

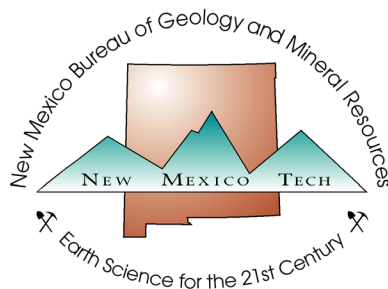
GEOLOGIC MAP OF THE
WILLIAMSBURG NW 75-MINUTE QUADRANGLE,
SIERRA COUNTY, NEW MEXICO

By
Andrew P. Jochems

December 2015
[Revised January 2019]

New Mexico Bureau of Geology and Mineral Resources
Open-file Digital Geologic Map OF-GM 251

Scale 1:24,000



This work was supported by the U.S. Geological Survey, National Cooperative Geologic Mapping Program (STATEMAP) under USGS Cooperative Agreement 06HQPA0003 and the New Mexico Bureau of Geology and Mineral Resources.

New Mexico Bureau of Geology and Mineral Resources, New Mexico Institute of Mining and Technology, 801 Leroy Place, Socorro, New Mexico, 87801-4796

The views and conclusions contained in this document are those of the author and should not be interpreted as necessarily representing the official policies, either expressed or implied, of the U.S. Government or the State of New Mexico.

CONTENTS

INTRODUCTION.....	3
GEOLOGIC SETTING.....	4
GEOCHRONOLOGY.....	4
STRATIGRAPHY.....	5
Paleozoic Rocks.....	5
Eocene-Oligocene Volcanism.....	5
Miocene-Pliocene Basalt.....	10
Quaternary-Tertiary Basin Fill.....	11
Quaternary Deposits.....	14
STRUCTURAL GEOLOGY.....	14
REFERENCES.....	16
Appendix A: Detailed unit descriptions.....	20
Appendix B: Clast count data.....	32
Appendix C: Paleocurrent data.....	42
Appendix D: $^{40}\text{Ar}/^{39}\text{Ar}$ age data.....	69

Note on Private-Land Access in the Williamsburg NW Quadrangle

Like many 7.5-minute quadrangles in the Palomas basin, the Williamsburg NW quadrangle covers a mix of public (~55%) and private (~45%) land. Access to approximately half of the private land on this quadrangle was restricted during the active phase of this project. Therefore, completion of this geologic map relied heavily on interpretations of aerial photography and existing maps of various scales. All users of this map should obtain permission from local owners before entering their lands.

INTRODUCTION

This report accompanies the Geologic Map of the Williamsburg NW 7.5-Minute Quadrangle, Sierra County, New Mexico (NMBGMR OF-GM 251). Its purpose is to discuss the geologic setting and history of the area, and to identify and explain significant stratigraphic and structural relationships uncovered during the course of mapping.

The Williamsburg NW quadrangle is located in the western Palomas basin where it abuts the Salado Mountains and Garcia Peaks (Fig. 1). Major drainages crossing the quadrangle are Salado Creek, Cuchillo Negro Creek, and Palomas Creek. The highest location in the quadrangle is 1893 m (~6210 ft) above sea level (asl) atop Garcia Peak at 267224 mE/3670445 mN (all locations reported in NAD83 UTM 13S). The lowest point is 1395 m (4577 ft) asl where Palomas Creek exits the quadrangle at 277460 mE/3667689 mN. Access to the quadrangle is via county roads, including CO20, 23, and 79 (collectively known as Calle de los Ranchos), which connect the broad plain in the eastern part of the quadrangle with NM-187 (old US Highway 85) south of Williamsburg. Calle de los Ranchos drops into the valley of Palomas Creek and meets San Miguel Road near old San Miguel Church. This road then climbs out of the valley and heads to the town of Cuchillo to the northeast. NM-52 just crosses the northeastern corner of the quadrangle ~2 km west of Cuchillo. County Road BO77 (also known as Molino Viejo Road) provides access to lands south of Salado Creek and can be accessed from the community of Las Palomas.

Early geologic mapping and reconnaissance work in this part of the Palomas basin was done by Gordon and Graton (1907), Gordon (1910), and Harley (1934). Mapping by Jahns (1955) laid the groundwork for

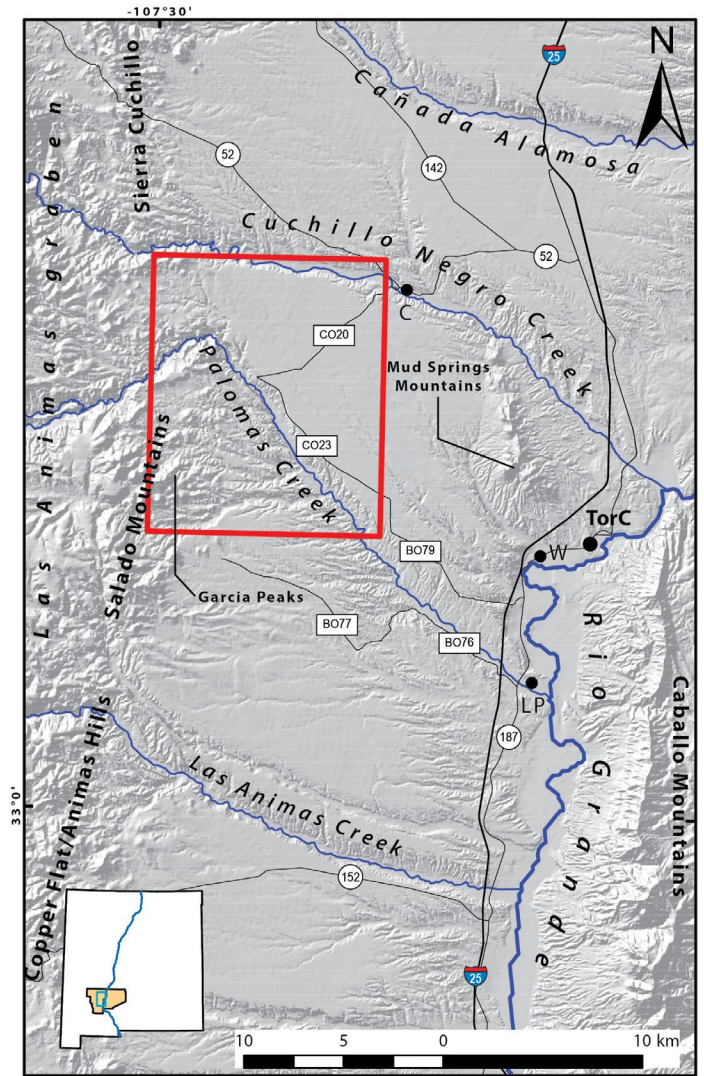


Figure 1. Relief map showing major physiographic features of the Palomas basin and surrounding areas. The basin is bordered on the east by the Caballo Mountains and on the west by the Animas-Salado uplifts and Sierra Cuchillo. Williamsburg NW quadrangle is outlined in red. Inset map shows location in Sierra County, New Mexico; blue line is the Rio Grande. Abbreviations for local communities: C = Cuchillo, LP = Las Palomas, TorC = Truth or Consequences, W = Williamsburg.

volcanic stratigraphy in the area. Harrison et al. (1993) produced a 1:100,000 scale geologic map that includes the Williamsburg NW quadrangle and surrounding country. The southwest corner of the quadrangle was mapped at 1:24,000 by Mayer (1987); additional theses with mapping in or near the quadrangle are those of Lamarre (1974) and McMillan (1979). Surrounding quadrangles mapped at 1:24,000 include Chise to the northwest (Jahns et al., 2006), Priest Tank to the north (Heyl et al., 1983), Cuchillo to the east (Maxwell and Oakman, 1990), and Williamsburg to the southeast (Jochems and Koning, 2015).

This report includes a geologic setting and summary of

local geochronology data before describing mapped units and their depositional settings by age, oldest to youngest. Stratigraphic correlations to surrounding quadrangles are described in the report, as is the structural geology of the area. Finally, detailed unit descriptions, clast counts, paleocurrent measurements, and $^{40}\text{Ar}/^{39}\text{Ar}$ age data are provided as appendices.

GEOLOGIC SETTING

The Williamsburg NW 7.5-minute quadrangle is located in the southern part of the Rio Grande rift, a series of *en echelon* basins stretching from northern Colorado to northern Mexico (Hawley, 1978; Chapin and Cather, 1994). The quadrangle includes the western part of an east-tilted half-graben filled with Miocene-Pleistocene sediment known as the Palomas basin (Fig. 1). The western border (i.e. hanging wall) of the Palomas basin is defined by the Animas Hills and Salado Mountains, east-dipping fault-block uplifts of mostly Paleozoic sedimentary through Oligocene volcanic bedrock. The Salado Mountains intersect the western 3-4 km of the Williamsburg NW quadrangle as the Garcia Peaks, with rugged topography formed from quartz diorite and andesite. These rocks form part of a large stock intruding Paleozoic through Eocene units that are observed to the south (Mayer, 1987). Oligocene volcanic units to the north are not intruded by the stock and form hills of moderate relief that are the continuation of the Animas-Salado fault blocks. The Salado block steps left to become the Sierra Cuchillo within several km of the northern boundary of the quadrangle (Jahns, 1955).

Exposed just south of the Williamsburg NW quadrangle is the Chavez Canyon fault, a Laramide structure defining the northern margin of the Rio Grande uplift (Mayer, 1987; Seager and Mayer, 1988). In the map area, the Eocene Rubio Peak Formation overlies the Permian Abo and Pennsylvanian Bar B Formations. This relationship suggests erosion of several thousand feet of the Permian Yeso Formation and younger Cretaceous strata concomitant with Laramide uplift (Kottlowski, 1963; Seager and Mayer, 1988).

Eocene-Oligocene volcanic rocks exposed throughout the quadrangle record the transition from arc-style magmatism to rift-related volcanism. Volcanic tuffs and flows exposed in the quadrangle reflect large ignimbrite eruptions and later calc-alkalic volcanism of the Mogollon-Datil volcanic field (Seager et al., 1984; Chapin

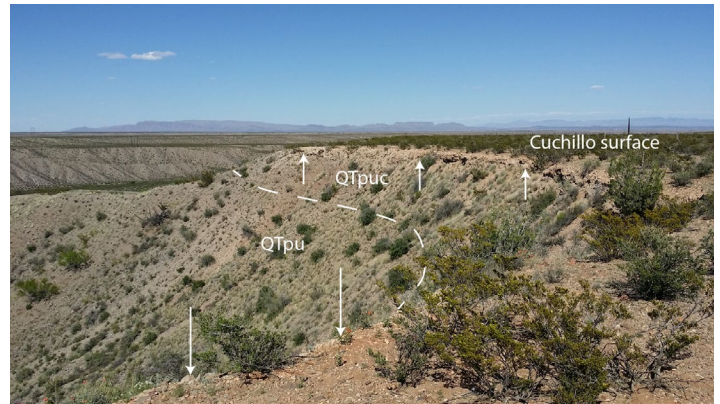


Figure 2. Calcrete (white arrows) with stage IV carbonate morphology underlying the Cuchillo surface south of Cuchillo Negro Creek. Similar pedogenic carbonate horizons up to 2 m thick are observed throughout the eastern part of the quadrangle atop gravel of the upper coarse piedmont facies of the Palomas Formation (QTpuc). Dashed line shows contact between QTpuc and finer-grained facies of upper Palomas piedmont (QTpu). View is toward the northeast.

et al., 2004).

The eastern part of the quadrangle is dominated by a gently inclined ($\leq 1.5^\circ$) plain known as the Cuchillo surface. This surface slopes toward the east and is considered the constructional surface of the Plio-Pleistocene Palomas Formation, basin-fill sediment deposited in large fans coalescing toward the deepest part of the Palomas basin in the Williamsburg area. Magnetostratigraphic data suggests that the surface dates to ~ 0.8 Ma in most places (Mack et al., 1993, 1998). The Cuchillo surface is underlain by a petrocalcic horizon featuring stage III-IV carbonate morphology as much as 2 m thick (Fig. 2). However, this soil and the surface is commonly eroded atop the westernmost exposures of the Palomas Formation in the quadrangle, where coarse gravels of the upper Palomas Formation (QTpuc) form an erosional pediment on older rocks.

GEOCHRONOLOGY

Although existing geochronologic data from the Williamsburg NW quadrangle is lacking, Lamarre (1974) reported a K/Ar age of 43.7 ± 1.7 Ma for a hornblende andesite dike intruding a reverse fault southwest of the map area. He considered this dike to be genetically related to the Garcia Peaks intrusive complex. Based on a similar mineralogic character, it may be close in age to the large dike intruding laharic deposits of the Rubio Peak Formation in the southwest quadrangle.

Table 1. Summary geochronology for rocks dated in the Williamsburg NW quadrangle.

Unit	Map Symbol	Method	n ^a	Age (Ma)	2σ Error (Ma)	MSWD ^b	Brief Description
Basalt flow	Tb	⁴⁰ Ar/ ³⁹ Ar	4	4.57	± 0.02	3.13	Lowest flow overlying lower Palomas gravels along Palomas Creek.
Basalt flow	Tb	⁴⁰ Ar/ ³⁹ Ar	6	5.54	± 0.03	2.16	Flow overlying middle Santa Fe Group sediment along Salado Creek.
Andesite-quartz diorite (flow)	Tad	⁴⁰ Ar/ ³⁹ Ar	4	40.35	± 0.05	29.99	Hypidiomorphic, slightly vesicular, fine- to medium-grained andesite.

Note: Groundmass concentrate analyzed for Tb samples; biotite separate analyzed for Tad sample. Weighted mean ages are given for each sample.

^an = number of plateau ages used in mean.

^bMSWD = mean square weighted deviation.

Three new ⁴⁰Ar/³⁹Ar ages were obtained for rocks in the Williamsburg NW quadrangle during the course of mapping (Table 1). The older age of 40.35 ± 0.05 Ma was found for biotite in an andesitic extrusive equivalent of the Garcia Peaks stock at 270141 mE/3670002 mN. This age was determined for a sample exhibiting slight alteration; however, weighted mean and integrated ages agree within error and argon loss in the sample was therefore considered minimal (L. Peters, pers. comm., 2015). The andesite age implies a middle to late Eocene time frame for intrusion of the main stock body and associated dikes and eruption of occasional flows onto the surface.

The younger ⁴⁰Ar/³⁹Ar ages of 4.57 ± 0.02 Ma and 5.54 ± 0.03 Ma were obtained for two basalt flows capping early Palomas Formation gravels along Palomas Creek (271084 mE/3675538 mN) and uppermost gravels, sands, and muds of the middle-lower Santa Fe Group along Salado Creek (271695 mE/3669792 mN), respectively. These ages suggest that Palomas Formation gravels were deposited atop the middle-lower Santa Fe Group in proximal alluvial fan settings after the earliest Pliocene.

STRATIGRAPHY

Paleozoic Rocks

Paleozoic rocks are only sparingly exposed in the map area, and were not investigated in the field due to private land access restrictions. The two units exposed at the surface are the Pennsylvanian Bar-B Formation (Pb) and the Permian Abo Formation (Pa). The Bar-B Formation

outcrops along the western border of the quadrangle. Locally, it has been described as nodular limestone and mudstone with a middle zone of calcite-cemented chert and quartz pebble conglomerate (Lamarre, 1974; Mayer, 1987). Lamarre (1974) reported a late Virgilian-early Wolfcampian(?) fusulinid species from fossiliferous Bar-B beds. The Bar-B Formation was likely deposited on a shallow marine shelf with occasional deposition of turbidites (Kues and Giles, 2004).

The Abo Formation is also found along the western quadrangle border, apparently thrust upon itself at 268710 mE/3671141 mN (Mayer, 1987; Harrison et al., 1993). Mayer (1987) described the Abo Formation as red beds of cross-stratified sandstone and siltstone. These facies were deposited in fluvial and floodplain settings and are considered middle-late Wolfcampian in age (Lucas et al., 2012).

Eocene-Oligocene Volcanism

Several thousand feet of Permian through Cretaceous strata are missing in the Williamsburg NW quadrangle (Kottlowski, 1963; Seager and Mayer, 1988), as is any syn- or post-orogenic unit associated with the Laramide orogeny, such as the Love Ranch Formation. However, both Love Ranch conglomerate and a Laramide fault (the Chavez Canyon fault) are located just south of the map area (Seager and Mayer, 1988). The absence of the Love Ranch Formation or a similar sedimentary package in the Williamsburg NW quadrangle implies that it was a topographically and structurally high area during the Eocene.

The Eocene-Oligocene section exposed in the quadrangle

reflects the transition from arc-style magmatism to volcanism of the Mogollon-Datil volcanic field, including large ignimbrite eruptions and later calc-alkalic volcanism during initial Rio Grande rift extension (Seager et al., 1984). The initiation of this activity may be related to slab roll-back (Chapin et al., 2004). Although the volcanic section in the Williamsburg NW quadrangle is not as complete as other locations in the Animas-Salado uplifts and the nearby Black Range (e.g., Jochems et al., 2014), these rocks do span most of the history of Eocene-Oligocene volcanism in the area, beginning with the deposition of thick sequences of volcanoclastic deposits.

The Rubio Peak Formation (Trp) is the oldest Tertiary volcanic/volcanoclastic unit exposed in the Williamsburg NW quadrangle. Based on cross section A-A' and projecting to its lower contact in the Thumb Tank Peak quadrangle to the west, the Rubio Peak Formation has a thickness of at least 595 m. In places, the Rubio Peak rests on deeply erosional contacts with the Permian Abo or Pennsylvanian Bar-B Formations, resulting in angular unconformities of up to 10°.

Although mapped by previous workers as the Palm Park Formation (Lamarre, 1974; Mayer, 1987), the unit is designated the Rubio Peak Formation here because the clasts it contains are compositionally distinct from those in the Palm Park at its type locality in the southern Caballo Mountains, which are primarily andesite-latitude (e.g., Seager et al., 1971; Seager et al., 1975). In the map area, clasts range in composition from dacite to andesite to rhyolitic tuff. This observation suggests that the two units were sourced from different areas; however, the units interfinger in the southern part of the Palomas basin and workers generally consider them to be time-



Figure 4. View looking northwest toward the southern part of the Garcia Peaks. These rugged mountains are formed by andesite to quartz diorite (unit Tad) intruded into Paleozoic and lower Eocene strata after ~45 Ma. Laharc breccia and volcanoclastic deposits of the Rubio Peak Formation (Trp) form light-colored hills in the foreground.

correlative (e.g., Clemons, 1979).

The Rubio Peak Formation in the map area consists of breccia, conglomerate, and tuffaceous sandstone. Breccia is by far the most common lithofacies and was mostly deposited by lahars as implied by matrix-supported textures (Fig. 3). Clasts in these deposits include dacite (up to 50%), reddish plagioclase-phyric andesite, and tannish to whitish rhyolitic tuffs. Other breccias may have been deposited in or near vents, especially where clasts are angular and monolithic. Volcanoclastic facies commonly interfinger with andesitic flows containing 10-12% plagioclase and 5-7% hornblende phenocrysts. Ages determined for both lava flows and clasts found in laharc breccia of the Rubio Peak Formation and correlative Palm Park Formation range from 46.3 to 36.7 Ma (Clemons, 1979; Loring and Loring, 1980; McMillan, 2004).

Paleozoic strata and the Rubio Peak Formation are intruded by andesite to quartz diorite (Tad) of the Garcia Peaks stock in the Williamsburg NW quadrangle. The Garcia Peaks form rugged topography in the southwest part of the map area (Fig. 4). Intrusive contacts are sharp with nearly vertical abutments of igneous rock against volcanoclastic or sedimentary units in many locations. However, the unit exhibits somewhat concordant contacts with the Rubio Peak Formation in some locations; these are interpreted as correlative extrusive lavas lying on older volcanoclastic rocks. Contacts between the Rubio Peak and unit Tad are often paralleled by drainages, with streams and arroyos taking advantage of the comparatively weak volcanoclastic deposits at the margins of the intrusion.

Intrusive rocks of the Garcia Peaks stock are dense,



Figure 3. Lahar deposit in the Rubio Peak Formation (Trp). This is the most common lithofacies in the Rubio Peak throughout the Williamsburg NW quadrangle, and is typified by a tuffaceous matrix supporting angular to subrounded clasts of dacite, andesite, and perhaps rhyolitic tuff. Pack is 0.6 m tall.

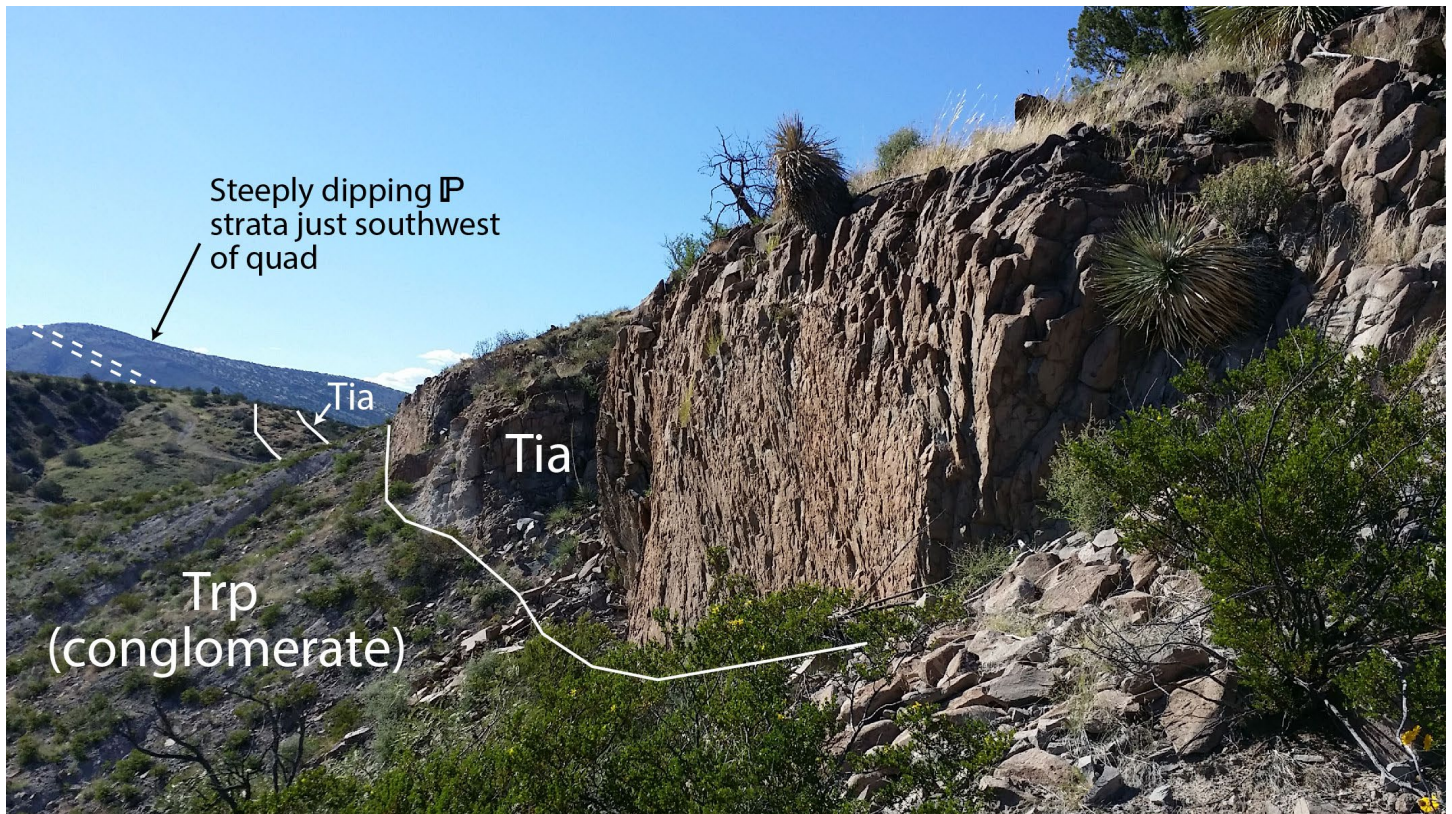


Figure 5. Andesite dike (Tia) intruding laharic conglomerate and breccia of the Rubio Peak Formation (Trp). Plagioclase- and hornblende-bearing dike is up to 30 m wide and does not intrude strata younger than Eocene in age. Dipping Pennsylvanian beds just southwest of quadrangle boundary are located in the footwall of the north-vergent Chavez Canyon fault in the Salado Mountains.

porphyritic, and have 8-10% hornblende, 5% biotite, trace to 3% plagioclase, and trace to 2% quartz phenocrysts, with rare biotite overprinting hornblende crystals. However, petrographic analysis of these rocks by Mayer (1987) show that they may contain as much as 40% plagioclase and range in composition from quartz diorite to andesite porphyry with scant evidence of metamorphism. He also notes the presence of diorite porphyry (his unit *Td*) that may represent a second stock or a deeper part of the Garcia Peaks body. This unit was not mapped due to land access restrictions but may crop out along the western boundary of the quadrangle between the high point of the Garcia Peaks and Palomas Creek. On the flanks of the main intrusive body are subordinate extrusive units, including an andesite flow at 270141 mE/3670002 mN. This flow has 14-15% plagioclase, 10% hornblende, and 2-5% biotite phenocrysts, and was dated at 40.35 ± 0.05 Ma (Table 1). This age broadly supports middle to late Eocene intrusion and related extrusive events of the Garcia Peaks stock.

Other intrusive rocks observed in the quadrangle include a large andesite dike (Tia) in the southwest corner of the map area and smaller dikes (Ti) mapped primarily by reconnaissance and using aerial photography. A small

plug is observed at 269561 mE/3674902 mN, but its composition could not be determined due to restricted land access. The large dike (Fig. 5) is up to 30 m across and faulted in at least three locations. It intrudes the Rubio Peak Formation and is buried by thin deposits of Palomas Formation gravels. Compositionally, this dike may be similar to the dike intruding the Chavez Canyon fault to the south, for which Lamarre (1974) provided a K/Ar date of 43.7 ± 1.7 Ma.

Following deposition of the Rubio Peak Formation and intrusion of the Garcia Peaks stock, local- to regional-scale andesite, dacite, rhyolite, and ignimbrites were erupted from the Mogollon-Datil volcanic field. The Sugarlump Tuff (Tsl) is the earliest of these observed. It is lithic-rich (~15-20%), contains up to 6% biotite phenocrysts, and underlies valley floors in the northwest corner of the quadrangle. The Sugarlump is in both depositional and fault contact with the Rubio Peak Formation throughout that area (Fig. 6), where it attains a maximum thickness of 35-45 m.

The Kneeling Nun Tuff (Tkn), well exposed in this part of the southern Rio Grande rift, unconformably overlies the Sugarlump and is typified by outflow facies featuring dense welding and high phenocryst content (25-30%

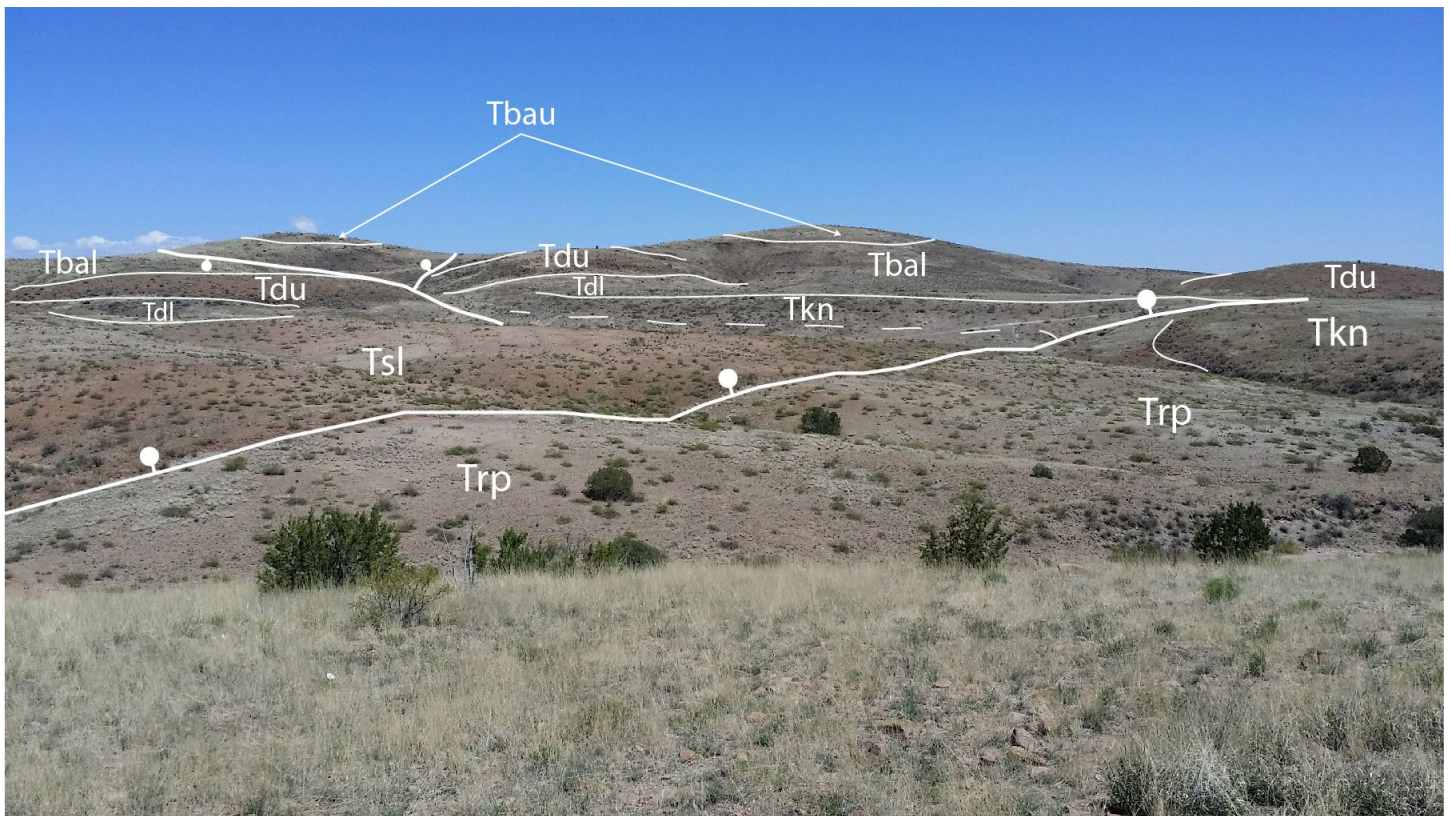


Figure 6. Fault contact (foreground) between the Sugarlump Tuff (Tsl) and Rubio Peak Formation (Trp) in the northwestern quadrangle. Simplified Eocene-Oligocene volcanic stratigraphy and additional faults are shown in the background; refer to geologic map for unit designations. Contacts are shown as thin lines and normal faults as thick lines; balls and bars shown on downthrown blocks of faults. View is toward the northeast.

sanidine+quartz+biotite). A maximum thickness for this unit is approximately 150 m near the bend of Palomas Creek, but this could not be confirmed due to restricted field access. This is close to the maximum thickness for outflow facies of the Kneeling Nun Tuff in other locations around the periphery of its source area, the Emory cauldron (Elston et al., 1975). Only ~20-30 m are preserved in the northwest corner of the quadrangle.

The Kneeling Nun Tuff on the Williamsburg NW quadrangle is found some 25-30 km beyond the northeastern margin of the Emory cauldron (Ericksen et al., 1970; Elston et al., 1975; Abitz, 1984). It appears to have covered considerable paleotopography formed on the surface of the Sugarlump Tuff given abrupt, steeply dipping contacts in many locations. Locally high relief may have been present to the north of Indian Creek during Kneeling Nun deposition where the tuff quickly pinches out. Note, however, that faults may account for some anomalously steep contacts and truncation of these rocks. The total eruptive volume of the Kneeling Nun is thought to have exceeded 900 km³ (Elston et al., 1975). The Sugarlump and Kneeling Nun tuffs are assigned ⁴⁰Ar/³⁹Ar ages of ~35.6 and 35.3 Ma (McIntosh et al., 1991), respectively; these ages are scaled upward by 1.3%

in this report to account for a revised sanidine monitor age of 28.201 Ma for the Fish Canyon Tuff advocated by Kuiper et al. (2008).

The Eocene-Oligocene volcanic section in the Williamsburg NW quadrangle is capped by a series of dacitic to andesitic lavas, tuffs, and tuff breccias as well as rare volcanoclastic sediment exposed in the northwest corner of the map (Fig. 6). Dacitic lava flows (Tdl) rest unconformably on the Sugarlump Tuff and are conformably overlain by dacitic tuffs and tuff breccias (Tdu), except in a few locations where the flows are cut by paleovalleys filled with volcanoclastic sediment (see below). Phenocrysts in both units include 2-16% plagioclase, 1% quartz, and trace amounts of biotite, sanidine, and perhaps pyroxene, with lower phenocryst percentages and smaller crystal size in the lower dacitic flows (Tdl). Tuff breccia in the upper dacitic unit (Tdu) contains up to 20% pumice fragments as well as light gray, aphyric clasts that may be rhyolite. A vitrophyre (Tdv) with deformed xenoliths of red, aphanitic material locally underlies Tdu and serves as a prominent marker across several faults (Fig. 7). Dacitic units in the quadrangle are correlative to units *Tdt* of Heyl et al. (1983) and *Td* of Jahns et al. (2006).



Figure 7. Vitrophyre (Tdv) underlying dacitic tuff. Reddish xenoliths of aphanitic material are abundant. Locally, these inclusions may be plastically deformed. Sledge hammer is 35 cm long.

Volcaniclastic sediment (Tds) cuts flows in the upper part of unit Tdl and consists of non-cemented siltstone and very fine-grained sandstone filling paleovalleys. The position of this mechanically weak deposit on steep slopes has proven favorable for at least one landslide at 268050 mE/3681151 mN. Although in a similar stratigraphic position as an air-fall tuff (unit *Twt*) described by Heyl et al. (1983), rounded grains and cross-stratification confirm this unit as a distinct sedimentary deposit (Fig. 8).

The dacitic package is unconformably overlain by a suite of basaltic andesite lavas that are regionally extensive

along the eastern margin of the Black Range. In the map area, these flows are divided into lower and upper units distinguished primarily by phenocryst content. The lower basaltic andesite (Tbal) is aphanitic with no more than ~2% phenocrysts (mostly pyroxene), whereas the upper unit (Tbau) contains 2-4% pyroxene and trace to 2% olivine. These flows correlate to units *Tb* and *Tyaf* of Heyl et al. (1983), respectively, and more generally to the *Ta* units of Jahns and others (2006). They may also correlate to units *T4ba* of Seager et al. (1982), *Tba2* of Jochems et al. (2014), and/or the Bear Springs basaltic andesite of the southern Black Range (Elston, 1957). No ages have been obtained for the dacite to basaltic andesite package in the map area, but Seager et al. (1984) obtained a K-Ar age of

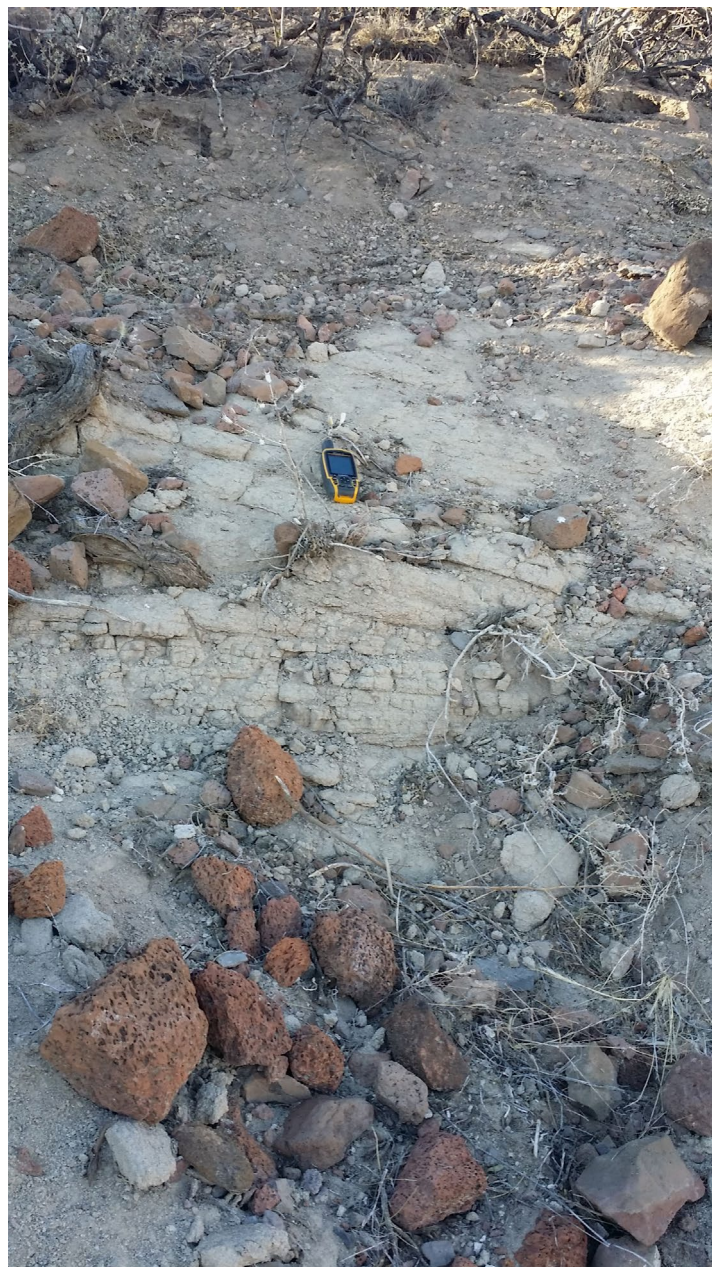


Figure 8. Cross-stratified volcaniclastic sediment (Tds) in the northern part of the quadrangle. Yellow GPS unit is 15 cm long.

28.1 ± 0.6 Ma for presumably correlative basaltic andesite west of Hillsboro.

Several small exposures of a relatively loose, unaltered tephra occur near the southwest corner of the quadrangle (not mappable at 1:24,000 scale). This unnamed ash is no more than 5 m thick in these locations where it fills paleochannels in the middle-lower Santa Fe Group. A sample of this quartz-rich (15-30%) ash was analyzed by electron microprobe, and backscattered electron images show large, intact phenocrysts (Fig. 9). An $^{40}\text{Ar}/^{39}\text{Ar}$ age has yet to be attained for this sample.

Miocene-Pliocene Basalt

Relatively thin (12-20 m) packages of basalt flows are present along Palomas and Salado Creeks in the west-central part of the quadrangle. These flows are dense to vesicular or scoriaceous; these textures plus phenocryst percentages distinguish individual flows (e.g., Compton, 1985). Overall, phenocrysts include 2-5% pyroxene and 2-3% olivine with disseminated magnetite. A sample collected from the lowermost flow exposed across from

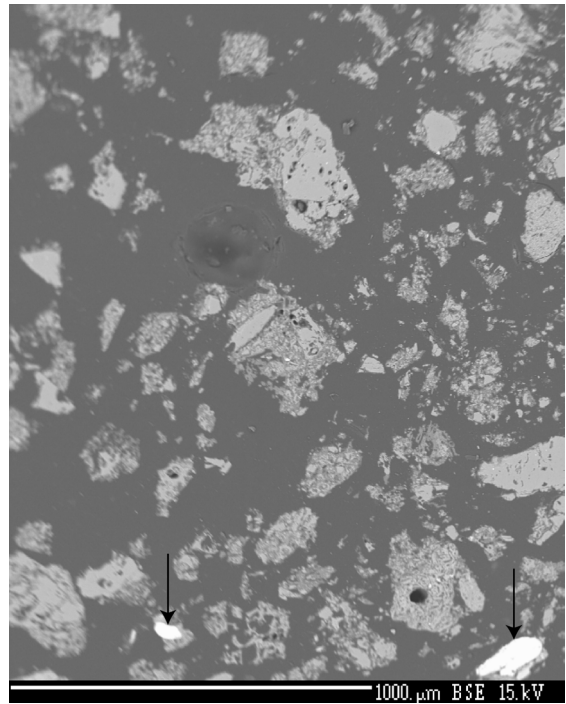


Figure 9. Backscattered electron image of tephra collected from small, isolated deposits of an ash in the southern part of the quadrangle. Sample exhibits large, relatively unaltered phenocrysts and glass shards (arrows). Low degree of alteration is unusual for ash of this age and phenocryst size implies a nearby source area. Field of view is ~1.5 mm.

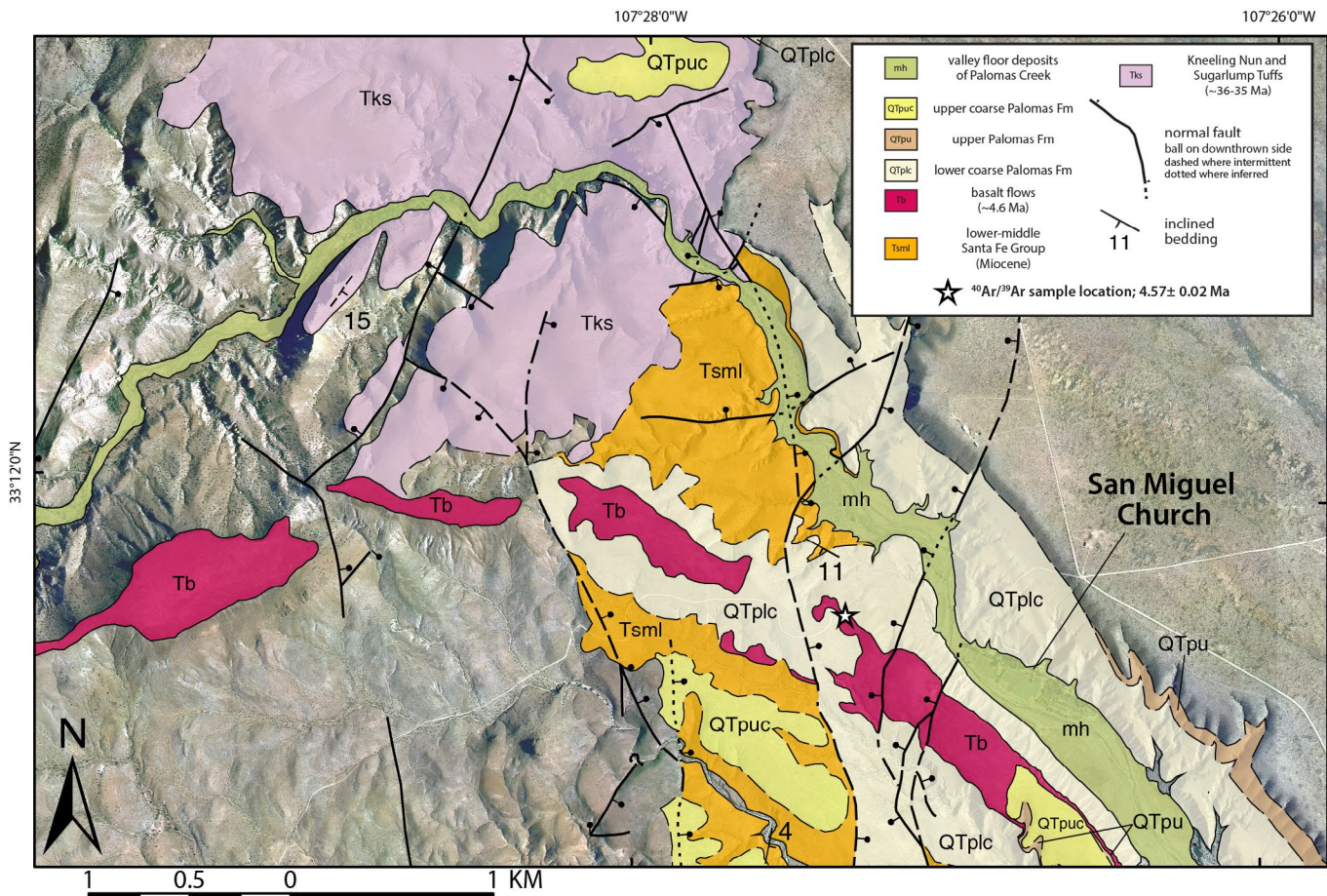


Figure 10. Orthophoto showing Pliocene basalt flows (Tb) that parallel the modern drainage of Palomas Creek. Outcrops of Kneeling Nun Tuff have apparent dips of ~15° toward the southeast.

San Miguel Church was dated at 4.57 ± 0.02 Ma ($^{40}\text{Ar}/^{39}\text{Ar}$; Table 1). Another thin flow found along Salado Creek was dated at 5.54 ± 0.03 Ma ($^{40}\text{Ar}/^{39}\text{Ar}$).

The series of basalt flows along Palomas Creek define one of the more intriguing topographic features of the Williamsburg NW quadrangle. These flows underlie elongate mesas that closely mimic the modern course of Palomas Creek (Fig. 10), which bends abruptly toward the southeast near 269894 mE/3677753 mN, where the creek enters a constriction formed by resistant cliffs of Kneeling Nun Tuff. If these basalt flows occupied a former canyon of Palomas Creek, then their age (~ 4.6 Ma) suggests that a large drainage was crossing the Salado uplift in a similar manner to the modern stream in early Pliocene time. Hence, this segment of the range was likely uplifted sometime during the late Miocene or earliest Pliocene. This line of evidence also demonstrates the Palomas Creek is likely an antecedent drainage. Importantly, the ancestral Rio Grande entered the Palomas basin in the early Pliocene (Mack et al., 1993). Clast lithologies in distal piedmont facies of the Palomas Formation (Jochems and Koning, 2015) imply that the ancestral Palomas Creek and other tributaries heading in the Black Range quickly integrated to the ancestral Rio Grande, probably because they already flowed toward a similarly positioned bolson prior to its arrival.

The 5.54 Ma Salado Creek basalt flow provides an important age constraint for pre-Palomas Formation basin fill. This flow interfingers with reddish, moderately to well-cemented conglomerate, sandstone, and lesser mudstone inferred to be upper Miocene in age (uppermost unit Tsml). It appears that proximal portions of the Palomas basin were filling with relatively coarse sediment perhaps correlative with the Rincon Valley Formation of Seager and others (1971) through the latest Miocene. Coarse, unconsolidated gravels of the Palomas Formation (unit QTpu) have cut a pedimented surface on the Miocene basin fill above the basalt. Projection of contacts to the east indicates that the lowest Palomas Formation (unit QTplc) locally lies with angular unconformity on lower-middle Santa Fe Group sediment and is younger than latest Miocene in age.

Quaternary-Tertiary Basin Fill

Oligocene through early Pleistocene deposition of basin-fill deposits formed the Santa Fe Group, a diverse set of lithofacies found throughout the Rio Grande rift

(stratigraphy shown and discussed in numerous works including Seager et al., 1982; Seager et al., 1987; Connell, 2008; and Koning et al., 2013). In the southern rift, the Santa Fe Group has been divided into as many as three formations (e.g., Seager et al., 1971); these broadly encompass the Oligocene-early Miocene, middle-late Miocene, and Pliocene-early Pleistocene. Miocene (and potentially Oligocene) basin fill is described in this report as the middle-lower Santa Fe Group (Tsml). Pliocene-early Pleistocene basin fill is described as the Palomas Formation (QTplc, QTpt, QTpm, QTpu, QTpuc).

Exposures of middle-lower Santa Fe Group beds are restricted to the western half of the Williamsburg NW quadrangle. The unit has an estimated average thickness of 150-300 m, with potential basinward thickening to as much as 500(+) m. These beds consist of moderately well-consolidated, predominantly silica-cemented, pebbly sandstone and conglomerate that are massive, imbricated, or cross-stratified. Clasts consist of subangular to subrounded basaltic andesite and felsites with scarce Paleozoic sedimentary lithologies. The texture of most middle-lower Santa Fe Group beds is consistent with debris-flow, fluvial, or sheet-flood deposition in the proximal to medial areas of large alluvial fans. Middle-lower Santa Fe Group beds may be in depositional or fault contact with the Rubio Peak Formation and typically underlie an angular unconformity with younger Palomas Formation gravels. They are nearly always tilted much more than the overlying Palomas Formation (up to 30° ; Fig. 11). Based on color and clay content, the upper part



Figure 11. Tilted pebbly conglomerate and pebbly sandstone of the middle-lower Santa Fe Group (Tsml). Dips are typically twice as much or more than those in the Palomas Formation (up to 30°).

of unit Tsml is tentatively correlated to the Rincon Valley Formation of Seager et al. (1971). It is not known whether older (Oligocene to early Miocene) basin-fill strata are represented in the quadrangle.

Basin fill in the western Palomas basin is dominated by the Plio-Pleistocene Palomas Formation. The term

“Palomas” was first applied to outcrops of upper Santa Fe Group basin fill by Gordon and Graton (1907), Gordon (1910), and Harley (1934). Lozinsky and Hawley (1986) formally defined the Palomas Formation and additional detailed descriptions of the unit are found in their work and Lozinsky (1986). Fossil data (summarized by Morgan and Lucas, 2012), basalt radiometric ages (Bachman and Mehnert, 1978; Seager et al., 1984; this study), and magnetostratigraphic data (Repenning and May, 1986; Mack et al., 1993, 1998) indicate an age range of approximately 5.0-0.8 Ma for the Palomas Formation. The basal Palomas is likely on the older end of this range in the Williamsburg NW quadrangle, where as much as 60 m of nearly flat sand and gravel beds underlie a 4.6 Ma basalt flow.

In the Williamsburg NW quadrangle, the Palomas Formation attains a maximum thickness of 257 m and consists of sandy gravel, pebbly sand, and subordinate sandy silt and mud. These facies can be delineated into five lithofacies, all of which were deposited in proximal to medial positions of coalesced alluvial fans (bajadas) in the western Palomas basin: (1) lower coarse-grained piedmont (QTplc); (2) transitional gravels and sands (QTpt); (3) middle fine-grained piedmont (QTpm); (4) upper, mostly fine-grained piedmont (QTpu); and (5) upper coarse-grained piedmont (QTpuc). Paleocurrent data suggest that the large fan complexes in which these lithofacies were deposited emanated primarily from ancestral drainages of Cuchillo Negro and Palomas Creeks. Interfingering between these units may be complex, but approximate source areas can be estimated through observation of clast lithologies in alluvial fan gravels. All lithofacies thicken toward the east and southeast (i.e. toward the basin center).

Lithofacies 1 is up to 73 m thick and includes pebbly sand/sandstone and sandy pebble-cobble gravel/conglomerate in massive, tabular, matrix-supported debris-flow beds or in lenticular, imbricated to cross-stratified, fluvially deposited beds. This unit is distinguished from underlying middle-lower Santa Fe Group basin fill by weaker cementation and lower tilt angles. However, basal beds of this unit may dip substantially more than overlying Palomas Formation facies (up to 6°). The lower coarse lithofacies underlies the ~4.6 Ma Palomas Creek basalt flows.

Lithofacies 2 is up to 43 m thick and well-exposed along Palomas Creek in the southern part of the quadrangle; in places, it may be vertically gradational with Lithofacies

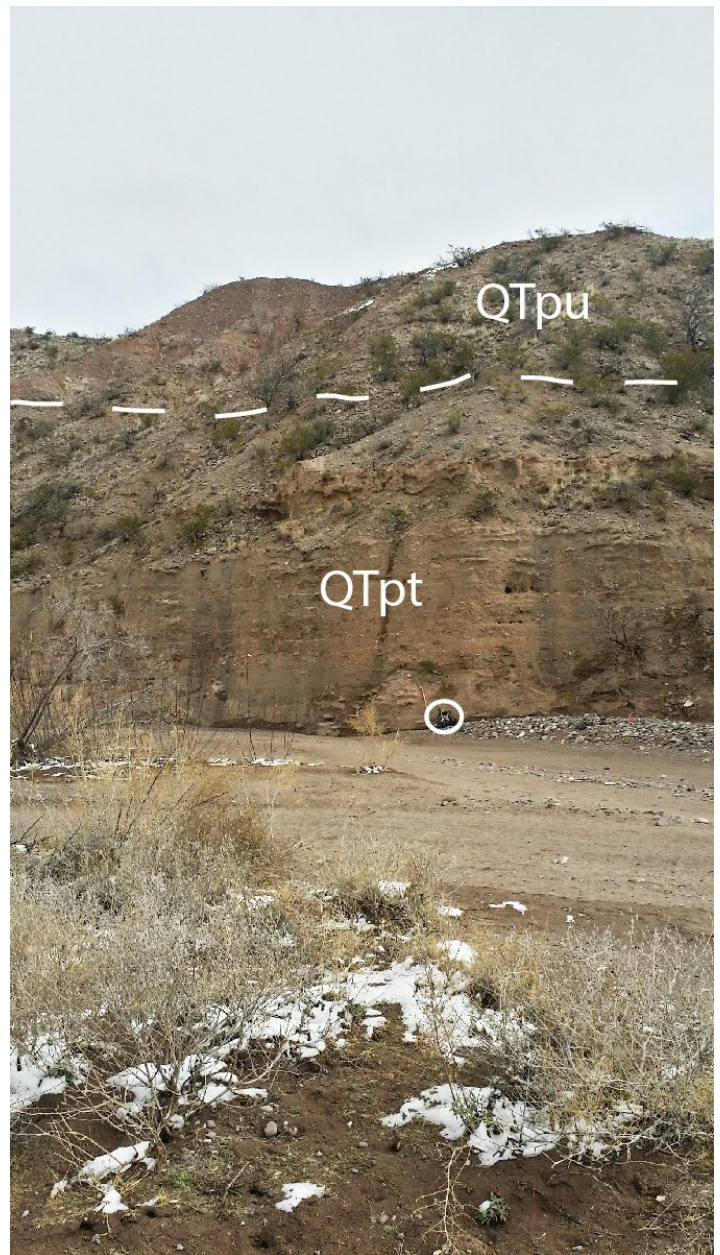


Figure 12. Contact between the transitional (QTpt) and upper piedmont facies (QTpu) of the Palomas Formation along Palomas Creek just upstream of its confluence with Salado Creek. QTpt beds in this location are moderately calcite-cemented sandstone and conglomerate that form prominent ledges below the redder, poorly cemented, fine-grained beds of the upper piedmont. Pack (white circle) is 0.6 m tall.

1. It pinches out toward the north and is not observed along Cuchillo Negro Creek. Lithofacies 2, likely fluvial in origin, consists of calcite-cemented sandstone and conglomerate that form small to prominent ledges along Palomas Creek (Fig. 12); these beds clearly interfinger with finer-grained deposits to the north and south (Jochems and Koning, 2015). Sparry calcite cement in these beds could be phreatic in origin (Mack et al., 2000).

Lithofacies 3, 20-81 m thick, includes brownish to

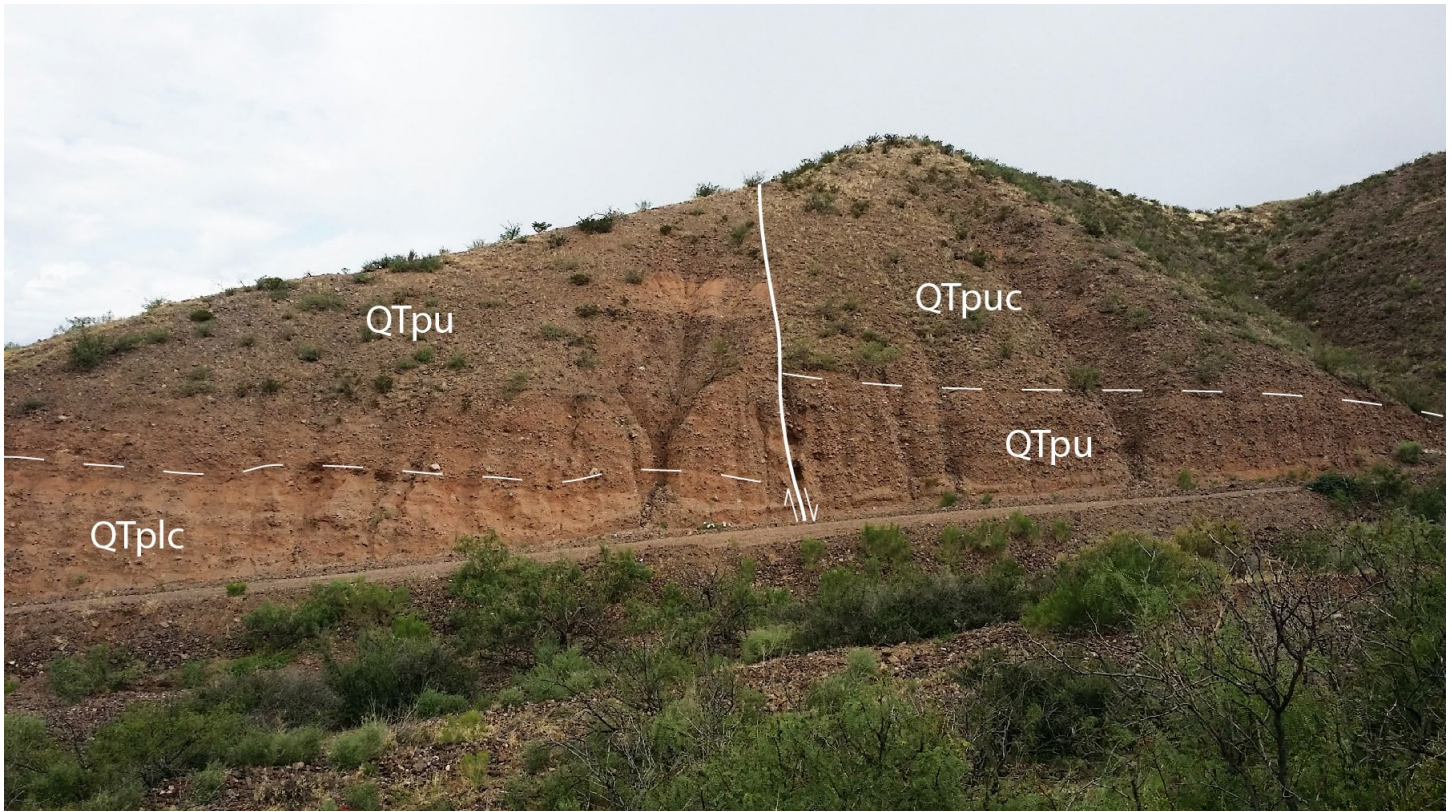


Figure 13. Contact between the upper piedmont facies (QTpu) and lower coarse piedmont facies (QTplc) in the footwall of the Palomas Creek fault along roadcut at 273925 mE/3672745 mN. The upper coarse facies (QTpuc) present in the hanging wall is typified by imbricated and/or cross-stratified, amalgamated channel-fills.

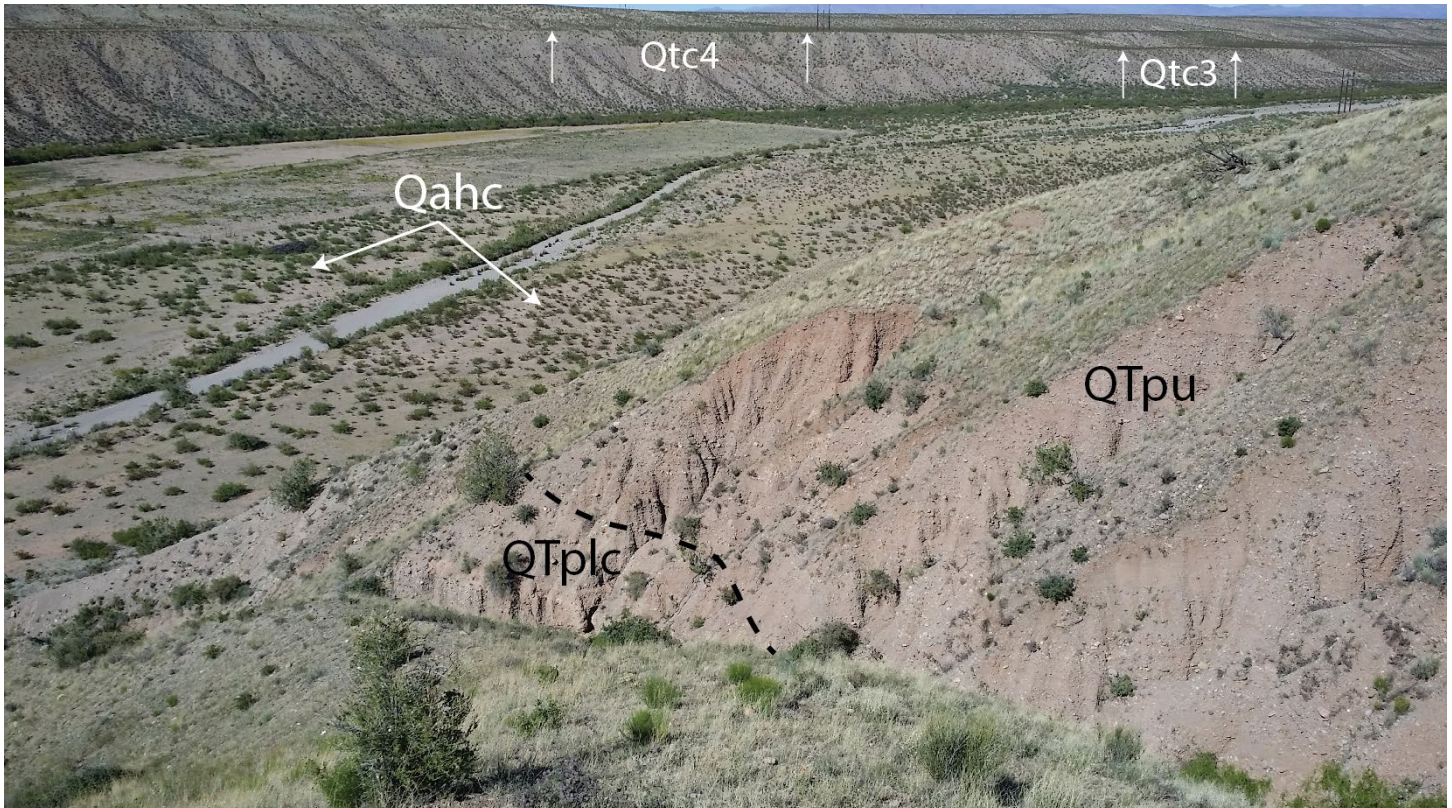


Figure 14. Historical alluvium (Qahc) and middle to late Pleistocene terrace deposits (Qtc4 and Qtc3, treads above white arrows) of Cuchillo Negro Creek (middle ground). Also shown is the contact between upper piedmont facies (QTpu) and lower, coarse-grained piedmont facies of the Palomas Formation (QTplc). View is toward the northeast.

pinkish, pebbly silt and mud to very fine- or fine-grained sand with $\leq 15\%$ gravelly channel fills. Finer-grained beds represent deposition in extral-channel settings, perhaps with some eolian-derived material present. Stage II-III calcic paleosols are common. Lithofacies 3 is laterally gradational with Lithofacies 2 in most places; this relationship is especially clear to the south along Palomas Creek (Jochems and Koning, 2015).

Lithofacies 4 is 20-60 m thick and includes sand, silt, and mud featuring abundant buried paleosols with Bw, Btk, and Bk horizons. A distinct reddish hue is imparted by abundant clay bridges and films in the matrix of gravelly channel fills or by clay-rich overbank deposits. This unit is mostly comprised ($>60\%$) of beds deposited in extra-channel or interfluvial settings.

Finally, Lithofacies 5 is 12-52 m thick and composed of well-imbricated, often amalgamated, pebble-cobble gravel with up to 20% Pliocene basalt clasts (Fig. 13). It reflects an upward coarsening that is observed elsewhere in the Palomas basin (e.g., Jochems and Koning, 2015; Koning et al., 2015). In the eastern part of the quadrangle, Lithofacies 5 is usually capped by a stage III-IV petrocalcic horizon underlying the Cuchillo geomorphic surface. However, thin deposits in the southwestern part of the quadrangle correlated to Lithofacies 5 are likely erosional pediment gravels.

Quaternary Deposits

The Quaternary history of the Williamsburg NW quadrangle is marked by drainage integration and down-cutting. The canyons of Cuchillo Negro and Palomas Creeks are 60-90 m deep in many places and are lined by suites of up to seven stream terrace deposits (units Qtc and Qtp, respectively). These gravelly units underlie flat, drainage-parallel surfaces (Fig. 14), and may represent sedimentation controlled by glacial-interglacial climatic fluctuations. One model suggested for the formation of terrace deposits elsewhere in southern New Mexico hypothesizes that these deposits formed in three stages: (1) incision in the Rio Grande and the lower valleys of its tributaries during full glacial conditions; (2) aggradation during the transition to interglacial intervals due to decreased water to sediment ratios; and (3) stability for the remainder of interglacial intervals (Gile et al., 1981). Application of this model to the terrace suites observed in the Williamsburg NW quadrangle suggests that these deposits have been forming since roughly 700 ka. This time frame is constrained by the ~ 800 ka Cuchillo

geomorphic surface (Mack et al., 1993).

More recent deposits span the Holocene and include low-lying stream terraces and alluvial fans. The valley floors of Cuchillo Negro and Palomas Creeks each have widespread historical deposits (Qahc and Qahp, respectively) that signify aggradation over the late Holocene. These deposits are cut by straight to meandering arroyo channels that experience localized deposition of sand and gravel during high-flow events associated with summer monsoon storms (e.g., Mack et al., 2008).

STRUCTURAL GEOLOGY

Nearly all mapped structures in the Williamsburg NW quadrangle are related to extension of the Rio Grande rift. One exception is a possible northeast-trending anticline that appears to warp beds of the Rubio Peak Formation along the western border of the map; however, this structure could not be assessed in the field due to land access restrictions. If it is indeed an anticline, its hinge apparently exhibits a NE-SW trend that is unexpected, given the regional NE-SW compressive fabric commonly associated with Laramide deformation (e.g., Seager and Mack, 1986; Seager and Mayer, 1988; Seager et al., 1997). Alternatively, this feature could be related to intrusion of the Garcia Peaks stock, as Mayer (1987) suggested for similarly oriented folds in the Pennsylvanian Bar-B Formation. A small, southwest-dipping thrust fault mapped by Mayer (1987) and Harrison et al. (1993) near 268710 mE/3671141 mN is more suggestive of Laramide



Figure 15. East-down normal fault zone cutting the middle-lower Santa Fe Group (Tsm1); finer-grained lithofacies in footwall, coarse-grained sandstones and conglomerates in hanging wall. Vertical throw on right fault is estimated at 100 m. 270415 mE/3669197 mN (NAD83 UTM 13S). View is toward the northeast.

deformation.

Deformation in the quadrangle is typified by high-angle (56° to near vertical), mostly north-trending normal faults that vary in timing but are generally Neogene-Quaternary in age. In the western part of the map area, a series of east-down faults juxtapose Miocene basin fill against Eocene volcanoclastic and intrusive units. These faults are dip-slip and have estimated throws of up to ~ 120 m. One such structure crosses Salado where it juxtaposes different lithofacies of the middle-lower Santa Fe Group (Fig. 15). It continues to the south where it offsets the ~ 0.8 Ma Cuchillo surface, constraining the most recent rupture event along this fault to the early-



Figure 16. Carbonate cementation commonly observed in damage zones of faults cutting the Palomas Formation in the Williamsburg NW quadrangle. Note rotated clasts in damage zone.

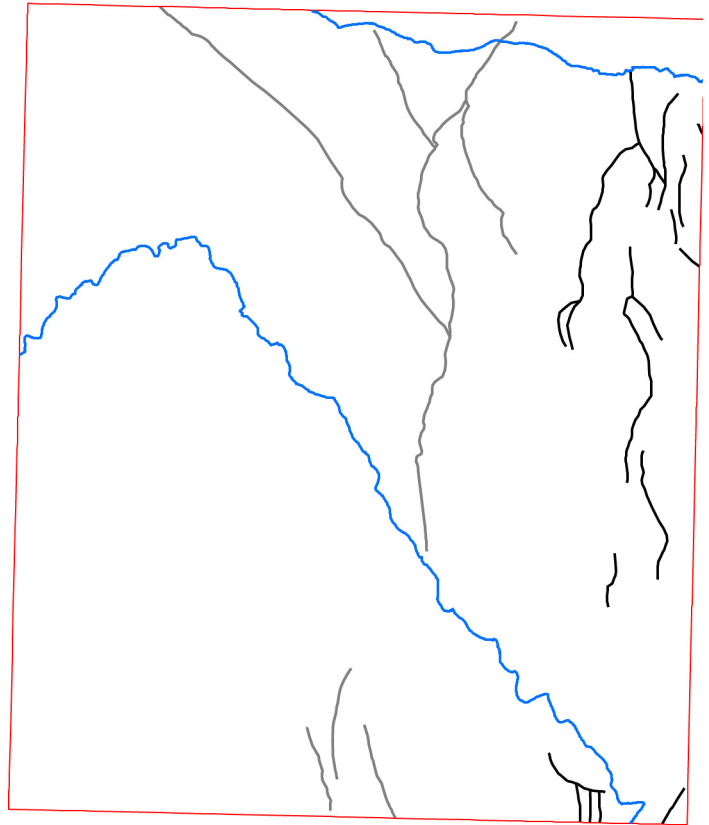


Figure 17. Palomas Creek and Cuchillo Negro Creek fault zones shown in gray and black, respectively. Palomas and Cuchillo Negro Creeks in blue. Williamsburg NW quadrangle in red.

middle Pleistocene if not more recently.

Farther east, north-trending faults include both east- and west-dipping structures, and display modest offset (< 20 m) of the ~ 4.6 Ma Palomas Creek basalt flows. None of these faults are directly observed to offset middle-late Pleistocene deposits, although the elevation of basal terrace strath surfaces drop somewhat between correlative deposits upstream of San Miguel Church. These faults are characterized by common carbonate cementation in damage zones 0.2-1 m thick (Fig. 16).

Two fault zones, the Palomas Creek and Cuchillo Negro Creek fault zones, exhibit evidence for Quaternary offset in the eastern half of the quadrangle (Fig. 17). The Palomas Creek fault (Fig. 13) forms a prominent ($\leq 6-8$ m high) east-down scarp on the Cuchillo surface stretching from Palomas to Cuchillo Negro Creeks. Machette and others (1998) considered the most recent rupture event (MRE) along this fault to be < 750 ka based on scarp morphology and the fact that it cuts the Cuchillo surface. These workers assigned an MRE age of < 130 ka for the series of smaller ($\leq 4-6$ m high), often short ($< 1-2$ km long) scarps in the eastern part of the quadrangle (Fig.



Figure 18. Cuchillo Negro fault zone scarp near 278010 mE/3679150 mN. Bottom of west-down scarp is shown by arrows. Scarp is 3.5 m high.

18). These scarps comprise the Cuchillo Negro fault zone. Slip rates for both fault zones are less than 0.2 mm/yr (Machette et al., 1998). The west-to-east progression of younger faulting indicates a basin-ward shift in tectonism throughout the late Neogene and Quaternary.

ACKNOWLEDGMENTS

Mapping of the Williamsburg NW quadrangle was funded by the STATEMAP program, which is jointly supported by the U.S. Geological Survey and the New Mexico Bureau of Geology & Mineral Resources (NMBGMR). I thank Dr. J. Michael Timmons of NMBGMR for logistical support. I am greatly indebted to the following landowners for access to their private properties: the Bierner family, the Grijalva family, Mr. and Mrs. Michael Root, Mr. Adam Sanchez, Mr. Wesley Whitney, and Las Palomas Land & Cattle Company (particularly caretakers Mr. Jonathan Beaty and Mr. John Walker). Dr. Bill McIntosh and Lisa Peters of the NMBGMR Argon Lab provided ages on Eocene andesite and Miocene-Pliocene basalt in the quadrangle. Dr. Nelia Dunbar (NMBGMR) analyzed tephra collected near Salado Creek. Dan Koning of NMBGMR provided valuable thoughts and discussion on Palomas Formation basin-fill stratigraphy. Finally, this map and report greatly benefited from a thorough review by Dr. William Seager (NMSU).

REFERENCES

- Abitz, R.J., 1986, Geology of mid-Tertiary volcanic rocks of the east-central Black Range, Sierra County, New Mexico: implications for a double-cauldron complex in the Emory cauldron, *in* Clemons, R.E., King, W.E., Mack, G.H., and Zidek, J., eds., *Truth or Consequences Region: New Mexico Geological Society Guidebook 37*, p. 161-166.
- Bachman, G.O., and Mehnert, H.H., 1978, New K-Ar dates and the late Pliocene to Holocene geomorphic history of the Rio Grande region, New Mexico: *Geological Society of America Bulletin*, v. 89, p. 283–292.
- Birkeland, P.W., 1999, *Soils and geomorphology*: Oxford, UK, Oxford University Press, 448 p.
- Birkeland, P.W., Machette, M.N., and Haller, K.M., 1991, Soils as a tool for applied Quaternary geology: *Utah Geological and Mineral Survey Miscellaneous Publication 91-3*, 63 p.
- Chapin, C.E., and Cather, S.M., 1994, Tectonic setting of the axial basins of the northern and central Rio Grande rift, *in* Keller, G.R., and Cather, S.M., eds., *Basins of the Rio Grande rift: Structure, Stratigraphic, and Tectonic Setting: Geological Society of America Special Paper 291*, p. 5-25.
- Chapin, C.E., McIntosh, W.C., and Chamberlin, R.M., 2004, The late Eocene-Oligocene peak of Cenozoic volcanism in southwestern New Mexico, *in* Mack, G.H., and Giles, K.A., eds., *The Geology of New Mexico: A Geologic History: New Mexico Geological Society Special Publication 11*, p. 271–293.
- Clemons, R.E., 1979, *Geology of Good Sight Mountains and Uvas Valley, southwest New Mexico*: New Mexico Bureau of Mines and Mineral Resources Circular 169, 32 p.
- Compton, R.R., 1985, *Geology in the field*: New York, John Wiley & Sons, 398 p.
- Connell, S.D., 2008, Refinements to the stratigraphic nomenclature of the Santa Fe Group, northwestern Albuquerque Basin, New Mexico: *New Mexico Geology*, v. 30, no. 1, p. 14–35.
- Elston, W.E., 1957, *Geology and mineral resources of Dwyer quadrangle, Grant, Luna, and Sierra Counties*,

- New Mexico: New Mexico Bureau of Mines and Mineral Resources Bulletin 38, 88 p.
- Elston, W.E., Seager, W.R., and Clemons, R.E., 1975, Emory cauldron, Black Range, New Mexico: source of the Kneeling Nun Tuff, *in* Seager, W.R., Clemons, R.E., and Callender, J.F., eds., *Las Cruces Country: New Mexico Geological Society Guidebook 26*, p. 283-292.
- Ericksen, G.E., Wedow, H., Jr., Eaton, G.P., and Leland, G.R., 1970, Mineral resources of the Black Range Primitive Area, Grant, Sierra, and Catron Counties, New Mexico: U.S. Geological Survey Bulletin 1319-E, 162 p.
- Gile, L.H., Peterson, F.F., and Grossman, R.B., 1966, Morphological and genetic sequences of carbonate accumulation in desert soils: *Soil Science*, v. 101, p. 347-360.
- Gile, L.H., Hawley, J.W., and Grossman, R.B., 1981, Soils and geomorphology in the Basin and Range area of southern New Mexico—Guidebook to the Desert Project: New Mexico Bureau of Mines and Mineral Resources Memoir 39, 222 p.
- Gordon, C.H., 1910, Sierra and central Socorro Counties, *in* Lindgren, W., Graton, L.C., and Gordon, C.H., eds., *The Ore Deposits of New Mexico: U.S. Geological Survey Professional Paper 68*, p. 213-285.
- Gordon, C.H., and Graton, L.C., 1907, Lower Paleozoic formations in New Mexico (abs.): *Journal of Geology*, v. 15, p. 91-92.
- Harley, G.T., 1934, The geology and ore deposits of Sierra County, New Mexico: New Mexico Bureau of Mines and Mineral Resources Bulletin 10, 220 p.
- Harrison, R.W., Lozinsky, R.P., Eggleston, T.L., and McIntosh, W.C., 1993, Geologic map of the Truth or Consequences 30 x 60 minute quadrangle: New Mexico Bureau of Mines and Mineral Resources Open-file Report 390, scale 1:100,000.
- Hawley, J.W., comp., 1978, Guidebook to Rio Grande rift in New Mexico and Colorado: New Mexico Bureau of Mines and Mineral Resources Circular 163, 241 p.
- Heyl, A.V., Maxwell, C.H., and Davis, L.L., 1983, Geology and mineral deposits of the Priest Tank quadrangle, Sierra County, New Mexico: U.S. Geological Survey Miscellaneous Field Studies Map MF-1665, scale 1:24,000.
- Ingram, R.L., 1954, Terminology for the thickness of stratification and parting units in sedimentary rocks: *Geological Society of America Bulletin*, v. 65, p. 937-938.
- Jahns, R.H., 1955, Geology of the Sierra Cuchillo, New Mexico, *in* Fitzsimmons, J.P., ed., *South-central New Mexico: New Mexico Geological Society Guidebook 6*, p. 158-174.
- Jahns, R.H., McMillan, K., and O'Brien, J.D., 2006, Geologic map of the Chise quadrangle, Sierra County, New Mexico: New Mexico Bureau of Geology and Mineral Resources Open-file Geologic Map OF-GM 115, scale 1:24,000.
- Jochems, A.P., and Koning, D.J., 2015, Geologic map of the Williamsburg 7.5-minute quadrangle, Sierra County, New Mexico: New Mexico Bureau of Geology and Mineral Resources Open-file Geologic Map OF-GM 250, scale 1:24,000.
- Jochems, A.P., Kelley, S.A., Seager, W.R., Cikoski, C.T., and Koning, D.J., 2014, Geologic map of the Hillsboro 7.5-minute quadrangle, Sierra County, New Mexico: New Mexico Bureau of Geology and Mineral Resources Open-file Geologic Map OF-GM 242, scale 1:24,000.
- Koning, D.J., Grauch, V.J.S., Connell, S.D., Ferguson, J., McIntosh, W., Slate, J.L., Wan, E., and Baldrige, W.S., 2013, Structure and tectonic evolution of the eastern Española Basin, Rio Grande rift, north-central New Mexico, *in* Hudson, M.R., and Grauch, V.J.S., eds., *Geological Society of America Special Paper 494*, p. 185-219.
- Koning, D.J., Jochems, A.P., and Cikoski, C.T., 2015, Geologic map of the Skute Stone Arroyo 7.5-minute quadrangle, Sierra County, New Mexico: New Mexico Bureau of Geology and Mineral Resources Open-file Geologic Map OF-GM 252, scale 1:24,000.
- Kottlowski, F.E., 1963, Paleozoic and Mesozoic strata of southwestern and south-central New Mexico: *New Mexico Bureau of Mines and Mineral Resources Bulletin 79*, 100 p.
- Kues, B.S., and Giles, K.A., 2004, The late Paleozoic Ancestral Rocky Mountains system in New Mexico,

- in* Mack, G.H., and Giles, K.A., eds., *The Geology of New Mexico: A Geologic History*: New Mexico Geological Society Special Publication 11, p. 95–136.
- Kuiper, K.F., Deino, A., Hilgen, F.J., Krijgsman, W., Renne, P.R., and Wijbrans, J.R., 2008, Synchronizing rock clocks of Earth history: *Science*, v. 320, p. 500–504.
- Lamarre, A.L., 1974, Fluorite in jasperoid of the Salado Mountains, Sierra County, New Mexico: Significance to metallogeny of the western United States [Unpublished M.S. thesis]: London, Canada, University of Western Ontario, 134 p.
- Loring, A.K., and Loring, R.B., 1980, K/Ar ages of middle Tertiary igneous rocks from southern New Mexico: Isochron/West, *Bulletin of Isotopic Geochronology*, no. 28, p. 17–19.
- Lozinsky, R.P., 1986, Geology and late Cenozoic history of the Elephant Butte area, Sierra County, New Mexico: New Mexico Bureau of Mines and Mineral Resources Circular 187, 40 p.
- Lozinsky, R.P., and Hawley, J.W., 1986, The Palomas Formation of south-central New Mexico—A formal definition: *New Mexico Geology*, v. 8, no. 4, p. 73–82.
- Lucas, S.G., Krainer, K., Chaney, D.S., Dimichele, W.A., Voigt, S., Berman, D.S., and Henrici, A.C., 2012, The lower Permian Abo Formation in the Fra Cristobal and Caballo Mountains, Sierra County, New Mexico, *in* Lucas, S.G., McLemore, V.T., Lueth, V.W., Spielmann, J.A., and Krainer, K., eds., *Geology of the Warm Springs Region*: New Mexico Geological Society Guidebook 63, p. 345–376.
- Machette, M.N., Personius, S.F., Kelson, K.I., Haller, K.M., and Dart, R.L., 1998, Map and data for Quaternary faults and folds in New Mexico: U.S. Geological Survey Open-file Report 98-521, 443 p.
- Mack, G.H., Salyards, S.L., and James, W.C., 1993, Magnetostratigraphy of the Plio-Pleistocene Camp Rice and Palomas Formations in the Rio Grande rift of southern New Mexico: *American Journal of Science*, v. 293, p. 49–77.
- Mack, G.H., Salyards, S.L., McIntosh, W.C., and Leeder, M.R., 1998, Reversal magnetostratigraphy and radioisotopic geochronology of the Plio-Pleistocene Camp Rice and Palomas Formations, southern Rio Grande rift, *in* Mack, G.H., Austin, G.S., and Barker, J.M., eds., *Las Cruces Country II: New Mexico Geological Society Guidebook 49*, p. 229–236.
- Mack, G.H., Cole, D.R., and Treviño, L., 2000, The distribution and discrimination of shallow, authigenic carbonate in the Pliocene-Pleistocene Palomas Basin, southern Rio Grande rift: *Geological Society of America Bulletin*, v. 112, no. 5, p. 643–656.
- Mack, G.H., Leeder, M.R., and Carothers-Durr, M., 2008, Modern flood deposition, erosion, and fan-channel avulsion on the semiarid Red Canyon and Palomas Canyon alluvial fans in the southern Rio Grande rift, New Mexico, U.S.A.: *Journal of Sedimentary Research*, v. 78, no. 7, p. 432–442, doi:10.2110/jsr.2008.050.
- Maxwell, C.H., and Oakman, M.R., 1990, Geologic map of the Cuchillo quadrangle, Sierra County, New Mexico: U.S. Geological Survey Geologic Quadrangle Map GQ-1686, scale 1:24,000.
- Mayer, A.B., 1987, Structural and volcanic geology of the Salado Mountains-Garcia Peaks area, Sierra County, New Mexico [Unpublished M.S. thesis]: Las Cruces, New Mexico State University, 61 p.
- McCraw, D.J., and Love, D.W., 2012, An overview and delineation of the Cuchillo geomorphic surface, Engle and Palomas Basins, New Mexico, *in* Lucas, S.G., McLemore, V.T., Lueth, V.W., Spielmann, J.A., and Krainer, K., eds., *Geology of the Warm Springs Region*: New Mexico Geological Society Guidebook 63, p. 491–498.
- McIntosh, W.C., Kedzie, L.L., and Sutter, J.F., 1991, Paleomagnetism and $^{40}\text{Ar}/^{39}\text{Ar}$ ages of ignimbrites, Mogollon-Datil volcanic field, southwestern New Mexico: *New Mexico Bureau of Mines and Mineral Resources Bulletin 135*, 79 p.
- McMillan, D.K., 1979, Crystallization and metasomatism of the Cuchillo Mountain laccolith, Sierra County, New Mexico [Unpublished Ph.D. dissertation]: Palo Alto, Stanford University, 217 p.
- McMillan, N.J., 2004, Magmatic record of Laramide subduction and the transition to Tertiary extension: Upper Cretaceous through Eocene igneous rocks of New Mexico, *in* Mack, G.H., and Giles, K.A., eds.,

- The Geology of New Mexico: A Geologic History: New Mexico Geological Society Special Publication 11, p. 249–270.
- Morgan, G.S., and Lucas, S.G., 2012, Cenozoic vertebrates from Sierra County, southwestern New Mexico, *in* Lucas, S.G., McLemore, V.T., Lueth, V.W., Spielmann, J.A., and Krainer, K., eds., *Geology of the Warm Springs Region: New Mexico Geological Society Guidebook 63*, p. 525–540.
- Munsell Color, 2009, Munsell soil color book: X-Rite, Grand Rapids, MI.
- Repenning, C.A., and May, S.R., 1986, New evidence for the age of lower part of the Palomas Formation, *in* Clemons, R.E., King, W.E., Mack, G.H., and Zidek, J., eds., *Truth or Consequences region: New Mexico Geological Society Guidebook 37*, p. 257–260.
- Seager, W.R., and Mack, G.H., 1986, Laramide paleotectonics of southern New Mexico, *in* Peterson, J.A., ed., *Paleotectonics and Sedimentation in the Rocky Mountain Region, United States: American Association of Petroleum Geologists Memoir 41*, p. 669–685.
- Seager, W.R., and Mack, G.H., 2003, *Geology of the Caballo Mountains, New Mexico: New Mexico Bureau of Geology and Mineral Resources Memoir 49*, 136 p.
- Seager, W.R., and Mayer, A.B., 1988, Uplift, erosion, and burial of Laramide fault blocks, Salado Mountains, Sierra County, New Mexico: *New Mexico Geology*, v. 10, no. 3, p. 49–53.
- Seager, W.R., Hawley, J.W., and Clemons, R.E., 1971, *Geology of San Diego Mountain area, Doña Ana County, New Mexico: New Mexico Bureau of Mines and Mineral Resources Bulletin 97*, 38 p.
- Seager, W.R., Clemons, R.E., and Hawley, J.W., 1975, *Geology of Sierra Alta quadrangle, Doña Ana County, New Mexico: New Mexico Bureau of Mines and Mineral Resources Bulletin 102*, 56 p., map scale 1:24,000.
- Seager, W.R., Clemons, R.E., Hawley, J.W., and Kelley, R.E., 1982, *Geology of northwest part of Las Cruces 1° x 2° sheet, New Mexico: New Mexico Bureau of Mines and Mineral Resources Geologic Map 53*, scale 1:125,000.
- Seager, W.R., Shafiqullah, M., Hawley, J.W., and Marvin, R.F., 1984, New K-Ar dates from basalts and the evolution of the southern Rio Grande rift: *Geological Society of America Bulletin*, v. 95, no. 1, p. 87–99.
- Seager, W.R., Hawley, J.W., Kottlowski, F.E., and Kelley, S.A., 1987, *Geology of east half of Las Cruces and northeast El Paso 1° x 2° sheets, New Mexico: New Mexico Bureau of Mines and Mineral Resources Geologic Map 57*, scale 1:125,000.
- Seager, W.R., Mack, G.H., and Lawton, T.F., 1997, Structural kinematics and depositional history of a Laramide uplift-basin pair in southern New Mexico: implications for development of intraforeland basins: *Geological Society of America Bulletin*, v. 109, p. 1389–1401.
- Soil Survey Staff, 1992, *Keys to soil taxonomy: U.S. Department of Agriculture*.
- Udden, J.A., 1914, Mechanical composition of clastic sediments: *Geological Society of America Bulletin*, v. 25, p. 655–744.
- Wentworth, C.K., 1922, A scale of grade and class terms for clastic sediments: *Journal of Geology*, v. 30, p. 377–392.

APPENDIX A

Detailed descriptions of lithologic units on the
Williamsburg NW 7.5-minute quadrangle

UNIT DESCRIPTIONS

The units described below were mapped using aerial photography coupled with field checks. Stereogrammetry software (Stereo Analyst for ArcGIS 10.1, an ERDAS extension, version 11.0.6) permitted accurate placement of geologic contacts. Grain sizes follow the Udden-Wentworth scale for clastic sediments (Udden, 1914; Wentworth, 1922) and are based on field estimates. The term “clast(s)” refers to the grain size fraction greater than 2 mm in diameter. Descriptions of bedding thickness follow Ingram (1954). Colors of sediment are based on visual comparison of dry samples to Munsell Soil Color Charts (Munsell Color, 2009). Soil horizon designations and descriptive terms follow those of Birkeland et al. (1991), Soil Survey Staff (1992), and Birkeland (1999). Stages of pedogenic calcium carbonate morphology follow those of Gile et al. (1966) and Birkeland (1999). Description of sedimentary and igneous rocks was based on inspection using a hand lens and, in some cases, a Bausch & Lomb StereoZoom 5 microscope.

Surface characteristics and relative landscape position were used in mapping middle Pleistocene to Holocene units. Surface processes dependent on age (e.g., desert pavement development, clast varnish, calcium carbonate accumulation, and eradication of original bar-and-swale topography) can be used to differentiate stream terrace, alluvial fan, and valley floor deposits. Younger deposits are generally inset below older deposits. However, erosion may create a young surface on top of an older deposit, so Quaternary deposits were field-checked to identify this relationship.

QUATERNARY

Anthropogenic, hillslope, and landslide units

- daf Disturbed or artificial fill (modern) – Sand and gravel that has been moved by humans to form earthen dams or levees, or has been removed for construction.
- Qca Colluvium and alluvium, undivided (Holocene to middle Pleistocene) – Poorly sorted gravel with subordinate silt and sand forming aprons at the base of high angle slopes. Gravel is typically angular to subangular (minor subrounded). Maximum thickness 6 m (20 ft).
- Qls Landslide deposit (late to middle Pleistocene?) – Unstratified/massive sand and gravel comprising translational slide material. Light yellowish brown to pale brown (2.5Y 6-7/3). Weakly consolidated. Very fine- to coarse-grained sand is very poorly to poorly sorted, angular to subrounded, and composed of approximately 85% lithic and 15% feldspar grains, with <2% clay films. Gravel is poorly sorted, angular to subrounded, and consists of 50-70% pebbles, 30-40% cobbles, and 10-20% boulders of Tdu, Tbal, and Tbau. One deposit is located on failure plane formed on weak volcanoclastic sand (Tds). Maximum thickness 8 m (26 ft) thick.

Valley-floor units dominated by modern and historical sediment (<50-600 yr old)

- Qam Modern alluvium (modern to ~50 years old) – Unconsolidated sandy gravel and gravelly sand underlying channels and forming transverse to longitudinal bars with 0.7-1.25 m (2.3-4 ft) of local relief. Thickness likely no more than 3 m (10 ft). Unit subdivided along two major drainages in quad:
 - Qamc Modern alluvium of Cuchillo Negro Creek – Sandy pebble-cobble gravel and gravelly sand. Unconsolidated and massive to trough cross-bedded to well-imbricated. Gravel is poorly to moderately sorted, subrounded to well-rounded, and consists of 60-90% pebbles, 10-40% cobbles, and up to 2% boulders. Clast lithologies are approximately 45% andesite+dacite, 30-35% Paleozoic carbonate and detrital sedimentary lithologies, 20% felsites (e.g., Tkn), and 5-10% chert and Tsml conglomerate. Sand is dark grayish brown (10YR 4/2), poorly sorted, subrounded to rounded, and

fine- to coarse-grained with approximately 55% lithic (volcanic), 25% feldspar, and 20% quartz grains. Lithic sand grains are somewhat less heterogeneous than Qamp.

- Qamp Modern alluvium of Palomas Creek – Sandy pebble-cobble-boulder gravel and gravelly sand; gravel is more common in longitudinal bars that commonly feature >50% pebbles. Unconsolidated and massive to rippled to well-imbricated. Gravel is very poorly to moderately sorted and rounded to well-rounded. Clast lithologies are approximately 40% andesite (e.g., Tba), 30% felsites (aphanitic flow-banded rhyolite and tuffs), 15-20% Tad, and 10-15% Tb and Paleozoic sedimentary lithologies. Sand is gray to grayish brown (10YR 5/1-2), moderately to well-sorted, subrounded to well-rounded, and fine- to medium-grained with approximately 40% lithic (volcanic+mafic+chert), 35% quartz, and 25% feldspar grains. Sand contains more mafic and chert grains than Qamc.
- Qamh Modern and historical alluvium, undivided (modern to ~600 years old) – Modern alluvium (Qam) and subordinate historical alluvium (Qah). See detailed descriptions of each individual unit.
- Qah Historical alluvium (~50 to ~600 years old) – Pebbly sand and sandy gravel in very thin to thick, tabular to lenticular beds underlying very low terraces. Unconsolidated, clast- to matrix-supported, and planar cross-stratified, horizontal-planar to ripple cross-laminated, or imbricated (gravel). Gravel is moderately to very well-sorted, subangular to subrounded, and consists of 85-90% pebbles, 5-10% cobbles, and <5% boulders. Common clast lithologies include basalt, dacite, and tuff. Sand consists of grayish brown to brown (10YR 5/2 to 6/3), moderately to very well-sorted, subangular to subrounded, fine to coarse grains composed of 50-60% lithics (volcanic, including mafic minerals), 20-30% feldspar, and up to 20% quartz. Retains bar-and-swale topography with up to 50 cm (20 in) of relief. Somewhat vegetated with no soil development and commonly mantled by 5-10 cm (2-4 in) of silt to fine sand derived from sheet flooding. Tread height up to 1.6 m (5.2 ft) above modern grade. Maximum thickness 3 m (10 ft). Unit subdivided along two major drainages in quad:
- Qahc Historical alluvium of Cuchillo Negro Creek – Sandy pebble-cobble gravel and clayey sand in thin to thick (3-60 cm), tabular to broadly lenticular beds. Unconsolidated, non- to weakly calcareous, clast-supported, and massive to well-imbricated and/or trough cross-stratified. May be horizontal-planar laminated in clayey sand beds. Gravel is poorly sorted, subrounded to well-rounded, and consists of 70-90% pebbles, 10-30% cobbles, and up to 3% boulders. Clast lithologies include approximately 45% intermediate volcanics (e.g., plagioclase-phyric andesite, Tba), 40% felsites (e.g., Tkn, flow-banded rhyolite), 10% Pa, and 5% Paleozoic carbonates. Finer-grained beds and matrix of gravel beds consist of brown (10YR 4/3), poorly sorted, subangular to rounded, very fine- to medium-grained sand composed of approximately 50% lithics (volcanic+mafic+Pa), 30% quartz, and 20% feldspar. Sandy beds typically thinner and more tabular than gravelly beds. Deposit is capped by an A horizon (<10 cm thick) and is moderately bioturbated by fine to very coarse roots. Tread height 1.4-1.6 m (4.6-5.2 ft) above modern grade.
- Qahp Historical alluvium of Palomas Creek – Gravelly sand and subordinate gravelly channel-fills in thin to medium (4-25 cm), lenticular beds. Deposit is sandier (fine- to medium-grained) in upper layers, except for upper 40 cm (16 in) of moderately calcareous, sandy silt. This upper interval may also contain 5-20% clay. Unconsolidated, weakly calcareous, internally ripple cross-laminated to planar or trough cross-stratified. Planar cross-bed foresets are up to 15 cm (6 in) thick. Gravel is imbricated, poorly sorted, rounded to well-rounded, and consists of 75-85% pebbles and 15-25% cobbles. Clast lithologies are dominated by Tb, Tad, various Eocene-Oligocene andesites, and Pa. Sand and gravel matrix is brown (10YR 4-5/3), well-sorted, subrounded to well-rounded, very fine- to fine-grained, and composed of approximately 45% lithics (volcanic+mafic), 30% quartz, and 25% feldspar. Little to no soil development observed. Bioturbated by very fine to medium roots and burrows. Tread height up to 1.7 m (5.6 ft) above modern grade.
- Qahm Historical and modern alluvium, undivided (modern to ~600 years old) – Historical alluvium (Qah) and subordinate modern alluvium (Qam). See detailed descriptions of each individual unit.
- Qahy Historical and younger alluvium, undivided (~50 years old to early Holocene) – Historical alluvium (Qah) and subordinate younger alluvium (Qay). See detailed descriptions of each individual unit.
- Qary Recent (historical + modern) and younger alluvium, undivided (modern to early Holocene) – Recent alluvium (Qah + Qam) and subordinate younger alluvium (Qay). See detailed descriptions of each individual unit.

Valley-floor units dominated by younger sediment (~600-11,000 yr old)

- Qay Younger alluvium (Holocene) – Sandy gravel in medium to thick (25-85 cm), tabular beds underlying low terraces. Unconsolidated, strongly calcareous, and massive to moderately imbricated. Gravel is poorly sorted, subangular to subrounded, and consists of 75-90% pebbles, 10-25% cobbles, and up to 5% boulders. Clast lithologies include Tertiary volcanic and Paleozoic sedimentary lithologies primarily reworked from QTpu and QTpuc. Matrix consists of dark yellowish brown (10YR 3/6), moderately sorted, subangular to rounded, very fine- to medium-grained sand composed of approximately 70% lithic (volcanic), 15% feldspar, and 15% quartz grains with up to 5% clay chips. Darker and browner than other valley floor units. Retains subdued bar-and-swale topography with less than 30 cm (12 in) of local relief. Dark A horizon is observed in upper 20 cm (8 in). No varnish observed on clasts at surface. Tread height 1.8-4 m (6-13 ft) above modern grade. Maximum thickness 4 m (13 ft).
- Qaym Younger and modern alluvium, undivided (modern to early Holocene) – Younger alluvium (Qay) and subordinate modern alluvium (Qam). See detailed descriptions of each individual unit.
- Qayh Younger and historical alluvium, undivided (~50 years old to early Holocene) – Younger alluvium (Qay) and subordinate historical alluvium (Qah). See detailed descriptions of each individual unit.
- Qayr Younger and recent (historical + modern) alluvium, undivided (modern to early Holocene) – Younger alluvium (Qay) and subordinate recent alluvium (Qah + Qam). See detailed descriptions of each individual unit.

Terrace deposits of Cuchillo Negro Creek

- Qtc Terrace deposit of Cuchillo Negro Creek (late to middle Pleistocene) – Imbricated, sandy gravel occurring in fill and strath terrace deposits with surfaces higher than those associated with Qay. Clast compositions are dominated by intermediate to felsic, Eocene-Oligocene volcanic lithologies derived from the Sierra Cuchillo to the west with subordinate Paleozoic sedimentary lithologies (especially Pa). Locally subdivided into four deposits:
- Qtc1 First or lowest terrace deposit of Cuchillo Negro Creek (late Pleistocene) – Sandy pebble-cobble-boulder gravel in medium to thick (20-65 cm), mostly tabular beds. Unconsolidated to weakly carbonate-cemented in places, clast-supported, and moderately well-imbricated. Gravel is very poorly to poorly sorted, subrounded to well-rounded, and consists of 40-60% pebbles, 30-40% cobbles, and 10-20% boulders. Clast lithologies include approximately 45% intermediate volcanics, 40% felsites, 10% Paleozoic sedimentary lithologies (including Pa), and 5% Tb. Clast imbrication is mostly SSE (140-180°). Matrix consists of yellowish brown (10YR 5/4), poorly to moderately sorted, subangular to rounded, very fine- to medium-grained sand composed of approximately 55% lithics (volcanic), 25% feldspar, and 20% quartz. Moderately bioturbated by fine to coarse roots. Stage I carbonate morphology observed. Varnish on 10-15% of clasts at surface. Tread is 5-11 m (16.5-36 ft) above modern grade. 1.7-3.8 m (5.6-12.5 ft) thick.
- Qtc2 Second or middle-lower terrace deposit of Cuchillo Negro Creek (late Pleistocene) – Sandy pebble-cobble gravel in medium to thick (20-50 cm), tabular beds. Unconsolidated, weakly calcareous, clast-supported, and well-imbricated. Gravel is poorly sorted, subrounded to well-rounded, and consists of 55-60% pebbles, 35-45% cobbles, and 0-5% boulders. Clast lithologies include approximately 60% intermediate volcanics, 30% felsites, and 10% Paleozoic sedimentary lithologies (including Pa) and Tb. Matrix consists of brown (7.5YR 4-5/4), poorly sorted, subrounded to well-rounded, very fine- to coarse-grained sand composed of 50% lithics (volcanics), 30% feldspar, and 10% quartz with 10-12% reddish clay chips. Lower 40 cm (16 in) moderately well-cemented by clay bridges. Stage I+ carbonate morphology in upper 50 cm (20 in) indicated by carbonate coats on 70-90% of clasts. Varnish on 55-70% of clasts at surface. Tread is 15-24 m (49-79 ft) above modern grade. 4-11 m (13-36 ft) thick.
- Qtc3 Third or middle-upper terrace deposit of Cuchillo Negro Creek (middle Pleistocene) – Sandy

pebble-cobble gravel in medium to thick (25-70 cm), tabular to lenticular beds. Weakly consolidated, moderately calcareous, clast-supported, and moderately well-imbricated to planar cross-stratified (foresets 25-40 cm thick). Gravel is poorly sorted, subrounded to well rounded, and consists of 55-65% pebbles and 35-45% cobbles of approximately 85% volcanic lithologies and 15% Paleozoic carbonates. Clast imbrication is NNE to ESE (030-110°). Matrix consists of reddish brown (5YR 5/4), poorly to moderately sorted, subangular to well-rounded, fine- to coarse-grained sand composed of approximately 60% lithics (volcanics), 20% quartz, and 20% feldspar. Soil development uncommon (likely eroded). Varnish on 40-45% of clasts at surface. Tread is 28-45 m (92-148 ft) above modern grade. 6-8 m (20-26 ft) thick.

- Qtc4 Fourth or upper terrace deposit of Cuchillo Negro Creek (middle Pleistocene) – Sandy pebble-cobble-boulder gravel in medium to thick (20-100 cm), broadly lenticular to tabular beds. Unconsolidated, non- to weakly calcareous, and imbricated to vaguely trough cross-stratified. Gravel is poorly sorted, subrounded to well-rounded, and consists of 50-85% pebbles, 15-50% cobbles, and 0-10% boulders. Clast lithologies include Tertiary volcanic and Paleozoic sedimentary lithologies exposed in the southern Sierra Cuchillo range. Clast imbrication is generally ENE to ESE (060-130°). Matrix consists of brown to strong brown (7.5YR 4/4 to 5/6), very poorly to moderately sorted, mostly rounded, very fine- to coarse-grained sand composed of 50-70% lithics (volcanic>>carbonate), 20-30% feldspar, and 10-20% quartz grains with up to 10% clay chips and films. Upper 1-1.5 m (3.3-5 ft) of deposit consists of gravelly sand. A 30 cm (12 in) thick zone of stage III carbonate morphology is observed in places. Varnish on 40-80% of clasts at surface. Tread is 54-67 m (177-220 ft) above modern grade. 3-11 m (10-36 ft) thick.

Terrace deposits of Palomas Creek

- Qtp Terrace deposit of Palomas Creek (late to middle Pleistocene) –Imbricated, sandy gravel occurring in fill and strath terrace deposits with surfaces higher than those associated with Qay. Clast compositions are dominated by Tad and other volcanic lithologies derived from the eastern Black Range and Garcia Peaks with subordinate Paleozoic sedimentary lithologies (especially Pa). Locally subdivided into four deposits:

Qtp1 First or lowest terrace deposit of Palomas Creek (late Pleistocene) – Sandy pebble-cobble-boulder gravel in medium to thick (20-60 cm), broadly lenticular beds. Weakly consolidated, weakly to moderately calcareous, clast-supported, and massive to well-imbricated to trough cross-stratified. Gravel is very poorly to poorly sorted, rounded to well rounded, and consists of 45-75% pebbles, 25-45% cobbles, and up to 15% boulders. Clast lithologies include approximately 40% Tad, 30% andesite (e.g., Tba), 20% felsites (e.g., Tkn), and 10% Tb and Paleozoic sedimentary lithologies. Matrix consists of dark brown (7.5YR 3/4) to yellowish brown (10YR 5/4), poorly to moderately sorted, rounded to well-rounded, very fine- to medium-grained sand composed of approximately 55% lithics (volcanic), 20% feldspar, and 20% quartz; ~5% of grains are fragments of Fe-Mn oxide minerals. Occasionally, beds have up to 35% clasts with partial or whole Mn-oxide coats. Stage I+ carbonate morphology observed in upper 1.3 m (4.3 ft) where 45% of clasts have partial carbonate coats. Varnish on 10-15% of clasts at surface. Tread is 9-13 m (30-43 ft) above modern grade. 3-7 m (10-23 ft) thick.

Qtp2 Second or middle-lower terrace deposit of Palomas Creek (late Pleistocene) – Sandy pebble-cobble-boulder gravel in thin to thick (8-90 cm), tabular beds. Occasional sand lenses. Unconsolidated, non- to slightly calcareous, clast-supported, and well-imbricated. Gravel is poorly sorted, subrounded to well-rounded, and consists of 60-80% pebbles, 30-45% cobbles, and ≤15% boulders. Clast lithologies include 10-20% basalt or basaltic andesite (Tb + Tba), 5-15% crystal- or lithic-rich tuff (e.g., Tkn, Tsl), up to 10% Paleozoic siltstone and chert, and <5% hornblende porphyry. Matrix consists of brown (7.5YR 4/3), poorly to moderately sorted, subangular to rounded, fine- to coarse-grained sand composed of approximately 50% lithics (volcanic+ chert), 30% feldspar, and 20% quartz with up to 5% clay films. Tread is 14-22 m (46-72 ft) above modern grade. 2-5 m (7-16 ft) thick.

Qtp3 Third or middle-upper terrace deposit of Palomas Creek (middle Pleistocene) – Sandy pebble-cobble-boulder gravel in medium to thick (20-90 cm), broadly lenticular beds. Unconsolidated, non- to weakly carbonate-cemented, clast-supported, and well-imbricated with subordinate broad cross-

stratification. Gravel is poorly sorted, subrounded to rounded, and consists of 50-80% pebbles, 15-40% cobbles, and 5-15% boulders. Clast lithologies include up to 55% basalt or basaltic andesite (Tb + Tba) with 35% total Tkn, aphanitic rhyolite, and Tad. Matrix consists of brown to light brown (7.5YR 5-6/3), poorly to moderately sorted, subangular to rounded, very fine- to medium-grained sand composed of approximately 60% lithics (volcanic), 25% feldspar, and 15% quartz. Deposit exhibits stage I+ carbonate morphology with 50% of clast surfaces coated up to 80% by carbonate (including rare rinds). Varnish on 40-45% of clasts at surface. Tread is 27-40 m (89-131 ft) above modern grade. 2-7 m (7-23 ft) thick.

- Qtp4 Fourth or upper terrace deposit of Palomas Creek (middle Pleistocene) – Sandy pebble-cobble-boulder gravel with brown (7.5YR 4-5/3) matrix. Varnish on 55-75% of clasts at surface. Soil development uncommon (likely eroded). Tread is 48-53 m (157-174 ft) above modern grade. 3-7 m (10-23 ft) thick.

Terrace deposits of other streams

- Qtg Tributary terrace deposit (late to middle Pleistocene) – Relatively thin sandy gravel underlying terraces alongside drainages other than Cuchillo Negro and Palomas Creeks. Surfaces typically feature weakly to moderately varnished clasts and topsoils with weak calcium carbonate accumulation (stage I to II carbonate morphology). Locally subdivided into four deposits:

- Qtg1 First or lowest tributary terrace deposit of other streams (late Pleistocene) – Sandy pebble-cobble gravel in thick (40-50 cm), lenticular beds. Unconsolidated, very weakly calcareous, clast-supported, and well-imbricated. Gravel is poorly sorted, subangular to rounded, and consists of 50-60% pebbles, 40-50% cobbles, and 0-10% boulders of Tb, Tad, and/or felsites. Matrix consists of brown (7.5YR 4/4), moderately sorted, subangular to subrounded silt to fine-grained sand with approximately 50% lithics (volcanic+mafic), 30% quartz, and 20% feldspar. Tread is 5-8 m (16-26 ft) above modern grade. 3-4 m (10-13 ft) thick.

- Qtg2 Second or middle-lower tributary terrace deposit of other streams (late Pleistocene) – Sandy pebble-cobble gravel in thin to very thick, tabular to lenticular beds. Unconsolidated and massive to imbricated. Gravel is poorly to moderately sorted, subangular to subrounded, and consists of 70-75% pebbles, 25-30% cobbles, and up to 2% boulders. At least 80% of clast lithologies are intermediate to felsic volcanics. Matrix consists of brown (7.5YR 4/4), poorly sorted, subangular to subrounded silt to medium-grained sand with approximately 40% quartz and subequal percentages of feldspar and lithics. Surface features very weak desert pavement. Tread is 10-23 m (33-75 ft) above modern grade. 3-9 m (10-30 ft) thick.

- Qtg3 Third or middle-upper tributary terrace deposit of other streams (middle Pleistocene) – Sandy gravel in medium to thick, tabular to lenticular beds. Unconsolidated and well-imbricated. Tread is 26-30 m (85-98 ft) above modern grade. 5-6 m (16-20 ft) thick.

- Qtg4 Fourth or upper tributary terrace deposit of other streams (middle Pleistocene) – Sandy gravel in medium to thick, tabular to lenticular beds. Unconsolidated and well-imbricated. Tread is 34-38 m (112-125 ft) above modern grade. 3-7 m (10-23 ft) thick.

Alluvial-fan units dominated by modern and historical sediment (<50-600 yr old)

- Qfam Modern fan alluvium (modern to ~50 years old) – Sandy gravel in channels and low-lying bars of modern fan surfaces. Unconsolidated and commonly imbricated. Gravel is very poorly sorted, angular to subrounded,

and consists of 40-55% pebbles, 40-50% cobbles, and 10-20% boulders. Matrix consists of dark brown (10YR 3/3), very poorly sorted, angular to subrounded, fine- to very coarse-grained sand composed of approximately 55% lithics (volcanic+chert), 35% quartz, and 10% feldspar. Generally inset against Qfah or Qfay. Maximum thickness 3 m (10 ft).

- Qfah Historical fan alluvium (~50 to ~600 years old) – Sandy gravel and pebbly sand in thin to medium (9-20 cm), tabular beds underlying alluvial fans graded to the surface of Qfah. Unconsolidated, slightly calcareous, and mostly clast-supported. Gravel is very poorly to poorly sorted, angular to subrounded, and composed of 60-80% pebbles (up to 3 cm across) and 20-40% cobbles. Matrix consists of brown (7.5YR 4/4), poorly sorted, subangular to subrounded, very fine- to medium-grained sand composed of approximately 50% lithics, 40% quartz, and 10% feldspar grains. Deposit features upper A horizon up to 11 cm (4.3 in) thick; otherwise, little to no soil/carbonate development. Bioturbated by medium to very coarse roots. 0.6 to perhaps 3 m (2-10 ft) thick.
- Qfahm Historical and modern fan alluvium, undivided (modern to ~600 years old) – Historical alluvium (Qfah) and subordinate modern alluvium (Qfam) deposited on alluvial fans. See detailed descriptions of each individual unit.
- Qfahy Historical and younger fan alluvium, undivided (~50 years old to early Holocene) – Historical alluvium (Qfah) and subordinate younger alluvium (Qfay) deposited on alluvial fans. See detailed descriptions of each individual unit.
- Qfary Recent (historical + modern) and younger fan alluvium, undivided (modern to early Holocene) – Recent fan alluvium (Qfah + Qfam) and subordinate younger fan alluvium (Qfay). See detailed descriptions of each individual unit.

Alluvial-fan units dominated by younger sediment (~600-11,000 yr old)

- Qfay Younger fan alluvium (Holocene) – Pebbly sand and gravel in thin to thick, tabular to lenticular or broadly wavy beds underlying alluvial fans graded to the surface of Qfay. Loose, clast- to matrix-supported, and massive to weakly imbricated. Gravel is poorly sorted, angular to subrounded, and consists of 85% pebbles, 10-15% cobbles, and 0-5% boulders. Clast lithologies commonly include Tb, Tba, and rhyolite and vitric tuff reworked from QTp and Tsm. Clasts may be in open-framework texture with weak clay films. Matrix is a brown (10YR 4-5/3), very poorly to moderately sorted, subangular to rounded volcanic litharenite. Deposit is capped by topsoil with an A horizon 8-12 cm (3-5 in) thick. Stage I+ carbonate morphology occasionally observed. Base not observed in thickest deposits; perhaps up to 3 m (10 ft) maximum thickness.
- Qfaym Younger and modern fan alluvium, undivided (modern to early Holocene) – Younger alluvium (Qfay) and subordinate modern alluvium (Qfam) deposited on alluvial fans. See detailed descriptions of each individual unit.
- Qfahy Younger and historical fan alluvium, undivided (~50 years old to early Holocene) – Younger alluvium (Qfay) and subordinate historical alluvium (Qfah) deposited on alluvial fans. See detailed descriptions of each individual unit.
- Qfary Younger and recent (historical + modern) fan alluvium, undivided (modern to early Holocene) – Younger fan alluvium (Qfay) and subordinate recent fan alluvium (Qfah + Qfam). See detailed descriptions of each individual unit.

Older alluvial fans graded to stream terraces (late to middle Pleistocene)

- Qf1 Alluvial-fan deposits graded to lower terraces (late Pleistocene) – Sandy pebble-cobble gravel in thin to thick, tabular beds. Light brown to light yellowish brown (7.5-10YR 6/4) matrix. Unconsolidated, strongly

calcareous, clast- to matrix-supported, and massive to weakly imbricated. Stage I carbonate morphology in upper 60 cm (24 cm) of deposit. 3-4 m (10-13 ft) thick.

- Qf2 Alluvial-fan deposits graded to middle-lower terraces (late Pleistocene) – Sandy pebble-cobble gravel in medium to thick (30-100 cm), tabular beds. Unconsolidated, calcareous, and weakly imbricated. Gravel is poorly sorted, subangular to subrounded, and consists of 80-90% pebbles, 10-20% cobbles, and up to 1% boulders. Clast lithologies include Tertiary volcanics and Paleozoic sedimentary lithologies reworked from QTp. Lags and lenses of pebble and pebble-cobble gravel up to 20 cm (8 in) thick are observed in places. Matrix is reddish brown (5YR 4/4) to brown (7.5YR 5/4) and consists of sandy silt; approximately 60% of medium to coarse grains in matrix are composed of volcanic lithologies. Little to no carbonate development observed in deposit. Varnish on 60-70% of clasts at the surface. Maximum thickness 4 m (13 ft).
- Qf3 Alluvial-fan deposits graded to middle-upper terraces (middle Pleistocene) – Sandy pebble-cobble gravel in medium to very thick, tabular beds. Pinkish gray to light brown (7.5YR 6/2-3) matrix. Weakly consolidated, matrix-supported, and massive to weakly imbricated. Features stage II-III carbonate morphology in upper 70 cm (28 cm). Maximum thickness 5 m (16 ft).

QUATERNARY-TERTIARY

Basin-fill units

- QTp Palomas Formation of the Santa Fe Group (early Pleistocene to latest Miocene) – Sandy gravel/conglomerate, pebbly sand/sandstone, and subordinate sandy silt and mud in thin to thick, mostly tabular beds. In the Williamsburg NW quadrangle, this unit was deposited in proximal to medial positions of coalesced alluvial fans (bajadas) in the western Palomas basin. The term “Palomas” was first applied to outcrops of upper Santa Fe Group basin-fill by Gordon and Graton (1907), Gordon (1910), and Harley (1934). Lozinsky and Hawley (1986) formally defined the Palomas Formation and additional detailed descriptions of the unit are found in this work and Lozinsky (1986). Fossil data (summarized by Morgan and Lucas, 2012), basalt radiometric dates (Bachman and Mehnert, 1978; Seager et al., 1984; this study), and magnetostratigraphic data (Repenning and May, 1986; Mack et al., 1993; 1998; Seager and Mack, 2003) indicate an age range of approximately 5.0-0.8 Ma for the Palomas Formation, with a maximum age of approximately 5.5 Ma. The surface soil is marked by a petrocalcic horizon that is up to 2 m (6.6 ft) thick and commonly exhibits a stage IV carbonate morphology. However, this soil is generally eroded in the westernmost exposures of Palomas Formation beds in the quadrangle. More information on this petrocalcic horizon and the constructional surface developed on the Palomas Formation, the Cuchillo surface, can be found in McCraw and Love (2012). The lower part of the unit is intercalated with Palomas Creek basalt flows dated at 5.54-4.57 Ma ($^{40}\text{Ar}/^{39}\text{Ar}$). Maximum thickness 257 m (843 ft). Locally subdivided into five units:
- QTpuc Upper, coarse-grained piedmont facies of the Palomas Formation (early Pleistocene) – Sandy pebble-cobble gravel/conglomerate in medium to very thick (20-120 cm), tabular to lenticular beds. Clast-supported and massive to imbricated. Gravel is very poorly to poorly sorted, subangular to subrounded, and consists of 45-60% pebbles, 40-55% cobbles, and 0-5% boulders. Common clast lithologies include 30-50% Tba, 15-20% Tkn, and 5-20% Tb; unit also contains a markedly higher proportion (up to 10%) of Paleozoic carbonate clasts than other QTp facies. Matrix consists of yellowish red (5YR 5/6), moderately sorted, angular to subangular, fine- to coarse-grained sand composed of 50-60% lithics (volcanic), 20-25% quartz, and 20-25% feldspar with up to 5% clay films. Rare pebbly sand lenses may be ripple cross-laminated to trough cross-stratified. Generally unconsolidated but commonly features 1-1.5 m (3.3-4.9 ft) thick calcrete (stage IV carbonate morphology) in upper part; this calcrete is not found in western exposures of the unit that underlie erosional surfaces. Basal contact is typically scoured, forming up to 1.5 m (4.9 ft) of relief. 12-52 m (40-172 ft) thick.
- QTpu Upper piedmont facies of the Palomas Formation (early Pleistocene) – Sand, silt, and mud interbedded with subordinate sandy pebble-cobble gravel in medium to thick (12-100 cm), tabular to broadly lenticular beds. Mostly unconsolidated and non- to moderately calcareous. Sandy beds may be planar cross-stratified with foresets 15-30 cm (6-12 in) thick. Gravels are commonly imbricated and

silt/mud is massive. Gravel occurs in channel-fills constituting <40% of deposit and is composed of poorly sorted, subrounded to well-rounded pebbles (60-80%), cobbles (20-40%), and boulders (0-8%). Clast lithologies include 40-50% intermediate volcanics (including up to 30% Tba), up to 40% felsites (Tkn, flow-banded rhyolite), up to 10% Tad, and <5% each of Tb and Paleozoic sedimentary lithologies. Gravel matrix is reddish brown (5YR 4-5/4), very poorly to poorly sorted, subangular to subrounded, very fine- to coarse-grained sand composed of 55-70% lithics (volcanic+chert), 10-15% feldspar, and 5-10% quartz. Matrix may contain 10-25% reddish clay chips and films. Silt and mud beds are typically light red (2.5YR 6/6) to reddish brown (5YR 5/4), massive, and may feature 3-8% subrounded pebbles representing hyperconcentrated flow deposits (Seager and Mack, 2003). Elsewhere, sparse pebbles mark lags in otherwise uniformly fine-grained deposits. Buried paleosols are occasionally observed throughout unit and marked by the presence of clay argillans and carbonate masses; these soils feature Bw (cambic) to Btk or Bk horizons. 20-60 m (67-197 ft) thick; basin-ward (i.e. eastward) thickening is particularly apparent along Cuchillo Negro Creek.

- QTpm Middle piedmont facies of the Palomas Formation (early Pleistocene to late Pliocene) – Pebbly silt and mud to very fine- or fine-grained sand in eastern part of quad. Gravels constitute up to 15% of unit. Light brown to pink (7.5YR 6-7/3). Mostly unconsolidated and massive with common paleosols exhibiting stage II-III carbonate morphology (pervasive carbonate coats on clasts, abundant carbonate nodules). Interfingers with QTpt near or east of Palomas Creek. 20-81 m (66-265 ft) thick.
- QTpt Transitional piedmont facies of the Palomas Formation (early Pleistocene to late Pliocene) – Pebbly sand and sandy pebble gravel in thin to thick (5-75 cm), mostly tabular beds. Weakly to moderately consolidated, weakly to strongly cemented by calcite (latter forms prominent ledges), clast- to matrix-supported, and massive to planar cross-stratified (foresets up to 20 cm thick) to well-imbricated. Gravel is poorly to moderately sorted, subangular to subrounded, and consists of 50-95% pebbles and 5-40% cobbles. Clast lithologies include up to 55% Tad, 15-35% intermediate volcanics (e.g., Tba), up to 25% felsites, and up to 10% Paleozoic sedimentary lithologies (mostly Pa). Matrix is reddish brown (5YR 5/4) to brown (7.5YR 4-5/3), poorly sorted, subangular to subrounded, fine- to medium-grained sand composed of 55-75% lithics (volcanic+chert>>carbonate), 15-30% feldspar, and 10-25% quartz with almost no clay. Paleosols are less common than in other QTp units. Rare, lenticular to draped, carbonate-cemented sand bodies are observed. Maximum thickness 43 m (142 ft).
- QTplc Lower, coarse-grained piedmont facies of the Palomas Formation (late or middle to early Pliocene) – Pebbly sand/sandstone and sandy pebble-cobble gravel/conglomerate in the western and northern parts of the quadrangle. Thin- to thick-bedded (8-80 cm) and tabular to lenticular. Loosely to moderately consolidated, moderately silica- to carbonate-cemented, clast- to matrix-supported or open-framework, and massive to imbricated to trough or planar cross-stratified (foresets up to 15 cm thick). Horizontal-planar lamination is rarely observed. Gravel is poorly to moderately sorted, angular to subrounded, and consists of 45-90% pebbles and 10-50% cobbles; up to 20% boulders are found in rare beds. Clast lithologies include Tba, equigranular plagioclase-phyric andesite, flow-banded rhyolite, and reddish tuff. Matrix is yellowish brown (10YR 4/5) to light brownish gray or brownish gray (10YR 6/2-3), poorly sorted, subangular to rounded, fine- to coarse-grained sand composed of 25-70% lithics (volcanic), 10-40% quartz, and 20-35% feldspar. Maximum thickness 73 m (240 ft).

TERTIARY

Santa Fe Group basin-fill predating the Palomas Formation

Tsml Lower-middle Santa Fe Group, undivided (late to early Miocene) – Pebbly sandstone and conglomerate in thin to medium (minor thick), tabular to lenticular beds. Moderately consolidated (silica or calcite cementation) and massive to imbricated or cross-stratified; minor horizontal lamination in finer beds. Occasional open-framework texture in gravels. Gravel is poorly to well-sorted, subangular to subrounded, and consists of pebbles with subordinate cobbles. Clast lithologies dominated by Tba and felsites, with no Tb and only trace Paleozoic sedimentary lithologies observed. Matrix is yellowish red (5YR 5-6/6) to light brown (7.5YR 6/4), moderately sorted, subangular to subrounded, very fine- to medium-grained sand. Likely correlative, in part, to the Rincon Valley Formation of Seager et al. (1971). Maximum thickness at least 500 m (1640 ft) toward basin center.

Intrusive units

- Ti Undivided intrusive lithologies (Eocene to Oligocene) – Dikes, sills, small stocks, and plugs composed of varying mafic to felsic lithologies. Commonly form prominent ledges or buttes.
- Tia Andesitic dike (middle Eocene) – Light gray, weathering orange-tan, fine- to medium-grained, intrusive andesite forming dikes up to 30 m (98 ft) wide. Phenocrysts include 3-14% plagioclase (0.5-2 mm, subhedral; roughly 10% altered to clay), 4-9% hornblende (1-2.5 mm, euhedral needles), and trace to 2% pyroxene (1-2 mm, anhedral; typically altered to clay). Chilled margins are 1.5-2.5 m (5-8 ft) wide and contain up to 11% phenocrysts.
- Tad Andesite-quartz diorite stock (middle Eocene) – Light gray (N 7/), weathering gray to brown (7.5YR 5/1-2), porphyritic, fine- to coarse-grained, intrusive andesite to quartz diorite. Dense. Phenocrysts include 8-10% hornblende (1.5-4 mm, euhedral), 5% biotite (1-2 mm, subhedral to euhedral), trace to 3% plagioclase (0.5-2 mm, subhedral), and trace to 2% quartz (up to 1.5 mm, anhedral). Rare biotite phenocrysts overprint hornblende crystals. Forms main body of Garcia Peaks stock. An $^{40}\text{Ar}/^{39}\text{Ar}$ -dated sample returned an age of 40.35 +/- 0.05 Ma. Equivalent to units Td and Tqd of Mayer (1987). Thickness unknown.

Volcanic and volcanoclastic units

- Tb Basalt flows (early Pliocene to latest Miocene) – Dark gray (N 4/), weathering gray to grayish brown (10YR 5/1-2), aphanitic to aphanitic-porphyritic, very fine- to medium-grained basalt. Dense to somewhat vesicular or scoriaceous; scoria is most common in the lower and/or upper 0.3-0.5 m (1-1.6 ft) of a given flow. Phenocrysts include 2-5% pyroxene (up to 1 mm, anhedral) and 2-3% olivine (1-2 mm, anhedral; commonly weathered to a dull, greenish yellow mineral that may be iddingsite); may contain disseminated magnetite. Features trace to 1% xenoliths up to 3 cm (1.2 in) across of dark, lustrous material with common chlorite alteration. Abundant amygdules filled by calcite, silica, and/or zeolites. The lowermost flow of the Palomas Creek basalts was dated at 4.57 +/- 0.02 Ma; a separate flow along Salado Creek was dated at 5.54 +/- 0.03 Ma (both ages $^{40}\text{Ar}/^{39}\text{Ar}$). Forms prominent ledges. Flow packages are 12-20 m (39-66 ft) thick.
- Tba Basaltic andesite (late Oligocene?) – Aphanitic to aphanitic-porphyritic basaltic andesite; observed phenocrysts are fine-grained. Likely correlates to unit Tba2 of Jochems et al. (2014) in the Hillsboro quadrangle and Ta units of Jahns et al. (2006) in the Chise quadrangle. Subdivided into two units:
- Tbau Upper basaltic andesite – Very dark gray to gray (N 3-5/), weathering brown to grayish brown (10YR 4/3 to 6/2). Dense/non-vesicular and occasionally foliated (flow layering). Phenocrysts include 2-4% pyroxene (up to 1.5 mm, anhedral) and trace to 2% olivine (up to 1 mm, anhedral). Contains trace glass and disseminated magnetite. Correlates to unit Tyaf of Heyl et al. (1983). 10-20 m (33-66 ft) thick.

- Tbal Lower basaltic andesite – Black (10YR 2/1) to very dark gray or dark gray (10YR-2.5Y 3-4/1), weathering grayish brown (10YR 4-5/2) to gray (2.5Y 6/1). Typically vesicular and thinly foliated (flow layering). Phenocrysts include trace to 2% pyroxene (up to 1.5 mm, anhedral; typically unaltered) and trace olivine and plagioclase set in a slightly glassy groundmass. Up to 5% amygdules filled by calcite or silica. Correlates to unit Tb of Heyl et al. (1983). Forms ledges and moderate to steep rubbly slopes. 32-57 m (105-187 ft) thick.
- Td Dacitic lava flows and tuffs (late Oligocene?) – Aphanitic to porphyritic, fine- to medium-grained, dacitic flows, tuffs, tuff breccia, and minor interbedded volcanoclastic sediment. Correlates to Td units of Jahns et al. (2006) in the Chise quadrangle. Includes four subunits:
- Tdu Upper dacitic tuff and tuff breccia, with subordinate flows – Weak red (10R 4/4) to very dark gray (5YR 3/1), weathering reddish brown (2.5YR 4-5/4) or dark reddish gray (5YR 4/2). Dense to vesicular and porphyritic. Phenocrysts include 2-16% plagioclase (1-4 mm, anhedral to euhedral laths; common internal fractures), 1% quartz (up to 1 mm, anhedral), and trace amounts of biotite, sanidine, and pyroxene (0.5-2 mm, anhedral to subhedral). May be hypocrySTALLINE with glassy groundmass. Tuff and tuff breccia contain 10-20% fragments of pumice. Non- to weakly welded. Forms prominent ledges underlying higher ridges. 18-25 m (59-82 ft) thick.
- Tdv Vitrophyre – Black (N 2.5/), weathering dark grayish brown to grayish brown (10YR 4-5/2), aphanitic-porphyritic, fine- to medium-grained vitrophyre at base of Tdu. Phenocrysts include 3-6% plagioclase (up to 2 mm, anhedral to euhedral laths) set in a glassy groundmass. Contains deformed xenoliths of dusky red (10R 3/3), aphanitic lava. Forms prominent dark ledge or steep rubbly slopes. 2-11 m (7-36 ft) thick.
- Tds Volcanoclastic sand – Siltstone to very fine-grained sandstone in thin beds. Light grayish olive (10Y 6/2) and non-calcareous. Exhibits planar cross-stratification with foresets 15-20 cm (6-8 in) thick. Fills paleovalleys cut into Tdl. Maximum thickness 20 m (66 ft).
- Tdl Lower dacitic flows – Dark gray (7.5YR 4/1), weathering brown (7.5YR 4/2), vesicular and aphanitic-porphyritic. Phenocrysts include 2-4% plagioclase (1-3 mm, anhedral to euhedral laths), 2% hornblende (1.5-2 mm, anhedral to subhedral), 1-2% biotite (up to 1 mm, euhedral), and trace pyroxene (up to 1 mm, anhedral; coalescent with plagioclase). Contains 5-10% amygdules filled by calcite or silica. Forms small ledges. 15 m (49 ft) thick.
- Tks Kneeling Nun and Sugarlump Tuffs, undivided (late Eocene) – Kneeling Nun (Tkn) and Sugarlump (Tsl) tuffs mapped by vantage reconnaissance and air photo interpretation due to land access restrictions. See detailed descriptions of each individual unit.
- Tkn Kneeling Nun Tuff (late Eocene) – Pinkish gray (5YR 6/2), weathering brown (7.5YR 4-5/3), non-welded, slightly vesicular, porphyritic, fine- to medium-grained rhyolitic tuff. Phenocrysts include 12-15% sanidine (1-4 mm, subhedral to euhedral; chatoyant), 7-10% quartz (up to 2 mm, anhedral; commonly shattered), and trace to 2% biotite (0.5-2.5 mm, subhedral to euhedral). Contains 1-2% lithic fragments and pumice 0.5-1.3 cm (0.2-0.5 in) across. ⁴⁰Ar/³⁹Ar-dated at 35.34 +/- 0.10 Ma (McIntosh et al., 1991). 12-18 m (39-59 ft) thick.
- Tsl Sugarlump Tuff (late Eocene) – White (N 8.5-9/), weathering grayish brown (10YR 5/2), non-welded, aphanitic-porphyritic, fine- to medium-grained lithic tuff. Phenocrysts include 1-6% biotite (up to 2 mm, subhedral to euhedral; coppery luster) and trace to 2% hornblende (up to 1.5 mm; subhedral to euhedral). Contains 7-8% andesitic and 5-8% pumice fragments 2-7 and 0.4-1 cm (0.8-2.8 and 0.2-0.4 in) across, respectively. ⁴⁰Ar/³⁹Ar-dated at 35.63 +/- 0.15 Ma (McIntosh et al., 1991). Underlies low-lying ridges and valley floors with gentle topographic relief. Maximum thickness 33 m (109 ft).
- Trp Rubio Peak Formation (late to middle Eocene) – Laharic breccia, conglomerate, and tuffaceous sandstone in thin to very thick beds. Minor laminated mudstone. Variable color, including light reddish brown (2.5YR 6/3) to reddish yellow (7.5YR 6-7/6) to dark gray (2.5Y 4/1). Weakly to strongly consolidated, commonly silica-cemented/rarely calcareous, clast- to matrix-supported, and massive to rarely imbricated; mudstone may be laminated. Breccia and conglomerate clasts are very poorly to poorly sorted, angular to subrounded, and consist of 15-70% cobbles, 10-60% pebbles, 30-50% granules, and <5-30% boulders. Common clast lithologies are dacite and plagioclase-phyric andesite with minor pumice and lithic tuff; boulders of the latter form erosion-resistant pedestals in places. Matrix consists of poorly to moderately sorted, subangular to

subrounded silt to coarse-grained sand composed of approximately 40% feldspar (dominantly plagioclase), 15-40% lithics (including biotite+hornblende), and 20% quartz. Volcaniclastic cobble conglomerate and tuffaceous sandstone form the upper 40 m (130 ft) of the formation. Maximum thickness at least 595 m (1952 ft). Frequently interbedded with andesite:

Trpa Andesitic flows of the Rubio Peak Formation – Light gray, weathering buff, porphyritic, fine- to medium-grained, equigranular andesite. Phenocrysts include 10-12% plagioclase (1-3 mm, subhedral laths) and 5-7% hornblende (1-2 mm, euhedral). Typically around 4 m (13 ft) thick.

PALEOZOIC

- Pa Abo Formation (Wolfcampian) – Sandstone and siltstone in thin beds. Red to yellow where altered. Rippled to cross-stratified. 84 m (276 ft) thick [Description modified from Mayer, 1987].
- Pb Bar-B Formation (Desmoinesian to Virgilian) – Limestone and mudstone with subordinate shale and conglomerate. Limestone is typically thin-bedded and nodular with brachiopods, bryozoans, crinoids, and gastropods. Mudstone is red, calcareous, and interbeds with chert to quartz-rich pebble conglomerate in the upper part of the unit. 116 m (381 ft) thick [Description modified from Mayer, 1987].
- Pn Nakaye Formation (Atokan to Desmoinesian) – Grainstone to micritic wackestone and packstone. Lacy to globular chert occurs in micritic beds, whereas chert lenses/beds and nodules occur in grainstone and packstone. Fossils include horn corals, forams, crinoids, brachiopods, and bryozoans. 105 m (345 ft) thick [Description modified from Mayer, 1987]. Cross section only.
- Pr Red House Formation (Morrowan to Atokan) – Shale and subordinate limestone, siltstone, and conglomerate. Shale is black, red, or green, and fissile. Limestone features lacy chert near top of unit and contains forams and phylloid algae among other fossils. Conglomerate is cross-stratified and quartzose, and occurs in the upper part of the unit. 151 m (494 ft) thick [Description modified from Mayer, 1987]. Cross section only.

APPENDIX B

Clast-count data from the Williamsburg NW 7.5-minute quadrangle

This appendix contains tabulated clast-count data (lithology type and mean diameter, except where noted) from several geologic units exposed in the Williamsburg NW quadrangle. These units include the upper coarse piedmont facies of the Palomas Formation, the lower coarse piedmont facies of the Palomas Formation, the middle-lower Santa Fe Group, and the Rubio Peak Formation. Location coordinates for all counts are given in NAD83 UTM zone 13S.

TABLE B.1 CLAST TYPE AND DIAMETER (cm) FOR UNIT QT_{puc} (WAYPOINT 131022_4)

Date 10/22/13 n = 50
 UTM Location 3669019N, 273949E

	Crystal-poor felsic volcanics	Tuffs, undivided	Kneeling Nun tuff	Crystal-poor intermediate volcanics	Crystal-rich intermediate volcanics	Abo Formation	Sandstone and siltstone, undivided	Basalt
	2	3	1.5	5	5	4	3.5	4
	3	1	7.5	3.5	2	4.5	4	1
	2	6	3	1	3.5	3	1.5	2.5
	3	5	6	5	3.5			6
	1.5	2		4.5	2			3
	5	3.5		3	4.5			
		5		2	3			
				6	2			
				2	1.5			
				3	1.5			
				2.5	3.5			
mean diameter (cm)	2.8	3.6	4.5	3.4	2.9	3.8	3.0	3.3
n	6	7	4	11	11	3	3	5
% total	12	14	8	22	22	6	6	10

TABLE B.2 CLAST TYPE AND DIAMETER (cm) FOR UNIT QT_{plc} (WAYPOINT 140225_1-3b)

Date 02/25/14 n = 50
 UTM Location 3674753N, 271519E

	Crystal-poor felsic volcanics	Tuffs, undivided	Crystal-poor intermediate volcanics	Crystal-rich intermediate volcanics	Diorite porphyry	Sandstone and siltstone, undivided	Chert and jasperoid	Basalt
	4	4.5	4	2	0.5	1.5	4	8.5
	6	2		2	2.5	4.5	2	2
	4.5	11		2	4	1		4
		1		4.5	2.5			4.5
		2		3	7			2
		3		4.5				2
		6		5				3.5
		6		1.5				
		2		5				
		1		2.5				
		1.5		4.5				
		3.5		7.5				
				1				
				3				
				2				
				2.5				
				5				
mean diameter (cm)	4.8	3.6	4.0	3.4	3.3	2.3	3.0	3.8
n	3	12	1	17	5	3	2	7
% total	6	24	2	34	10	6	4	14

TABLE B.3 CLAST TYPE AND DIAMETER (cm) FOR UNIT QTplc (WAYPOINT 150305_3f)

n =27

Date 03/05/15

UTM Location 3681624N, 270528E

	Crystal-poor felsic volcanics	Tuffs, undivided	Crystal-poor intermediate volcanics	Crystal-rich intermediate volcanics	Diorite porphyry	Abo Formation	Sandstone and siltstone, undivided	Basalt	Other
	2	2	5	9 5 4 2 3 6 7 8 9 6 2	3 4	6		9 4.5 5 2 5 7 4.5 3.5	3 4
mean diameter (cm)	2.0	2.0	5.0	5.5	3.5	6.0		5.1	3.5
n	1	1	1	11	2	1	0	8	2
% total	4	4	4	41	7	4	0	30	7

TABLE B.4 CLAST TYPE AND DIAMETER (cm) FOR UNIT QTplc (WAYPOINT 160204_D)

n =100

Date 02/04/16

UTM Location 3681565N, 271094E

	Felsic volcanics	Tuffs, undivided	Kneeling Nun tuff	Vicks Peak tuff	Intermediate volcanics	Diorite porphyry	Paleozoic carbonates	Abo Formation	Chert and jasperoid	Basalt	Other
n	12	13	4		48	11	2	4	1	1	4
% total	12	13	4		48	11	2	4	1	1	4

*Clast dimensions measured but not recorded by specific lithology.

TABLE B.5 CLAST TYPE AND DIAMETER (cm) FOR UNIT QTplc (WAYPOINT 180816_3b)

n =96

Date 08/16/18

UTM Location 3669527N, 273411E

Crystal-poor felsic volcanics	Crystal-rich felsic volcanics	Tuffs, undivided	Kneeling Nun tuff	Crystal-poor intermediate volcanics	Crystal-rich intermediate volcanics	Diorite porphyry	Paleozoic carbonates	Sandstone and siltstone, undivided	Chert and jasperoid	Basalt	Other
2	5.5	2	6	4	3	2.5	3	3.5	6	5	6
3.5	4	1.5	3	2.5	2	4	2.5		5	2.5	4
2	3	2	4	6	2.5	3	4		5	4	3.5
3		2	4.5	5	4.5	1	2		2	5.5	2
3.5		5	2.5	4	2	2					2
2		3.5	4.5	3.5	4	3.5					4
2.5		2	4	4	2.5	4.5					4
4		2	3	6.5	1	4					3
2		4	4	4	4						4
2		3.5	2.5	2							3
3			2	4							5
2				5							
4				5.5							
				5							
				5.5							
				4.5							
				3.5							
				4.5							
				7							
				3							
				5							
mean diameter (cm)	2.7	2.8	3.6	4.5	2.8	3.1	2.9	3.5	4.3	4.3	3.7
n	13	10	11	21	9	8	4	1	3	4	9
% total	14	10	11	22	9	8	4	1	3	4	9

TABLE B.6 CLAST TYPE AND DIAMETER (cm) FOR UNIT TsmI (WAYPOINT 140108_2-4)

Date 01/08/14 n = 49
 UTM Location 3674168N, 271792E

	Crystal-poor felsic volcanics	Crystal-rich felsic volcanics	Tuffs, undivided	Crystal-poor intermediate volcanics	Crystal-rich intermediate volcanics	Diorite porphyry	Paleozoic carbonates
	1.5	2	3.5	3.5	1.5	12	4 2
	5.5	4	1	3	3.5		
	4	1.5	5	5.5	10		
		2	1	6	6		
		2	4	2	3		
		2.5	3	4.5	2.5		
		4.5	4.5	8.5	4.5		
		9.5	4	2	6.5		
				6	3		
				7	3		
				2	4		
				4	4.5		
				1	4.5		
					1.5		
mean diameter (cm)	3.7	3.5	3.3	4.2	4.1	12.0	3.0
n	3	8	8	13	14	1	2
% total	6	16	16	27	29	2	4

TABLE B.7 CLAST TYPE AND DIAMETER (cm) FOR UNIT TsmI (WAYPOINT 140227_3-3a)

Date 02/27/14 n = 51
 UTM Location 3669615N, 271542E

	Crystal-poor felsic volcanics	Tuffs, undivided	Crystal-poor intermediate volcanics	Crystal-rich intermediate volcanics	Diorite porphyry	Sandstone and siltstone, undivided	Chert and jasperoid	Basalt
	3	3	3	2	18	2	3.5	5.5
	3	4	1	3.5		3.5	3	6
	5.5		3	11.5		1.5		
	5		2	2.5		2.5		
	1.5		3	6.5				
	5.5		7	3.5				
	1			3				
	3.5			3				
	1.5			4.5				
	1.5			2				
	1			3				
	5			5				
	9			3				
				1.5				
				4.5				
				1.5				
				2.5				
				2.5				
				2.5				
				8				
				4				
mean diameter (cm)	3.5	3.5	3.2	3.8	18.0	2.4	3.3	5.8
n	13	2	6	21	1	4	2	2
% total	25	4	12	41	2	8	4	4

TABLE B.8 CLAST TYPE AND DIAMETER (cm) FOR UNIT Tsml (WAYPOINT 140828_3-1a)

Date 08/28/14

n = 50

UTM Location 3670355N, 271981E

	Crystal-poor felsic volcanics	Tuffs, undivided	Kneeling Nun tuff	Crystal-poor intermediate volcanics	Crystal-rich intermediate volcanics	Diorite porphyry	Paleozoic carbonates	Chert and jasperoid	Basalt
	2	3	3	5	1.5	4.5	3	3	4
	3	2	4	2	1	4.5			
	1.5		8	2.5	2.5				
	4			3					
	4.5			5					
	4			6					
	4			6					
				3					
				8					
				4					
				2					
				4					
				3.5					
				5					
				2.5					
				1.5					
				5					
				1.5					
				3					
				4.5					
				4					
				4.5					
				2.5					
				5					
				2.5					
				5					
				3					
				6					
				3					
				9					
mean diameter (cm)	3.3	2.5	5.0	4.1	1.7	4.5	3.0	3.0	4.0
n	7	2	3	30	3	2	1	1	1
% total	14	4	6	60	6	4	2	2	2

TABLE B.9 CLAST TYPE AND DIAMETER (cm) FOR UNIT Tsml (WAYPOINT 150128_1-3)

Date 01/28/15

n = 51

UTM Location 3673409N, 271235E

	Crystal-poor felsic volcanics	Tuffs, undivided	Kneeling Nun tuff	Crystal-poor intermediate volcanics	Crystal-rich intermediate volcanics	Diorite porphyry	Paleozoic carbonates	Sandstone and siltstone, undivided	Chert and jasperoid	Basalt
	1	12	8	1.5	5.5	5	1		1	2.5
	4	5.5	9.5	5.5	1		2.5		2.5	4.5
	3	10.5	3.5	2	3		6.5		0.5	2
	3.5	3		7	6					3
	2			2	1					4
	2.5			1.5						4.5
	5.5			2.5						10
	1.5			3.5						
	1			1.5						
	2.5			4.5						
				1.5						
				1.5						
				3						
				5						
				7						
mean diameter (cm)	2.7	7.8	7.0	3.3	3.3	5.0	3.3		1.3	4.4
n	10	4	3	15	5	1	3	0	3	7
% total	20	8	6	29	10	2	6	0	6	14

TABLE B.10 CLAST TYPE AND DIAMETER (cm) FOR UNIT TsmI (WAYPOINT 150129_2-3)

Date 01/29/15 n = 50
 UTM Location 3671992N, 271192E

	Crystal-poor felsic volcanics	Kneeling Nun tuff	Crystal-poor intermediate volcanics	Crystal-rich intermediate volcanics	Diorite porphyry	Abo Formation	Chert and jasperoid
	2.5 3	1	4.5	7 7.5 2 2 6 2.5 4 3.5 6 7 8 8.5 1 1 1 7.5 4 8 3 3.5 2 3 1.5 3	22 2.5 6 5 3 4 7 5 7 3 3 5 4.5 1	2.5 1 1.5 2.5	10 4 2
mean diameter (cm)	2.8	1.0	4.5	4.3	5.7	1.9	5.3
n	2	1	1	24	15	4	3
% total	4	2	2	48	30	8	6

TABLE B.11 CLAST TYPE AND DIAMETER (cm) FOR UNIT TsmI (WAYPOINT 180816_1d)

n = 90

Date		UTM Location											
08/16/18		3669635N, 271998E											
Crystal-poor felsic volcanics	Crystal-rich felsic volcanics	Tuffs, undivided	Kneeling Nun tuff	Crystal-poor intermediate volcanics	Crystal-rich intermediate volcanics	Diorite porphyry	Paleozoic carbonates	Abo Formation	Basalt	Other			
2	2.5	2	5	3	2	11.5	1.5	1.5	7	3			
3	2.5	2	4	2.5	12	4	7		2.5	4			
2	2	1.5	3	2	2.5	2.5			4.5	2			
2		3	3.5	3	4	2			2.5	3			
4		3.5	3	1.5	4	2.5				4			
1		2.5	3	4	3	2.5				3			
2.5			3.5	6	3	2.5				4			
3			2.5	3	4.5	2				3			
3				5	4	3.5							
2.5				6	4								
3.5				3	2.5								
2				3									
3.5				1.5									
2.5				2									
				3									
				3									
				4									
				1.5									
				1.5									
				3									
				4									
				2									
mean diameter (cm)	2.6	2.4	3.4	3.0	4.2	3.7	4.3	1.5	4.1	3.2			
n	14	6	8	28	10	9	2	1	4	5			
% total	16	3	9	31	11	10	2	1	4	6			

TABLE B.12 CLAST TYPE AND DIAMETER (cm) FOR UNIT Trp (WAYPOINT 141023_1-1b)

Date 10/23/14 $n = 25$

UTM Location 3668409N, 269549E

	Tuffs, undivided	Crystal-rich intermediate volcanics	
	1	3	
	2	3	
	3.5	2	
	2.5	3.5	
	2	4	
	2.5	10	
	1.5	7	
	2.5	15	
		2.5	
		19	
		4.5	
		4.5	
		8	
		0.5	
		3	
		3	
		3	
mean diameter (cm)	2.2	5.6	
n	8	17	
% total	32	68	

APPENDIX C

Paleocurrent data from the Williamsburg NW 7.5-minute quadrangle

This appendix contains tabulated paleocurrent direction data (azimuthal) measured from imbrication of gravels in certain geologic units exposed on the Williamsburg NW quadrangle. These units include the upper coarse, upper, and lower coarse piedmont facies of the Palomas Formation as well as the middle-lower Santa Fe Group predating the Palomas Formation. Location coordinates for all measurements are given in NAD83 UTM zone 13S. Mean paleocurrent directions from imbrication are shown on the geologic map.

TABLE C.1 IMBRICATION PALEOCURRENT MEASUREMENTS AT WAYPOINT 140826_1-1a					
		Flow direction measurements			
Northing	3673162	84	100	61	
Easting	273916	148	118	67	
Unit	QTpuc	119	101	124	
Mean	106	134	91	95	
Median	107	126	131	60	
n	30	127	102	65	
		145	72	95	
		135	96	106	
		130	60	127	
		135	107	120	

TABLE C.2 IMBRICATION PALEOCURRENT MEASUREMENTS AT WAYPOINT 140827A_2-3					
		Flow direction measurements			
Northing	3671514	179	153	215	
Easting	275372	186	171	203	
Unit	QTpuc	189	200	156	
Mean	172	175	220	149	
Median	175	192	130	140	
n	25	145	134		
		122	186		
		212	209		
		106	155		
		214	154		

TABLE C.3 IMBRICATION PALEOCURRENT MEASUREMENTS AT WAYPOINT 140827B_2-3					
		Flow direction measurements			
Northing	3671514	106	115	138	
Easting	275372	111	90	134	
Unit	QTpuc	134	102	101	
Mean	118	82	116	113	
Median	115	115	131	109	
n	25	146	99		
		153	110		
		114	125		
		118	159		
		100	126		

TABLE C.4 IMBRICATION PALEOCURRENT MEASUREMENTS AT WAYPOINT 150128A_1-1c					
		Flow direction measurements			
Northing	3673049	209	213	205	
Easting	272813	155	230	151	
Unit	QTpuc	159	196	111	
Mean	184	96	155	178	
Median	178	176	163	177	
n	25	125	234		
		123	204		
		129	203		
		239	234		
		252	244		

TABLE C.5 IMBRICATION PALEOCURRENT MEASUREMENTS AT WAYPOINT 150128B_1-1c					
		Flow direction measurements			
Northing	3673049	249	85	134	
Easting	272813	248	190	169	
Unit	QTpuc	145	161	156	
Mean	146	111	96	140	
Median	143	159	89	134	
n	28	120	130	166	
		91	281	237	
		139	159	170	
		123	172		
		125	93		

TABLE C.6 IMBRICATION PALEOCURRENT MEASUREMENTS AT WAYPOINT 150225A_2-2					
		Flow direction measurements			
Northing	3670042	65	65	144	96
Easting	276675	105	71	68	129
Unit	QTpuc	100	82	68	129
Mean	86	25	82	108	146
Median	88	21	109	114	45
n	35	48	88	109	
		48	88	141	
		61	88	96	
		61	109	83	
		65	109	44	

TABLE C.7 IMBRICATION PALEOCURRENT MEASUREMENTS AT WAYPOINT 150225B_2-2						
		Flow direction measurements				
Northing	3670042	205	127	110		
Easting	276675	147	150	131		
Unit	QTpuc	147	191	102		
Mean	132	88	191	102		
Median	129	88	134	154		
n	28	118	95	59		
		118	126	59		
		224	164	59		
		235	147			
		189	102			

TABLE C.8 IMBRICATION PALEOCURRENT MEASUREMENTS AT WAYPOINT 150225_2-3c						
		Flow direction measurements				
Northing	3668515	130	104	145	91	75
Easting	273661	121	104	88	125	50
Unit	QTpuc	121	104	128	74	119
Mean	94	57	71	102	86	50
Median	91	107	71	86	110	95
n	50	136	43	107	56	84
		111	91	109	54	90
		111	91	109	70	86
		114	86	60	33	86
		135	142	84	33	131

TABLE C.9 IMBRICATION PALEOCURRENT MEASUREMENTS AT WAYPOINT 150305_3i						
		Flow direction measurements				
Northing	3681228	76	44	141		
Easting	270899	76	46	145		
Unit	QTpuc	93	104	113		
Mean	86	161	16	113		
Median	90	54	16	108		
n	30	45	104	108		
		45	99	76		
		68	118	60		
		70	107	86		
		65	107	108		

TABLE C.10 IMBRICATION PALEOCURRENT MEASUREMENTS AT WAYPOINT 150430_3d						
		Flow direction measurements				
Northing	3680669	110	76	72	119	80
Easting	274303	174	154	72	91	80
Unit	QTpuc	70	134	42	72	160
Mean	105	140	121	72	72	160
Median	95	140	154	72	61	139
n	50	196	154	11	90	139
		161	96	40	120	94
		155	34	70	120	68
		175	160	54	120	73
		175	91	54	127	73

TABLE C.11 IMBRICATION PALEOCURRENT MEASUREMENTS AT WAYPOINT 150430_4b						
		Flow direction measurements				
Northing	3680281	84	118	85		
Easting	276173	92	130	122		
Unit	QTpuc	92	137	134		
Mean	101	91	169	114		
Median	94	104	72	107		
n	25	60	93			
		114	94			
		56	93			
		100	93			
		94	85			

TABLE C.12 IMBRICATION PALEOCURRENT MEASUREMENTS AT WAYPOINT 140826_1-1d						
		Flow direction measurements				
Northing	3672745	104	155	208		
Easting	273923	146	161	202		
Unit	QTpu	70	173	177		
Mean	155	111	98	93		
Median	164	122	183	202		
n	30	86	156	99		
		107	190	176		
		200	201	190		
		144	164	164		
		167	169	168		

TABLE C.13 IMBRICATION PALEOCURRENT MEASUREMENTS AT WAYPOINT 140827_2-4a				
Flow direction measurements				
Northing	3672239	99	175	158
Easting	274245	110	130	164
Unit	QTpu	139	98	117
Mean	126	167	139	151
Median	131	61	116	124
n	30	132	175	147
		140	178	76
		137	146	110
		89	117	77
		49	145	91

TABLE C.14 IMBRICATION PALEOCURRENT MEASUREMENTS AT WAYPOINT 150128A_1-5				
Flow direction measurements				
Northing	3673333	155	151	165
Easting	272416	123	156	203
Unit	QTpu	132	54	73
Mean	145	134	168	189
Median	151	121	156	134
n	25	114	174	
		51	199	
		173	178	
		146	136	
		113	156	

TABLE C.15 IMBRICATION PALEOCURRENT MEASUREMENTS AT WAYPOINT 150128B_1-5				
Flow direction measurements				
Northing	3673333	160	190	136
Easting	272416	139	145	131
Unit	QTpu	135	131	144
Mean	161	228	161	159
Median	159	126	202	166
n	27	177	175	148
		201	191	220
		156	169	
		199	134	
		144	109	

TABLE C.16 IMBRICATION PALEOCURRENT MEASUREMENTS AT WAYPOINT 150128A_1-5b					
		Flow direction measurements			
Northing	3672644	141	184	108	
Easting	272735	198	197	98	
Unit	QTpu	161	174	139	
Mean	147	174	175	179	
Median	147	158	109	124	
n	26	147	177	107	
		180	124		
		126	147		
		126	76		
		153	126		

TABLE C.17 IMBRICATION PALEOCURRENT MEASUREMENTS AT WAYPOINT 150128B_1-5b					
		Flow direction measurements			
Northing	3672644	54	54	110	
Easting	272735	75	68	133	
Unit	QTpu	54	121	55	
Mean	84	81	101	99	
Median	76	72	84	128	
n	25	76	52		
		90	60		
		64	75		
		129	88		
		76	102		

TABLE C.18 IMBRICATION PALEOCURRENT MEASUREMENTS AT WAYPOINT 150224A_1-1a					
		Flow direction measurements			
Northing	3670879	181	76	71	97
Easting	275178	86	76	115	
Unit	QTpu	31	131	115	
Mean	110	14	131	144	
Median	114	94	129	118	
n	31	94	158	137	
		91	158	137	
		91	158	125	
		121	100	111	
		81	114	97	

TABLE C.19 IMBRICATION PALEOCURRENT MEASUREMENTS AT WAYPOINT 150224B_1-1a				
Flow direction measurements				
Northing	3670879	81	63	176
Easting	275178	81	111	114
Unit	QTpu	81	111	81
Mean	100	81	154	81
Median	89	55	154	93
n	30	61	137	75
		61	40	169
		45	100	151
		112	84	106
		151	84	152

TABLE C.20 IMBRICATION PALEOCURRENT MEASUREMENTS AT WAYPOINT 150224_1-2c				
Flow direction measurements				
Northing	3670620	118	60	50
Easting	273871	107	60	121
Unit	QTpu	107	119	160
Mean	101	150	116	83
Median	107	35	76	134
n	30	106	69	24
		80	115	159
		91	115	109
		119	105	131
		119	86	81

TABLE C.21 IMBRICATION PALEOCURRENT MEASUREMENTS AT WAYPOINT 150224_1-3d					
Flow direction measurements					
Northing	3670185	93	112	133	127
Easting	276120	93	33	104	153
Unit	QTpu	64	161	121	100
Mean	106	64	63	121	100
Median	108	47	63	121	104
n	40	95	128	73	90
		95	128	73	135
		119	114	155	61
		119	120	164	61
		161	172	151	18

TABLE C.22 IMBRICATION PALEOCURRENT MEASUREMENTS AT WAYPOINT 150225_2-2b					
		Flow direction measurements			
Northing	3669570	12	95	21	
Easting	276407	12	95	21	
Unit	QTpu	19	60	48	
Mean	68	42	74	68	
Median	64	331	26	31	
n	30	148	56	142	
		148	76	129	
		126	161	118	
		106	107	118	
		358	15	23	

TABLE C.23 IMBRICATION PALEOCURRENT MEASUREMENTS AT WAYPOINT 150225_2-3						
		Flow direction measurements				
Northing	3667930	92	52	35	83	70
Easting	275868	87	43	87	83	96
Unit	QTpu	100	43	92	96	86
Mean	91	142	91	92	128	123
Median	92	156	91	70	128	108
n	50	174	94	36	128	85
		173	114	81	110	35
		87	108	127	127	93
		78	115	96	74	44
		80	39	37	74	109

TABLE C.24 IMBRICATION PALEOCURRENT MEASUREMENTS AT WAYPOINT 150225_2-3d				
		Flow direction measurements		
Northing	3668673	135	115	116
Easting	275462	154	115	96
Unit	QTpu	111	160	54
Mean	117	155	111	76
Median	121	132	121	89
n	25	132	146	
		64	121	
		124	71	
		98	158	
		143	122	

TABLE C.25 IMBRICATION PALEOCURRENT MEASUREMENTS AT WAYPOINT 150225_2-3g							
		Flow direction measurements					
Northing	3668876	45	100	98	86	164	
Easting	275585	56	100	154	110	164	
Unit	QTpu	105	57	194	59	181	
Mean	101	105	48	146	75	151	
Median	100	133	88	175	65	124	
n	50	133	80	162	67	72	
		133	116	71	61	75	
		129	111	110	131	75	
		129	111	46	70	43	
		155	91	46	88	43	

TABLE C.26 IMBRICATION PALEOCURRENT MEASUREMENTS AT WAYPOINT 150225_2-3i							
		Flow direction measurements					
Northing	3668520	56	94	124	129	97	108
Easting	276106	56	75	124	141	97	108
Unit	QTpu	20	89	150	60	57	106
Mean	98	15	89	154	44	78	134
Median	97	42	120	128	44	78	146
n	55	65	152	136	50	149	
		45	96	174	100	149	
		34	119	115	134	81	
		94	119	115	126	133	
		61	88	81	66	108	

TABLE C.27 IMBRICATION PALEOCURRENT MEASUREMENTS AT WAYPOINT 150226_3-1							
		Flow direction measurements					
Northing	3668731	10	182	194			
Easting	277601	191	182	194			
Unit	QTpu	155	199	154			
Mean	174	169	114	215			
Median	179	169	181	134			
n	25	131	179				
		102	179				
		198	203				
		198	294				
		160	164				

TABLE C.28 IMBRICATION PALEOCURRENT MEASUREMENTS AT WAYPOINT 150226_3-1a				
Flow direction measurements				
Northing	3668635	180	113	116
Easting	277553	238	162	154
Unit	QTpu	159	162	121
Mean	144	116	154	154
Median	147	82	124	154
n	30	175	166	199
		128	140	102
		128	140	180
		131	101	180
		96	101	174

TABLE C.29 IMBRICATION PALEOCURRENT MEASUREMENTS AT WAYPOINT 150305A_4b				
Flow direction measurements				
Northing	3679964*	109	84	281
Easting	277816*	81	71	284
Unit	QTpu	41	116	284
Mean	82	107	116	6
Median	83	106	116	6
n	25	106	141	
		106	114	
		81	59	
		19	59	
		83	106	

*Approximate location (± 30 m).

TABLE C.30 IMBRICATION PALEOCURRENT MEASUREMENTS AT WAYPOINT 150305B_4b				
Flow direction measurements				
Northing	3679964*	86	10	125
Easting	277816*	86	194	78
Unit	QTpu	86	51	51
Mean	64	139	51	51
Median	51	125	51	32
n	25	103	17	
		40	17	
		40	86	
		2	86	
		2	86	

*Approximate location (± 30 m).

TABLE C.31 IMBRICATION PALEOCURRENT MEASUREMENTS AT WAYPOINT 150408A_4a					
		Flow direction measurements			
Northing	3681411	162	128	154	
Easting	277566	174	128	120	
Unit	QTpu	174	124	160	
Mean	145	180	137	121	
Median	151	129	151	121	
n	25	139	155		
		185	155		
		95	174		
		95	174		
		110	174		

TABLE C.32 IMBRICATION PALEOCURRENT MEASUREMENTS AT WAYPOINT 150408B_4a					
		Flow direction measurements			
Northing	3681411	93	46	66	
Easting	277566	66	84	69	
Unit	QTpu	94	100	69	
Mean	72	70	60	44	
Median	70	70	60	102	
n	25	85	20		
		85	20		
		105	20		
		105	84		
		101	66		

TABLE C.33 IMBRICATION PALEOCURRENT MEASUREMENTS AT WAYPOINT 150408_4e						
		Flow direction measurements				
Northing	3681134	100	70	165	70	116
Easting	277949	95	36	165	73	94
Unit	QTpu	74	124	99	130	70
Mean	101	135	61	106	130	104
Median	103	111	101	106	115	103
n	50	111	78	124	114	103
		111	78	84	74	123
		139	78	70	74	127
		139	78	70	113	127
		86	101	70	116	121

TABLE C.34 IMBRICATION PALEOCURRENT MEASUREMENTS AT WAYPOINT 150408_5d							
		Flow direction measurements					
Northing	3681447	121	176	179	184	184	188
Easting	276868	122	160	179	173	150	
Unit	QTpu	140	158	209	176	150	
Mean	167	150	140	209	166	178	
Median	173	150	179	209	155	184	
n	51	148	135	184	173	151	
		128	186	184	176	174	
		169	186	150	176	174	
		220	134	150	163	158	
		220	86	150	199	188	

TABLE C.35 IMBRICATION PALEOCURRENT MEASUREMENTS AT WAYPOINT 150430_3c							
		Flow direction measurements					
Northing	3680735	51	55	48	86	61	
Easting	274321	91	55	48	26	2	
Unit	QTpu	62	52	59	107	31	
Mean	61	25	105	59	107	51	
Median	52	27	96	27	17	51	
n	50	50	126	0	44	37	
		50	126	43	346	78	
		125	126	43	22	78	
		125	41	37	60	36	
		125	129	144	60	19	

TABLE C.36 IMBRICATION PALEOCURRENT MEASUREMENTS AT WAYPOINT 150430_4c							
		Flow direction measurements					
Northing	3680292	75					
Easting	276159	55					
Unit	QTpu	70					
Mean	59	25					
Median	70	70					
n	5						

TABLE C.37 IMBRICATION PALEOCURRENT MEASUREMENTS AT WAYPOINT 131022_4									
		Flow direction measurements							
Northing	3669019	234	124	89	107	112	145	101	
Easting	273949	234	121	250	102	112	184	101	
Unit	QTplc	154	86	126	102	120	184	103	
Mean	139	123	91	145	122	109	147	205	
Median	125	201	91	156	140	109	125	97	
n	69	201	94	162	179	182	128	97	
		113	94	169	179	206	124	121	
		113	94	169	193	245	124	123	
		103	190	146	125	169	124	249	
		125	190	107	241	145	116		

TABLE C.38 IMBRICATION PALEOCURRENT MEASUREMENTS AT WAYPOINT 140107_1-2c									
		Flow direction measurements							
Northing	3675649	106	127	167	130	81	168	77	165
Easting	270875	105	149	167	130	79	134	126	109
Unit	QTplc	139	127	190	130	159	134	54	181
Mean	124	144	64	129	130	159	123	54	
Median	129	144	64	129	130	84	41	54	
n	73	155	129	170	101	116	43	54	
		155	125	184	101	166	121	95	
		150	161	125	191	166	121	127	
		150	101	104	191	65	85	127	
		150	209	130	109	74	85	165	

TABLE C.39 IMBRICATION PALEOCURRENT MEASUREMENTS AT WAYPOINT 140225_1-3b											
		Flow direction measurements									
Northing	3674753	41	97	54	74	99	92	140	101	105	104
Easting	271519	69	72	54	74	99	92	140	101	105	104
Unit	QTplc	69	59	89	74	99	105	118	94	141	104
Mean	101	52	59	89	74	99	115	118	94	141	100
Median	100	91	91	96	58	94	145	118	107	130	100
n	99	96	91	96	58	130	134	119	107	130	105
		96	91	96	58	130	134	119	136	104	120
		97	91	91	51	120	134	125	136	104	120
		97	86	100	51	116	164	139	128	107	120
		97	86	74	51	92	140	100	121	107	

TABLE C.40 IMBRICATION PALEOCURRENT MEASUREMENTS AT WAYPOINT 140826_1-3h					
		Flow direction measurements			
Northing	3669022	63	112	34	
Easting	271960	42	85	62	
Unit	QTplc	40	91	35	
Mean	61	78	53	32	
Median	60	45	111	80	
n	25	60	31		
		99	84		
		85	75		
		41	30		
		27	41		

TABLE C.41 IMBRICATION PALEOCURRENT MEASUREMENTS AT WAYPOINT 140826_1-3i					
		Flow direction measurements			
Northing	3668925	74	12	56	
Easting	271811	24	1	60	
Unit	QTplc	21	15	29	
Mean	41	39	9	11	
Median	34	19	34	81	
n	25	27	30		
		49	40		
		75	19		
		80	115		
		84	41		

TABLE C.42 IMBRICATION PALEOCURRENT MEASUREMENTS AT WAYPOINT 140828_3-1a						
		Flow direction measurements				
Northing	3670356	118	53	140	84	60
Easting	271981	116	101	117	104	107
Unit	QTplc	75	68	78	85	36
Mean	84	87	83	106	83	8
Median	84	44	45	124	110	49
n	50	104	30	102	142	57
		84	45	99	96	85
		132	124	80	78	29
		65	28	138	140	70
		104	66	78	90	60

TABLE C.43 IMBRICATION PALEOCURRENT MEASUREMENTS AT WAYPOINT 150128_1-4d				
Flow direction measurements				
Northing	3674226	109	67	143
Easting	272187	57	130	142
Unit	QTplc	145	116	69
Mean	131	114	71	157
Median	137	170	171	166
n	26	131	164	160
		159	166	
		139	68	
		134	122	
		166	127	

TABLE C.44 IMBRICATION PALEOCURRENT MEASUREMENTS AT WAYPOINT 150129A_2-1f				
Flow direction measurements				
Northing	3672148	154	169	
Easting	272780	118	170	
Unit	QTplc	125	134	
Mean	134	137	69	
Median	136	183	104	
n	20	149	70	
		134	124	
		151	150	
		147	149	
		130	92	

TABLE C.45 IMBRICATION PALEOCURRENT MEASUREMENTS AT WAYPOINT 150129B_2-1f				
Flow direction measurements				
Northing	3672148	155	133	
Easting	272780	84	120	
Unit	QTplc	63	108	
Mean	95	78	120	
Median	96	105	192	
n	20	115	31	
		112	56	
		95	26	
		80	70	
		81	97	

TABLE C.46 IMBRICATION PALEOCURRENT MEASUREMENTS AT WAYPOINT 150129C_2-1f				
Flow direction measurements				
Northing	3672148	64	27	
Easting	272780	19	34	
Unit	QTplc	38	57	
Mean	45	86	141	
Median	39	26	110	
n	20	6	61	
		44	346	
		59	347	
		88	40	
		24	35	

TABLE C.47 IMBRICATION PALEOCURRENT MEASUREMENTS AT WAYPOINT 150129_2-2d				
Flow direction measurements				
Northing	3672297	128	113	80
Easting	272094	161	119	35
Unit	QTplc	129	340	162
Mean	117	165	104	24
Median	118	94	154	118
n	25	100	100	
		115	155	
		156	125	
		103	119	
		98	157	

TABLE C.48 IMBRICATION PALEOCURRENT MEASUREMENTS AT WAYPOINT 150129A_2-4a				
Flow direction measurements				
Northing	3671343	179	123	149
Easting	272588	122	100	154
Unit	QTplc	144	89	111
Mean	115	100	120	142
Median	109	109	91	82
n	25	80	88	
		142	130	
		92	100	
		165	99	
		109	61	

TABLE C.49 IMBRICATION PALEOCURRENT MEASUREMENTS AT WAYPOINT 150129B_2-4a					
		Flow direction measurements			
Northing	3671343	89	134	127	
Easting	272588	56	126	79	
Unit	QTplc	122	130	115	
Mean	118	196	129	96	
Median	123	128	117	135	
n	26	109	124	131	
		106	135		
		149	87		
		119	96		
		129	105		

TABLE C.50 IMBRICATION PALEOCURRENT MEASUREMENTS AT WAYPOINT 150129_2-4c					
		Flow direction measurements			
Northing	3670880	91	120	138	
Easting	272665	100	114	126	
Unit	QTplc	68	38	43	
Mean	85	66	61	136	
Median	86	99	41	118	
n	26	55	80	66	
		103	34		
		115	71		
		68	103		
		32	130		

TABLE C.51 IMBRICATION PALEOCURRENT MEASUREMENTS AT WAYPOINT 150224_1-1							
		Flow direction measurements					
Northing	3670824	84	45	106	140	99	129
Easting	275149	120	45	126	126	51	49
Unit	QTplc	120	45	126	91	51	60
Mean	85	135	47	61	45	60	81
Median	78	154	133	101	48	116	
n	54	44	118	101	41	59	
		71	58	65	41	130	
		69	58	141	41	144	
		14	14	141	91	129	
		44	75	62	150	129	

TABLE C.52 IMBRICATION PALEOCURRENT MEASUREMENTS AT WAYPOINT 150224_1-1f				
Flow direction measurements				
Northing	3670944	146	139	166
Easting	274723	178	139	166
Unit	QTplc	155	160	156
Mean	161	192	176	156
Median	160	191	218	60
n	25	124	89	
		216	89	
		180	181	
		186	144	
		230	139	

TABLE C.53 IMBRICATION PALEOCURRENT MEASUREMENTS AT WAYPOINT 150224_1-3				
Flow direction measurements				
Northing	3670198	94	100	79
Easting	275527	115	110	97
Unit	QTplc	109	119	107
Mean	106	124	111	153
Median	108	94	114	122
n	25	108	152	
		151	52	
		151	55	
		95	77	
		95	77	

TABLE C.54 IMBRICATION PALEOCURRENT MEASUREMENTS AT WAYPOINT 150224A_1-3b				
Flow direction measurements				
Northing	3669626	121	109	97
Easting	275421	121	93	97
Unit	QTplc	150	104	95
Mean	114	151	150	116
Median	109	109	96	121
n	25	89	96	
		89	126	
		107	126	
		55	149	
		136	147	

TABLE C.55 IMBRICATION PALEOCURRENT MEASUREMENTS AT WAYPOINT 150224B_1-3b					
		Flow direction measurements			
Northing	3669626	91	147	121	
Easting	275421	86	121	64	
Unit	QTplc	134	173	102	
Mean	117	214	131	145	
Median	117	93	136	145	
n	30	131	134	46	
		123	133	97	
		117	80	97	
		117	111	91	
		117	111	111	

TABLE C.56 IMBRICATION PALEOCURRENT MEASUREMENTS AT WAYPOINT 150305A_3f					
		Flow direction measurements			
Northing	3681624	81	94	99	
Easting	270528	41	57	82	
Unit	QTplc	101	127	82	
Mean	96	301	63	121	
Median	97	155	99	79	
n	26	126	99	79	
		150	128		
		150	76		
		351	23		
		120	164		

TABLE C.57 IMBRICATION PALEOCURRENT MEASUREMENTS AT WAYPOINT 150305B_3f					
		Flow direction measurements			
Northing	3681624	135	119	71	
Easting	270528	96	119	81	
Unit	QTplc	96	184	127	
Mean	112	117	154	127	
Median	117	125	154	74	
n	25	94	109		
		333	109		
		105	78		
		172	45		
		172	92		

TABLE C.58 IMBRICATION PALEOCURRENT MEASUREMENTS AT WAYPOINT 150414A_2b			
Flow direction measurements			
Northing	3681358	178	126
Easting	275670	140	126
Unit	QTplc	164	158
Mean	142	144	170
Median	142	144	170
n	20	144	121
		177	121
		92	140
		92	140
		130	156

TABLE C.59 IMBRICATION PALEOCURRENT MEASUREMENTS AT WAYPOINT 150414B_2b			
Flow direction measurements			
Northing	3681358	126	148
Easting	275670	126	170
Unit	QTplc	126	255
Mean	134	140	179
Median	138	199	179
n	20	142	138
		142	82
		82	82
		82	64
		137	137

TABLE C.60 IMBRICATION PALEOCURRENT MEASUREMENTS AT WAYPOINT 150414C_2b			
Flow direction measurements			
Northing	3681358	156	98
Easting	275670	106	136
Unit	QTplc	106	136
Mean	100	46	150
Median	101	46	150
n	20	254	100
		254	68
		101	68
		70	68
		98	35

TABLE C.61 IMBRICATION PALEOCURRENT MEASUREMENTS AT WAYPOINT 150430_1					
		Flow direction measurements			
Northing	3681612	26	83	60	
Easting	271004	26	80	65	
Unit	QTplc	133	26	36	
Mean	59	49	51	36	
Median	49	94	42	46	
n	25	87	39		
		119	30		
		119	63		
		23	41		
		83	41		

TABLE C.62 IMBRICATION PALEOCURRENT MEASUREMENTS AT WAYPOINT 150430A_1d					
		Flow direction measurements			
Northing	3681297	99	131	23	
Easting	271218	46	131	136	
Unit	QTplc	84	170	136	
Mean	106	84	109	53	
Median	109	150	109	48	
n	25	150	171		
		150	45		
		154	45		
		199	24		
		131	52		

TABLE C.63 IMBRICATION PALEOCURRENT MEASUREMENTS AT WAYPOINT 150430B_1d					
		Flow direction measurements			
Northing	3681297	359	18	50	
Easting	271218	359	18	54	
Unit	QTplc	359	61	45	
Mean	33	359	51	45	
Median	45	45	49	33	
n	25	16	30		
		36	34		
		45	34		
		45	14		
		45	63		

TABLE C.64 IMBRICATION PALEOCURRENT MEASUREMENTS AT WAYPOINT 150430_1f				
Flow direction measurements				
Northing	3681617	40	116	101
Easting	271411	40	70	101
Unit	QTplc	74	61	111
Mean	85	124	73	86
Median	86	124	35	129
n	25	116	84	
		86	104	
		86	44	
		44	44	
		182	80	

TABLE C.65 IMBRICATION PALEOCURRENT MEASUREMENTS AT WAYPOINT 150430_2b				
Flow direction measurements				
Northing	3681252	97	120	34
Easting	272261	136	174	7
Unit	QTplc	136	174	7
Mean	84	111	174	91
Median	86	86	28	94
n	25	86	28	
		154	344	
		154	46	
		63	46	
		63	34	

TABLE C.66 IMBRICATION PALEOCURRENT MEASUREMENTS AT WAYPOINT 150430_2c				
Flow direction measurements				
Northing	3681236	53	121	91
Easting	272267	109	113	91
Unit	QTplc	139	154	89
Mean	105	139	150	135
Median	111	139	143	135
n	26	139	141	135
		60	6	
		60	26	
		79	26	
		79	91	

TABLE C.67 IMBRICATION PALEOCURRENT MEASUREMENTS AT WAYPOINT 150430_3a										
		Flow direction measurements								
Northing	3681597	157	101	125						
Easting	274118	133	172	125						
Unit	QTplc	133	172	125						
Mean	133	124	111	125						
Median	129	124	126	148						
n	26	111	126	133						
		111	132							
		88	156							
		151	131							
		169	131							

TABLE C.68 IMBRICATION PALEOCURRENT MEASUREMENTS AT WAYPOINT 140226_2-3a										
		Flow direction measurements								
Northing	3669449	121	124	100	106	117	121	141	105	139
Easting	272575	124	153	104	102	143	124	118	97	
Unit	Tsml	126	144	139	119	110	124	120	90	
Mean	124	151	126	136	105	97	124	119	148	
Median	124	91	150	119	116	101	152	144	117	
n	81	110	141	93	97	159	117	118	143	
		152	118	149	125	126	124	118	97	
		126	132	144	90	118	124	106	126	
		117	110	118	128	154	124	102	154	
		124	120	144	148	139	126	119	154	

TABLE C.69 IMBRICATION PALEOCURRENT MEASUREMENTS AT WAYPOINT 140227_3-2										
		Flow direction measurements								
Northing	3670328	115	153	131	109	125	115	151	136	
Easting	271516	144	158	110	124	135	144	118	156	
Unit	Tsml	100	115	111	136	151	136	118	156	
Mean	139	136	158	123	141	165	154	133	155	
Median	140	138	163	101	156	136	140	139	155	
n	75	154	104	121	148	164	154	144		
		140	133	133	137	156	153	141		
		125	113	139	145	133	163	109		
		154	157	144	163	106	157	156		
		113	152	141	130	155	152	151		

TABLE C.70 IMBRICATION PALEOCURRENT MEASUREMENTS AT WAYPOINT 140227_3-3										
		Flow direction measurements								
Northing	3669255	100	79	84	80	90	100	64	44	75
Easting	271467	74	104	71	44	51	74	72	59	75
Unit	Tsml	81	99	54	59	82	50	84	44	74
Mean	71	81	66	64	49	66	50	71	54	74
Median	71	50	94	75	80	91	71	71	66	51
n	86	71	84	64	44	75	72	64	66	51
		72	64	52	54	75	67	75	90	
		67	72	104	71	41	67	104	82	
		56	66	65	51	74	79	65	66	
		84	96	69	66	51	94	69	75	

TABLE C.71 IMBRICATION PALEOCURRENT MEASUREMENTS AT WAYPOINT 140828_3-1a										
		Flow direction measurements								
Northing	3670356	118	53	140	84	60				
Easting	271981	116	101	117	104	107				
Unit	Tsml	75	68	78	85	36				
Mean	84	87	83	106	83	8				
Median	84	44	45	124	110	49				
n	50	104	30	102	142	57				
		84	45	99	96	85				
		132	124	80	78	29				
		65	28	138	140	70				
		104	66	78	90	60				

TABLE C.72 IMBRICATION PALEOCURRENT MEASUREMENTS AT WAYPOINT 141023_1-4d										
		Flow direction measurements								
Northing	3670787	61	140	126						
Easting	271333	80	120	93						
Unit	Tsml	94	161	114						
Mean	94	135	66	124						
Median	94	90	83	108						
n	25	45	73							
		135	119							
		323	96							
		42	54							
		43	104							

TABLE C.73 IMBRICATION PALEOCURRENT MEASUREMENTS AT WAYPOINT 141024_2-4				
Flow direction measurements				
Northing	3670347	120	84	71
Easting	271358	114	120	139
Unit	TsmI	99	123	73
Mean	100	80	114	105
Median	106	106	109	114
n	25	116	133	
		55	76	
		63	81	
		68	115	
		91	126	

TABLE C.74 IMBRICATION PALEOCURRENT MEASUREMENTS AT WAYPOINT 141024A_2-4b				
Flow direction measurements				
Northing	3669683	91	64	
Easting	270899	49	63	
Unit	TsmI	100		
Mean	82	114		
Median	75	61		
n	12	116		
		106		
		76		
		74		
		69		

TABLE C.75 IMBRICATION PALEOCURRENT MEASUREMENTS AT WAYPOINT 141024B_2-4b				
Flow direction measurements				
Northing	3669683	106	149	
Easting	270899	120	129	
Unit	TsmI	105		
Mean	139	330		
Median	145	280		
n	12	146		
		156		
		144		
		131		
		181		

TABLE C.76 IMBRICATION PALEOCURRENT MEASUREMENTS AT WAYPOINT 150128_1-2d				
		Flow direction measurements		
Northing	3673255	99	84	74
Easting	271672	80	81	134
Unit	TsmI	174	85	169
Mean	121	119	104	142
Median	119	134	173	194
n	30	115	89	106
		155	91	118
		118	121	205
		95	101	141
		120	122	136

APPENDIX D

$^{40}\text{Ar}/^{39}\text{Ar}$ dating analyses from samples collected on the
Williamsburg NW 7.5-minute quadrangle

Sample 14WNW-1-AJ was collected from a basalt flow (Tb) west of Palomas Creek at 271084 mE/3675538 mN (NAD83 UTM 13S). Sample 14WNW-3-AJ was collected from an extrusive equivalent of unit Tad at 270141 mE/3670002 mN. Sample 14WNW-6-AJ was collected from a basalt flow (Tb) north of Salado Creek at 271695 mE/3669792 mN. NOTE: Sample ID numbers in the following reports mistakenly begin with "14HNW".

$^{40}\text{Ar}/^{39}\text{Ar}$ data are courtesy of the New Mexico Geochronology Laboratory, Socorro, NM.

Table 1. Summary of $^{40}\text{Ar}/^{39}\text{Ar}$ results and analytical methods

Sample	Lab #	Irradiation	mineral	age analysis	steps/analyses	Age	$\pm 2\sigma$	MSWD	comments
144-1-AJ	63323	272	groundmass concentrate	bulk step-heat	3	4.39	0.03	0.72	weighted mean
144-2-AJ	63325	272	groundmass concentrate	bulk step-heat	4	4.39	0.02	2.93	weighted mean
14HNW-1-AJ	63324	272	groundmass concentrate	bulk step-heat	4	4.57	0.02	3.13	weighted mean
14HNW-3-AJ	63285	272	biotite	bulk step-heat	4	40.35	0.05	29.99	weighted mean

Sample preparation and irradiation:

Minerals separated with standard heavy liquid, Franz Magnetic and hand-picking techniques.

Samples in NM-272 irradiated in a machined Aluminum tray for 8 hours in C.T. position, USGS TRIGA, Denver, Colorado.

Neutron flux monitor Fish Canyon Tuff sanidine (FC-2). Assigned age = 28.201 Ma (Kuiper et al., 2008).

Instrumentation:

Total fusion monitor analyses performed on a Argus VI mass spectrometer on line with automated all-metal extraction system. System = Jan

Step-heat analyses performed on a Argus VI mass spectrometer on line with automated all-metal extraction system. System = Obama

Multi-collector configuration: 40Ar-H1, 39Ar-Ax, 38Ar-L1, 37Ar-L2, 36Ar-CDD

Flux monitors fused with a Photon Machines Inc. CO₂ laser. Groundmass concentrate and biotite step-heated with a Photon Machine Inc. Diode laser.

Analytical parameters:

Sensitivity for the Argus VI with the Diode laser (step-heated samples) is 9.84e-17 moles/fA.

Sensitivity for the Argus VI with the CO₂ laser (fused monitors) is 4.62 e-17 moles/fA.

Typical system blank and background was 194, 1.76, 0.197, 4.92, 0.59 x 10⁻¹⁸ moles at masses 40, 39, 38, 37 and 36, respectively for the laser analyses.

J-factors determined by CO₂ laser-fusion of 6 single crystals from each of 8 radial positions around the irradiation tray.

Decay constants and isotopic abundances after Minn et al., (2000).

Table 1. Summary of $^{40}\text{Ar}/^{39}\text{Ar}$ results and analytical methods

Sample	Lab #	Irradiation	mineral	age analysis	steps/analyses	Age	$\pm 2\sigma$	MSWD	comments
14H-3-AJ	63603	276	groundmass concentrate	bulk step-heat	6	4.93	0.03	1.68	weighted mean
14HNW-6-AJ	63602	276	groundmass concentrate	bulk step-heat	6	5.54	0.03	2.16	weighted mean

Sample preparation and irradiation:

Minerals separated with standard heavy liquid, Franz Magnetic and hand-picking techniques.

Samples in NM-276 irradiated in a machined Aluminum tray for 16 hours in C.T. position, USGS TRIGA, Denver, Colorado.

Neutron flux monitor Fish Canyon Tuff sanidine (FC-2). Assigned age = 28.201 Ma (Kuiper et al., 2008).

Instrumentation:

Total fusion monitor analyses performed on a Argus VI mass spectrometer on line with automated all-metal extraction system. System = Jan

Step-heat analyses performed on a Argus VI mass spectrometer on line with automated all-metal extraction system. System = Obama

Multi-collector configuration: 40Ar-H1, 39Ar-Ax, 38Ar-L1, 37Ar-L2, 36Ar-CDD

Flux monitors fused with a Photon Machines Inc. CO₂ laser. Groundmass concentrate and biotite step-heated with a Photon Machine Inc. Diode laser.

Analytical parameters:

Sensitivity for the Argus VI with the Diode laser (step-heated samples) is 9.84e-17 moles/fA.

Sensitivity for the Argus VI with the CO₂ laser (fused monitors) is 4.62 e-17 moles/fA.

Typical system blank and background was 97.9, 0.39, 1.38, 8.17, 0.37 x 10⁻¹⁸ moles at masses 40, 39, 38, 37 and 36, respectively for the laser analyses.

J-factors determined by CO₂ laser-fusion of 6 single crystals from each of 8 radial positions around the irradiation tray.

Decay constants and isotopic abundances after Minn et al., (2000).

Table 2. $^{40}\text{Ar}/^{39}\text{Ar}$ analytical data.

ID	Power (Watts)	$^{40}\text{Ar}/^{39}\text{Ar}$	$^{37}\text{Ar}/^{39}\text{Ar}$	$^{36}\text{Ar}/^{39}\text{Ar}$ ($\times 10^{-3}$)	$^{39}\text{Ar}_k$ ($\times 10^{-15}$ mol)	K/Ca	$^{40}\text{Ar}^*$ (%)	^{39}Ar (%)	Age (Ma)	$\pm 1\sigma$ (Ma)
144-1-AJ , gm, 8.63 mg, J=0.0019637 \pm 0.05%, D=1 \pm 0, NM-272E, Lab#=63323-01										
Xi A	1	39.32	1.182	130.4	0.583	0.43	2.2	1.6	3.17	0.34
X B	1	33.88	1.231	109.9	0.797	0.41	4.4	3.8	5.40	0.28
X C	1	11.65	1.128	35.48	1.618	0.45	10.7	8.4	4.49	0.10
X D	2	5.979	1.129	16.12	1.958	0.45	21.7	13.8	4.66	0.06
X E	2	6.104	1.052	16.36	2.26	0.48	22.0	20.1	4.83	0.06
X F	2	5.394	1.191	14.00	2.59	0.43	24.9	27.3	4.83	0.05
X G	3	4.222	1.187	10.22	4.69	0.43	30.6	40.4	4.63	0.03
X H	5	3.045	1.069	6.289	7.21	0.48	41.6	60.5	4.53	0.02
I	7	2.570	4.701	5.803	4.97	0.11	47.4	74.4	4.38	0.03
J	10	2.836	4.583	6.666	6.63	0.11	43.0	92.9	4.38	0.02
K	15	2.797	4.312	6.414	2.55	0.12	44.1	100.0	4.43	0.04
Integrated age $\pm 2\sigma$			n=11		35.9	0.20		K2O=0.81	4.53	0.03
Plateau $\pm 2\sigma$ steps I-K			n=3	MSWD=0.72	14.149	0.112\pm0.010		39.5	4.39	0.03
Isochron$\pm 2\sigma$ steps B-K			n=10	MSWD=11.23		$^{40}\text{Ar}/^{36}\text{Ar}= 300\pm 4$			4.38	0.12
144-2-AJ , gm, 8.74 mg, J=0.0019549 \pm 0.04%, D=1 \pm 0, NM-272E, Lab#=63325-01										
X A	1	12.12	1.286	37.27	0.402	0.40	9.9	0.7	4.30	0.22
X B	1	7.322	0.9057	20.41	0.948	0.56	18.5	2.3	4.84	0.10
X C	1	2.090	0.5484	2.585	4.33	0.93	65.4	9.9	4.87	0.02
X D	2	1.502	0.4467	0.8243	6.39	1.1	86.1	21.0	4.60	0.01
X E	2	1.385	0.4169	0.4993	6.20	1.2	91.7	31.8	4.51	0.01
X F	2	1.368	0.4104	0.5094	5.36	1.2	91.3	41.1	4.44	0.01
X G	3	1.385	0.4309	0.5930	7.39	1.2	89.7	53.9	4.42	0.01
H	5	1.426	0.8480	0.8579	10.51	0.60	86.8	72.2	4.40	0.01
I	7	1.786	3.322	2.774	9.82	0.15	68.5	89.3	4.36	0.01
J	10	1.897	4.031	3.314	4.62	0.13	64.8	97.3	4.39	0.02
K	15	2.038	4.290	3.849	1.551	0.12	60.5	100.0	4.40	0.04
Integrated age $\pm 2\sigma$			n=11		57.5	0.36		K2O=1.29	4.48	0.01
Plateau $\pm 2\sigma$ steps H-K			n=4	MSWD=2.93	26.5	0.32 \pm0.47		46.1	4.39	0.02
Isochron$\pm 2\sigma$ steps A-K			n=11	MSWD=95.35		$^{40}\text{Ar}/^{36}\text{Ar}= 302\pm 19$			4.45	0.09
14HNW-1-AJ , gm, 12.77 mg, J=0.0019593 \pm 0.05%, D=1 \pm 0, NM-272E, Lab#=63324-01										
X A	1	21.94	1.351	68.00	0.238	0.38	8.9	0.3	6.97	0.43
X B	1	5.593	0.7699	13.60	1.149	0.66	29.1	1.7	5.83	0.09
X C	1	1.958	0.5748	2.071	5.53	0.89	70.9	8.4	4.96	0.02
X D	2	1.581	0.4577	0.9828	7.01	1.1	83.8	16.9	4.72	0.01
X E	2	1.506	0.4405	0.8139	6.80	1.2	86.3	25.2	4.63	0.01
X F	2	1.504	0.4414	0.8088	6.62	1.2	86.3	33.2	4.63	0.01
X G	3	1.480	0.4817	0.7654	11.60	1.1	87.2	47.3	4.60	0.01
H	5	1.484	0.6128	0.8377	19.8	0.83	86.5	71.3	4.58	0.01
I	7	1.788	2.010	2.260	13.02	0.25	71.3	87.1	4.55	0.01
J	10	2.236	4.493	4.386	8.08	0.11	57.6	97.0	4.61	0.02
K	15	1.974	3.239	3.209	2.51	0.16	64.6	100.0	4.56	0.03
Integrated age $\pm 2\sigma$			n=11		82.4	0.41		K2O=1.26%	4.65	0.01
Plateau $\pm 2\sigma$ steps H-K			n=4	MSWD=3.13	43.4	0.49 \pm0.67		52.7	4.57	0.02
Isochron$\pm 2\sigma$ steps A-K			n=11	MSWD=78.92		$^{40}\text{Ar}/^{36}\text{Ar}= 311\pm 18$			4.56	0.08

ID	Power (Watts)	⁴⁰ Ar/ ³⁹ Ar	³⁷ Ar/ ³⁹ Ar	³⁶ Ar/ ³⁹ Ar (x 10 ⁻³)	³⁹ Ar _K (x 10 ⁻¹⁵ mol)	K/Ca	⁴⁰ Ar* (%)	³⁹ Ar (%)	Age (Ma)	±1σ (Ma)
14HNW-3-AJ , Biotite, 4.32 mg, J=0.001944±0.02%, D=1±0, NM-272B, Lab#=63285-01										
X A	1	224.8	0.5285	739.6	0.361	0.97	2.8	0.6	22.41	1.16
X B	1	126.8	-0.0295	399.9	0.517	-	6.8	1.4	30.29	0.72
X C	1	28.36	0.2722	60.16	1.449	1.9	37.4	3.7	37.34	0.19
X D	2	16.46	0.1624	17.79	1.840	3.1	68.1	6.6	39.47	0.13
X E	2	14.56	0.0957	10.32	2.41	5.3	79.1	10.2	40.50	0.10
X F	2	13.66	0.0033	6.961	2.91	153.0	84.9	14.3	40.81	0.08
X G	3	12.92	-0.0130	4.245	5.89	-	90.3	22.3	41.01	0.04
X H	5	12.21	0.0296	2.019	14.13	17.2	95.1	38.8	40.84	0.02
I	7	11.81	0.0717	1.091	25.1	7.1	97.3	61.8	40.41	0.01
J	10	11.63	0.0143	0.5552	50.7	35.6	98.6	92.9	40.35	0.01
K	13	11.63	-0.0059	0.6472	13.34	-	98.4	98.9	40.23	0.02
L	17	11.65	0.0099	0.7342	2.48	51.8	98.1	100.0	40.23	0.09
Integrated age ± 2σ			n=12		121.2	15.7	K ₂ O=5.54%		39.72	0.02
Plateau ± 2σ		steps I-L	n=4	MSWD=29.99	91.654	23.272±39.144	75.6	40.35	0.05	
Isochron±2σ		steps A-L	n=12	MSWD=145.15		⁴⁰ Ar/ ³⁶ Ar= 289.3±7.2		40.41	0.19	

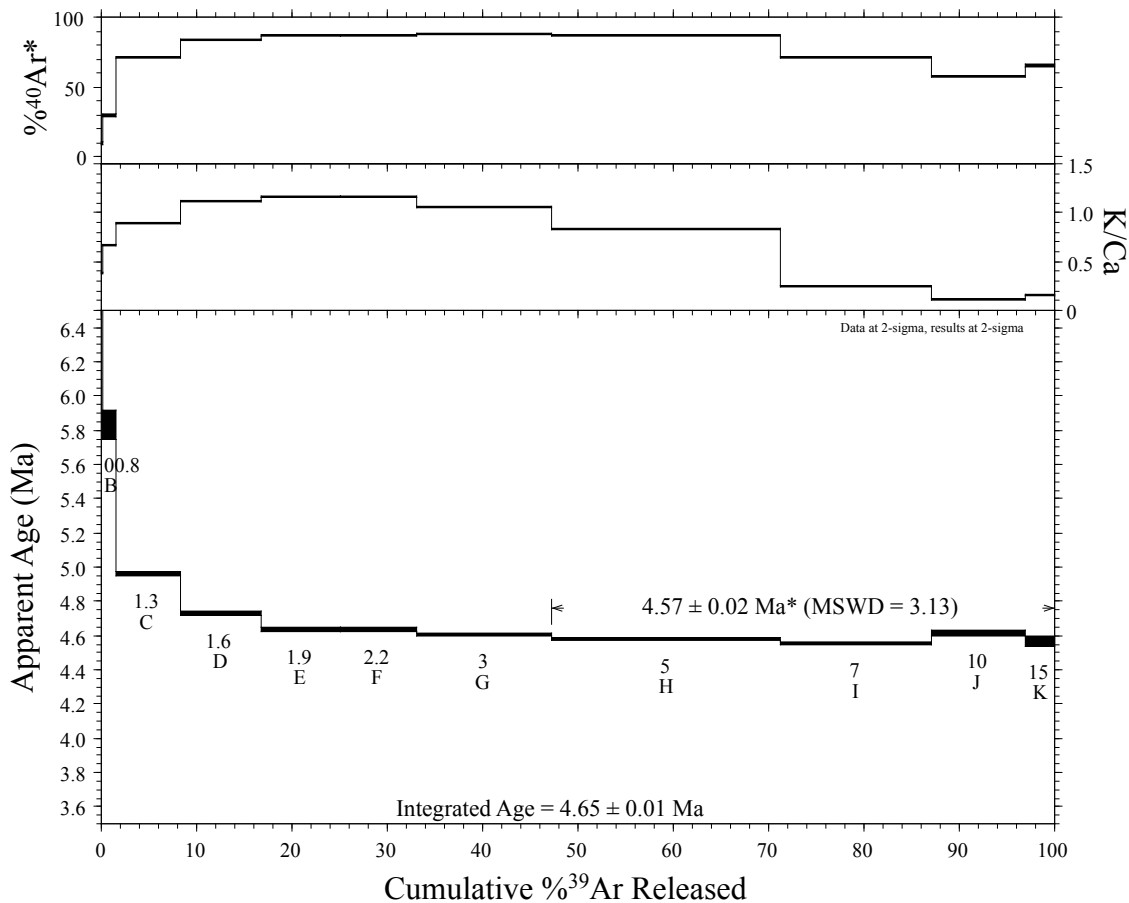
Notes:

Isotopic ratios corrected for blank, radioactive decay, and mass discrimination, not corrected for interfering reactions.
 Errors quoted for individual analyses include analytical error only, without interfering reaction or J uncertainties.
 Integrated age calculated by summing isotopic measurements of all steps.
 Integrated age error calculated by quadratically combining errors of isotopic measurements of all steps.
 Plateau age is inverse-variance-weighted mean of selected steps.
 Plateau age error is inverse-variance-weighted mean error (Taylor, 1982) times root MSWD where MSWD>1.
 Plateau error is weighted error of Taylor (1982).
 Decay constants and isotopic abundances after Minn et al. (2000).
 # symbol preceding sample ID denotes analyses excluded from plateau age calculations.
 Weight percent K₂O calculated from ³⁹Ar signal, sample weight, and instrument sensitivity.
 Ages calculated relative to FC-2 Fish Canyon Tuff sanidine interlaboratory standard at 28.201 Ma
 Decay Constant (LambdaK (total)) = 5.463e-10/a
 Correction factors:
 $(^{39}\text{Ar}/^{37}\text{Ar})_{\text{Ca}} = 0.00066 \pm 1\text{e-}05$
 $(^{36}\text{Ar}/^{37}\text{Ar})_{\text{Ca}} = 0.000264 \pm 1\text{e-}06$
 $(^{38}\text{Ar}/^{39}\text{Ar})_{\text{K}} = 0.013$
 $(^{40}\text{Ar}/^{39}\text{Ar})_{\text{K}} = 0.007614 \pm 0.000105$

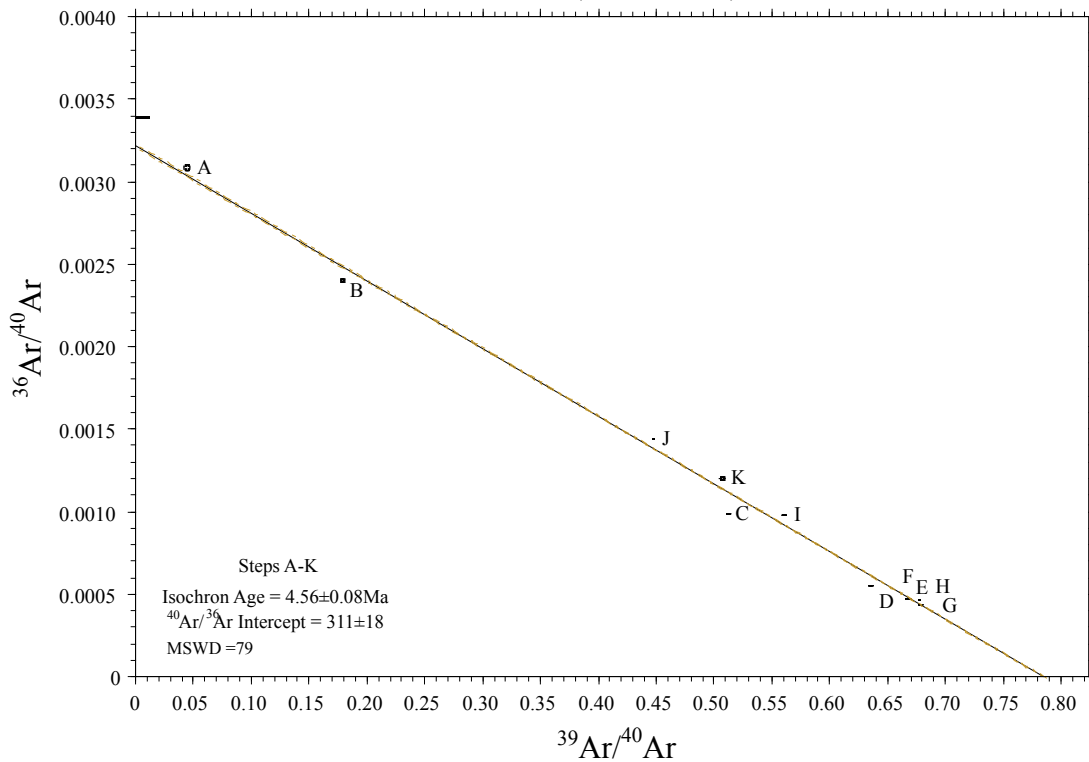
Table 2. $^{40}\text{Ar}/^{39}\text{Ar}$ analytical data.

ID	Power (Watts)	$^{40}\text{Ar}/^{39}\text{Ar}$	$^{37}\text{Ar}/^{39}\text{Ar}$	$^{36}\text{Ar}/^{39}\text{Ar}$ ($\times 10^{-3}$)	$^{39}\text{Ar}_K$ ($\times 10^{-15}$ mol)	K/Ca	$^{40}\text{Ar}^*$ (%)	^{39}Ar (%)	Age (Ma)	$\pm 1\sigma$ (Ma)
14H-3-AJ , whole rock, 12.15 mg, J=0.0039325 \pm 0.02%, D=1 \pm 0, NM-276A, Lab#=63603-01										
X A	1	16.81	2.179	54.52	0.719	0.23	5.2	0.9	6.26	0.65
X B	1	2.021	1.569	4.779	4.46	0.33	36.0	6.5	5.23	0.08
X C	1	0.8646	1.391	0.9223	15.92	0.37	80.5	26.4	5.01	0.02
D	2	0.7707	1.295	0.6112	14.42	0.39	89.1	44.4	4.94	0.02
E	2	0.7907	1.566	0.7632	10.02	0.33	86.4	56.9	4.92	0.02
F	2	0.8079	2.426	1.081	7.67	0.21	83.7	66.5	4.87	0.03
G	3	0.9186	4.851	2.074	9.52	0.11	75.0	78.4	4.97	0.04
H	5	1.071	7.849	3.427	9.09	0.065	63.8	89.7	4.94	0.04
I	7	1.039	8.985	3.692	2.57	0.057	64.0	92.9	4.81	0.08
X J	10	1.196	11.25	4.600	1.118	0.045	61.6	94.3	5.34	0.15
X K	15	1.197	14.46	5.586	4.54	0.035	58.9	100.0	5.12	0.08
Integrated age $\pm 2\sigma$			n=11		80.1	0.13		K ₂ O=0.64	4.99	0.03
Plateau $\pm 2\sigma$ steps D-I			n=6	MSWD=1.68	53.3	0.23 \pm0.28		66.6	4.93	0.03
Isochron $\pm 2\sigma$ steps A-K			n=11	MSWD=4.30		$^{40}\text{Ar}/^{36}\text{Ar}=301.3\pm 5.8$			4.94	0.04
14WNW-6-AJ , whole rock, 11 mg, J=0.0039232 \pm 0.02%, D=1 \pm 0, NM-276A, Lab#=63602-01										
Xi A	1	13.99	0.8064	44.40	1.705	0.63	6.6	1.3	6.63	0.38
X B	1	2.334	0.5593	5.172	7.72	0.91	36.1	7.0	6.05	0.06
X C	1	1.168	0.5299	1.337	20.6	0.96	69.2	22.3	5.79	0.02
X D	2	0.9870	0.5546	0.8077	19.05	0.92	79.6	36.4	5.63	0.01
E	2	0.9764	0.7281	0.8443	15.57	0.70	79.7	47.9	5.58	0.02
F	2	0.9615	1.092	0.9145	14.18	0.47	80.3	58.4	5.54	0.02
G	3	1.055	2.602	1.657	23.1	0.20	72.7	75.6	5.51	0.02
H	5	1.290	4.236	2.899	18.23	0.12	59.5	89.1	5.52	0.03
I	7	1.132	4.052	2.272	3.58	0.13	68.9	91.7	5.61	0.06
J	10	1.131	4.158	2.368	3.80	0.12	67.1	94.5	5.46	0.06
X K	15	2.548	6.742	7.510	7.38	0.076	34.0	100.0	6.23	0.07
Integrated age $\pm 2\sigma$			n=11		134.9	0.25		K ₂ O=1.20	5.59	0.02
Plateau $\pm 2\sigma$ steps E-J			n=6	MSWD=2.16	78.5	0.32 \pm0.48		58.1	5.54	0.03
Isochron $\pm 2\sigma$ steps B-K			n=10	MSWD=17.41		$^{40}\text{Ar}/^{36}\text{Ar}=310.6\pm 11.7$			5.51	0.08
Notes:										
Isotopic ratios corrected for blank, radioactive decay, and mass discrimination, not corrected for interfering reactions.										
Errors quoted for individual analyses include analytical error only, without interfering reaction or J uncertainties.										
Integrated age calculated by summing isotopic measurements of all steps.										
Integrated age error calculated by quadratically combining errors of isotopic measurements of all steps.										
Plateau age is inverse-variance-weighted mean of selected steps.										
Plateau age error is inverse-variance-weighted mean error (Taylor, 1982) times root MSWD where MSWD>1.										
Plateau error is weighted error of Taylor (1982).										
Decay constants and isotopic abundances after Minn et al. (2000).										
# symbol preceding sample ID denotes analyses excluded from plateau age calculations.										
Weight percent K ₂ O calculated from ^{39}Ar signal, sample weight, and instrument sensitivity.										
Ages calculated relative to FC-2 Fish Canyon Tuff sanidine interlaboratory standard at 28.201 Ma										
Decay Constant (LambdaK (total)) = 5.463e-10/a										
Correction factors:										
$(^{39}\text{Ar}/^{37}\text{Ar})_{\text{Ca}} = 0.0007064 \pm 4\text{e-}06$										
$(^{36}\text{Ar}/^{37}\text{Ar})_{\text{Ca}} = 0.0002731 \pm 0$										
$(^{38}\text{Ar}/^{39}\text{Ar})_K = 0.01261$										
$(^{40}\text{Ar}/^{39}\text{Ar})_K = 0.00808 \pm 0.00041$										

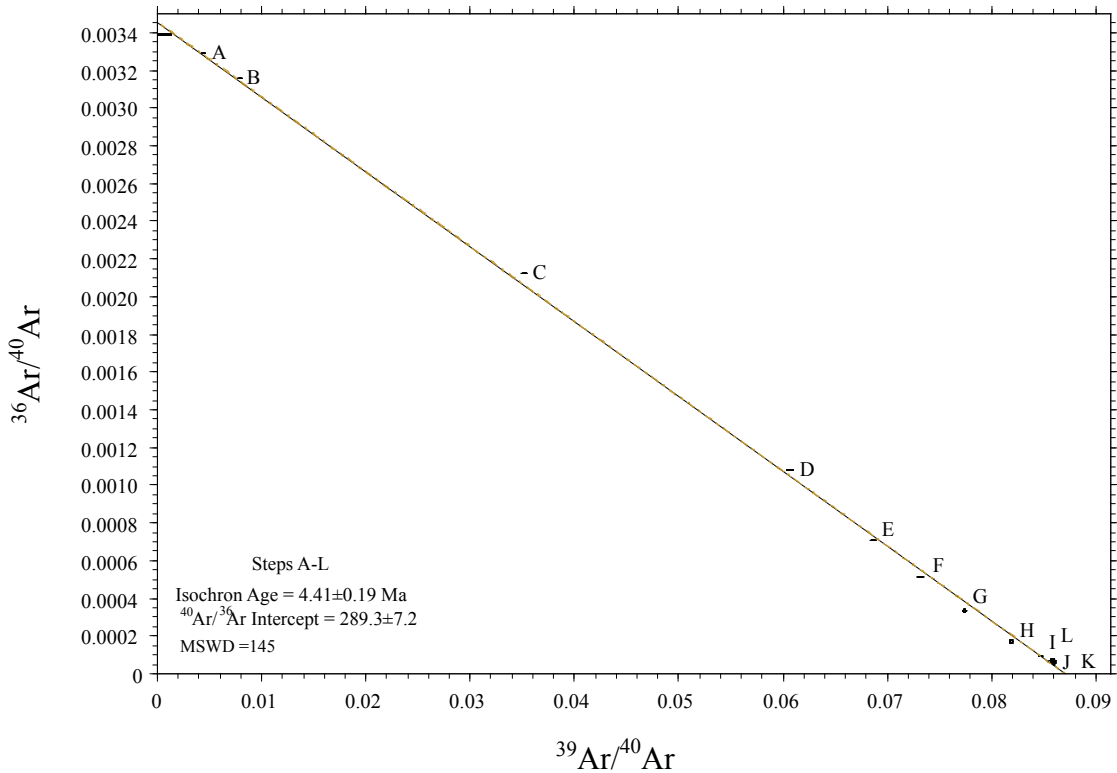
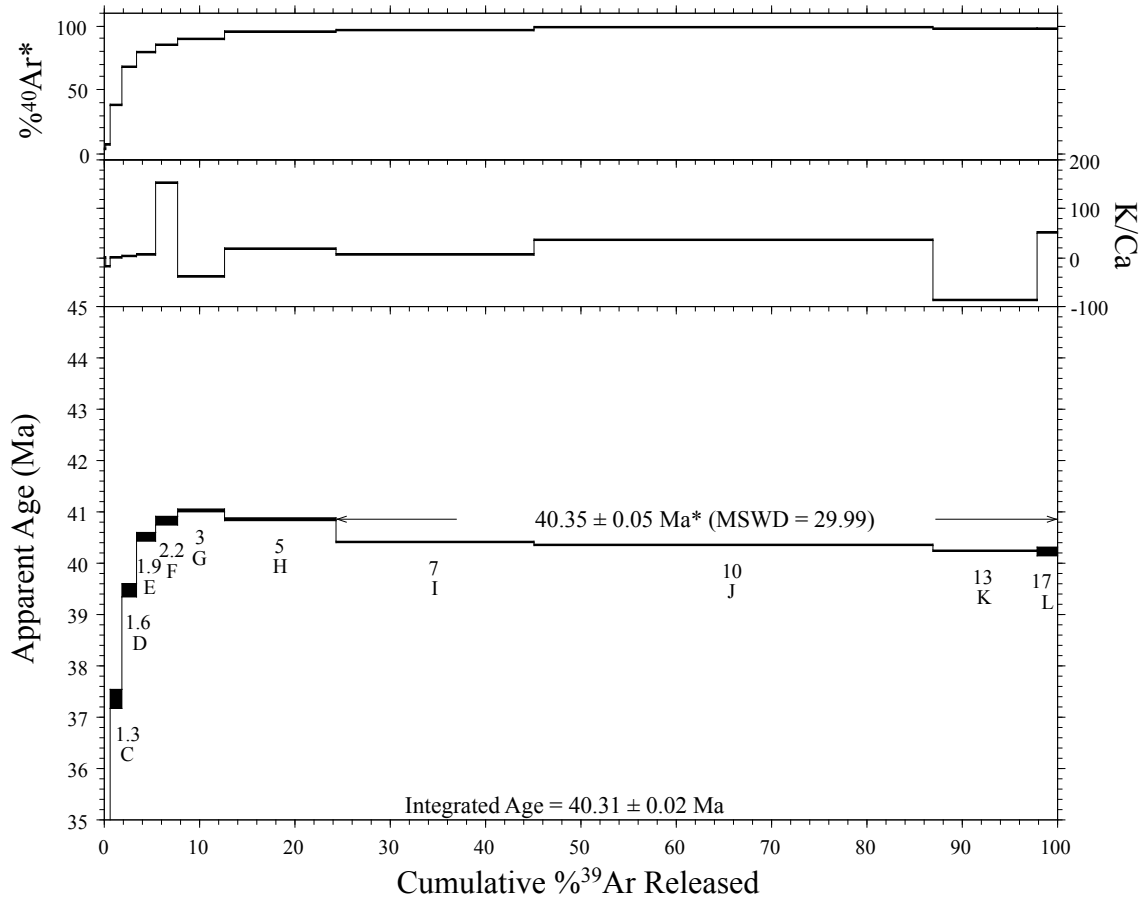
14HNW-1-AJ Groundmass Concentrate



63324-01 (14HNW-1-AJ)



14HNW-3-AJ Biotite



14WNW-6-AJ Groundmass Concentrate

